DENSITY, SPEED OF SOUND, REFRACTIVE INDEX AND ACTIVITY COEFFICIENTS AT INFINITE DILUTION FOR IONIC LIQUIDS

BY

NCOMEKA MGXADENI

Submitted in fulfilment of the academic requirements for the Masters of Applied Sciences

(Chemistry)

Durban University of Technology, Chemistry Department, Durban, South Africa

2017

PREFACE

This work was conducted in the Department of Chemistry, Durban University of Technology, ML Sultan Campus, Durban, South Africa in conjunction with University of KwaZulu-Natal, Howard College, Department of Chemical Engineering from February 2015 to October 2017. The work was supervised by Professor N. Deenadayalu, Professor D. Ramjugernath and Professor P. Naidoo.

DECLARATION

, **Ncomeka Mgxadeni** declare that:

- The work reported in this thesis, except from where generally indicated is my original work.
- This work has not been submitted to any degree or any examination at any other university.
- The thesis does not contain other people's information, diagrams and pictures or other data, unless particularly recognized as being sourced from different authors. Where other written sources have been cited, at that point their words have been re-written yet the general data ascribed to them has been referenced and where their correct words has been utilized, their written work has been set inside quotes, and referenced.
- This thesis does not contain text, graphs or tables copied and pasted from the internet unless particularly recognized, and the source being detailed in the thesis and in the reference section.

[redacted] 16/04/2018

Ncomeka Mgxadeni (Student) Date

As supervisors of this candidate, we approve this dissertation for submission:

[redacted] 16/04/2018

Prof. N. Deenadayalu Date

[redacted] 16/04/2018

Prof. D. Ramjugernath Date

16/04/2018

Prof. P. Naidoo Date

CONFERENCE ATTENDANCE

- **Poster presentation:** 42nd National Convention of the South African Chemical Institute (SACI), 29 – 4th December 2015, Southern Sun Elangeni Hotel, Durban.
- **Poster presentation:** National Inorganic Chemistry Conference and Carman Physical Chemistry Symposium of the South African Chemical Institute, 25 – 29th June 2017, Arabella Hotel and Spa, Hermanus, Western Cape.

ABSTRACT

In this study the experimental density, speed of sound, and refractive index for binary mixtures of an ionic liquid (IL): 1-butyl-3-methylimidazolium nitrate and activity coefficients at infinite dilution of organic solutes in the ionic liquid: 1-butyl-3-methylimidazolium hydrogen sulfate were determined.

The density, speed of sound, and refractive index of 1-butyl-3-methylimidazolium nitrate in pyridine or acetonitrile or thiophene have been reported at T = 298.15 K, 303.15 K, 308.15 K, 313.15 K and 318.15 K using an Anton Paar DSA 5000M vibrating U-tube densimeter and a RXA 156 refractometer. The derived properties namely: excess molar volume, isentropic compressibility and change in refractive index were calculated from density, speed of sound and refractive index, respectively. The results are discussed in terms of molecular interactions (hydrogen bond, dipole-dipole, or ion-solvent or interactions). The negative deviation of excess molar volume and the positive deviation in change in refractive index clearly indicates the strong interaction of 1-butyl-3-methylimidazolium nitrate with pyridine or acetonitrile or thiophene in solution. The positive values of isentropic compressibility for the system indicates that the mixtures were more compressible than the ideal mixture. The Redlich Kister smoothing polynomial was used to fit the excess molar volume and deviation in isentropic compressibility data. The Lorentz-Lorenz equation was used to predict the experimental density, or refractive index data and to correlate the excess molar volume. Gas liquid chromatography was used to determine activity coefficients at infinite dilution for 28 polar and non-polar organic solute: alkanes, cycloalkanes, alkenes, alkynes, aromatic hydrocarbons, alcohols, aldehydes, thiophene, pyridine and acetonitrile in an IL: 1-butyl-3-methylimidazolium hydrogen sulfate ([BMIM][HSO_4]). The measured values of activity

coefficients at infinite dilution for the solutes in [BMIM][HSO_4] were carried out at T = (313.15, 323.15, 333.15) K. Partial molar excess enthalpies at infinite dilution of the organic solutes in the ionic liquid have been calculated from the temperature dependence of activity coefficients at infinite dilution. The selectivity and capacity values for separation problems namely: hexane/benzene, heptane/benzene, cyclohexane/benzene, ethanol/benzene, heptane/pyridine, heptane/thiophene and methanol/acetone at T = 323.15 K were calculated and compared to literature values for similar ionic liquids, sulfolane and N-methyl-2-pyrolidinone (NMP). The IL [BMIM][HSO_4] gave both the highest selectivity and limiting capacity for the heptane/thiophene separation and would therefore be a suitable entrainer for this separation. New data from this study reveals that [BMIM][HSO_4] may be proposed as a replacement solvent for the separation of sulphur or nitrogen compounds from alkanes.

ACKNOWLEDGEMENTS

Greatness and Praise to Jehovah, the all mighty God who enabled me to accomplish this research work.

I offer my most extreme thanks to Prof. Nirmala Deenadayalu for her devoted supervision, her priceless assistance throughout this study and for introducing me to the World of Chemical Thermodynamics. Prof. Paramespri Naidoo and Prof. Deresh Ramjugernath, the co-supervisors are earnestly recognized for their direction, sincere kindness, understanding and selfless support that has expanded my insight into thermodynamics, as well as, fuelled my enthusiasm for research.

I would like to express my genuine thanks to:

Durban University of Technology for giving me the chance to embrace my research and the National Research Foundation (NRF) for financial support and for the purchase of the DSA 5000 M instrument.

University of KwaZulu-Natal Howard College and Thermodynamic Research Unit's laboratory technician, Mr Ayanda Khanyile and the School of Chemical Engineering's workshop staff, Mr Leon Augustyn thank you for your assistant.

Dr Mark Williams-Wayne, Marcin Durski, Dr Deepak Ekka and Dr Samuel Iwarere for their help with understanding the experimental procedures and calculations.

DUT Thermodynamics and Biomass Processing Research group for their help.

My family and friends for their encouragements.

My son (Lukholo Bukhobenkosi Melokuhle) for being my inspiration in everything I do and for being there for me in a unique and special way.

Table of Contents

LIST OF TABLES

LIST OF FIGURES

LIST OF SYMBOLS

ρ	=	density ($g \cdot cm^{-3}$).
V_m^E	=	excess molar volume ($cm^3 \cdot mol^{-1}$).
T	=	temperature (K).
x_1	=	mole fraction of the 1st component.
x_2	=	mole fraction of the 2nd component.
σ	=	standard deviation.
M_1	=	molar mass of the 1st component. ($g \cdot mol^{-1}$).
M_2	=	molar mass of the 2nd component. ($g \cdot mol^{-1}$).
A_i	=	polynomial coefficient.
N	=	polynomial degree.
n	=	number of experimental points.
N_A	=	Avogadro's number (mol^{-1}).
k	=	number of coefficients used in the Redlich-Kister correlation.
u	=	speed of sound ($m \cdot s^{-1}$).
κ_s	=	isentropic compressibility (Pa^{-1}).
Δn	=	refractive index deviation.
n^{id}	=	ideal refractive index.
R	=	molar refraction.

n = refractive index of mixture.

n_1 = refractive index of 1st component.

n_2 = refractive index of 2nd component.

γ_{13}^{∞} = activity coefficients at infinite dilution.

P_o = column outlet pressure.

J_2^3 = pressure correction term.

n_3 = number of moles of solvent in the column packing.

T_{col} = column temperature.

P_1^* = saturated vapour pressure of the solute at temperature *T.*

B_{11} = second virial coefficient of the pure solute.

V_1^* = molar volume of the solute.

V_1^{∞} = partial molar volume of the solute at infinite dilution in the solvent.

B_{12} = mixed second virial coefficient of the solute and the carrier gas.

t_R = retention time of the given solute.

t_G = retention time of the non-retainable component (gas).

q_{ov} = carrier gas flow at the column temperature and column outlet pressure.

q_o = flow rate measured with the bubble flow meter at the column outlet.

T_f = flow meter temperature measured with a thermometer.

P_W^* = saturated vapour of water at temperature T_f .

P_i = column inlet pressure.

$\Delta H_1^{E\infty}$ = partial molar excess enthalpy at infinite dilution.

S_{12}^{∞} = selectivity at infinite dilution.

k = capacity.

V_R = retention volume of the solute.

V_3 = solvent volume.

K = equilibrium partition coefficient.

R = universal gas constant.

V_G = gas hold up volume.

T_C = critical temperature.

V_C = critical volume.

Chapter 1

INTRODUCTION

1.1 Green Solvent

A growing area of research in the development of green technologies is devoted to designing new, environmentally friendly solvents (Brennecke and Maginn 2001; Alfonsi *et al.* 2008). Green chemistry, also called sustainable chemistry, is in the area of chemistry and chemical engineering that is focused in the development of chemical products and processes that reduce or wipe out the generation of a risky substance. Green chemistry principles require that: solvents should be non-toxic, readily biodegradable and synthesized by an environmentally friendly synthetic procedure, while also meeting technological and economic demands (Matzke *et al.* 2010). Approximately 20 million tons of volatile organic compounds (VOCs) are released into the atmosphere because of industrial processing operations (Allen, Shonnard and Prothero 2002). A new class of compounds called ionic liquids (ILs) are of interest to chemists and engineers due to their very low vapor pressure and low volatility. ILs can be designed for a specific application such as the separation of close boiling components. ILs are useful in many chemical applications: as novel solvent systems for organic synthesis, separation processes, and electrochemistry (Welton 1999; Rogers and Seddon 2003).

For ILs to be used effectively as entrainers, it is essential to know their interaction with different solutes. Experimental data for density, refractive index, and speed of sound and their derived properties, and activity coefficients at infinite dilution are necessary for many chemical, industrial, and biological processes, especially for mixtures containing the

extractant of interest, e.g., separation of close boiling mixtures and serving as input for process simulation (Alptekin and Canakci 2008; Ceriani *et al.* 2008).

In the petrochemical industries, the production of pure organic components requires their separation from streams containing similar classes of organic solvents using entrainers, e.g., N-methyl-2-pyrrolidone (NMP), N-formylmorpholine (NFM), and sulfolane. The separation of hydrocarbons is difficult to achieve due to their close boiling points. The continuous use of volatile organic solvents for industrial application is posing a considerable environmental concern, as they are highly toxic. Consequently, researchers are devoting much effort in seeking alternative solvents for wide scale industrial applications. Advanced distillation techniques such as extractive distillation or pressure swing distillation using an entrainer are used for the separation of close boiling point chemicals (Seader and Henley 2006). The entrainer must have high selectivity and capacity for the component to be separated. It must also have a relative volatility that is much lower than that of the components being separated. In order to use these separation methods the selectivity values calculated from activity coefficients at infinite dilution are required. It is therefore necessary to obtain experimental retention data from the gas liquid chromatography (GLC) technique for computing activity coefficients at infinite dilution and selectivities.

1.2 Aim of the Research

The aims of this study are:

To experimentally determine density, the speed of sound, and refractive index data for binary mixtures of the ionic liquid: 1-butyl-3-methylimidazolium nitrate and to determine activity coefficients at infinite dilution of organic solutes in the ionic liquid: 1-butyl-3-methylimidazolium hydrogen sulfate in order to calculate the selectivities.

1.3 Objectives of the Research

The objectives are to:

- to measure density, speed of sound and refractive index for the binary mixtures of ionic liquid 1-butyl-3-methyimidazolium nitrate ([BMIM][NO_3] + pyridine), ([BMIM][NO_3] + acetonitrile), ([BMIM][NO_3] + thiophene);
- to calculate excess molar volumes, isentropic compressibility and deviation in refractive index;
- measure the retention times for solutes using gas liquid chromatography (GLC);
- calculate the activity coefficient at infinite dilution;
- calculate the selectivity of the solvent for binary mixtures of close boiling components;
- calculate the capacity of the solvent for a particular solute at infinite dilution

1.4 Thesis Outline

- Chapter 1: context of the research
- Chapter 2: deals with the literature review (showing links to the topic)
- Chapter 3: outlines the experimental methods and theoretical frame work
- Chapter 4: details the experimental procedures
- Chapter 5: the results (tables, graphs) are presented
- Chapter 6: discussion of the experimental results obtained using DSA 5000M , RXA 156 and gas liquid chromatography.
- Chapter 7: the main points based on the results are presented

Chapter 2

LITERATURE REVIEW

2.1 Definition of Ionic Liquids

Ionic liquids (ILs) are salts that have a melting temperatures below 100 ^{o}C (Lehmann *et al.* 2010), that also act as "green solvents" (Welton 1999). The room temperature ionic liquids (RTILs), are organic salts in a mixture of organic/inorganic cations and anions which are held together by columbic forces and are liquid at room temperature.

2.2 History of Ionic Liquids

Gabriel and Weiner (1888) discovered the protic ionic liquid: ethanolammonium nitrate with the melting point of 52 – 55 ^{o}C. Walden (1914) observed that the earliest room temperature ionic liquid: ethylammonium nitrate had a melting point of 12 ^{o}C. The IL was formed by the neutralization of ethylamine with concentrated nitric acid (Walden 1914). Chum *et al.* (1975) and Wilkes *et al.* (1982) synthesized ionic liquids centred on alkyl substituted imidazolium and pyridinium cations with tetra halogen aluminate anions, to use as probable electrolytes in batteries. Wilkes and Zaworotko (1992) synthesised the air stable 1-ethyl-3-imidazolium based ionic liquids which consisted of the anions: acetate ($CH_3CO_2^-$), nitrite (NO_2^-), hexafluorophosphate (PF_6^-) and tetrafluoroborate (BF_4^-), allowing a much wider range of applications in research such as electrochemistry, polymer chemistry, organic synthesis and biocatalysts. These ionic liquids can be synthesised on the bench top; they can retain water from the environment, however they do not react with water. Current synthesis techniques

involve ionic liquid that can be created by combining diverse ions like the ones shown in Figure 2.1.

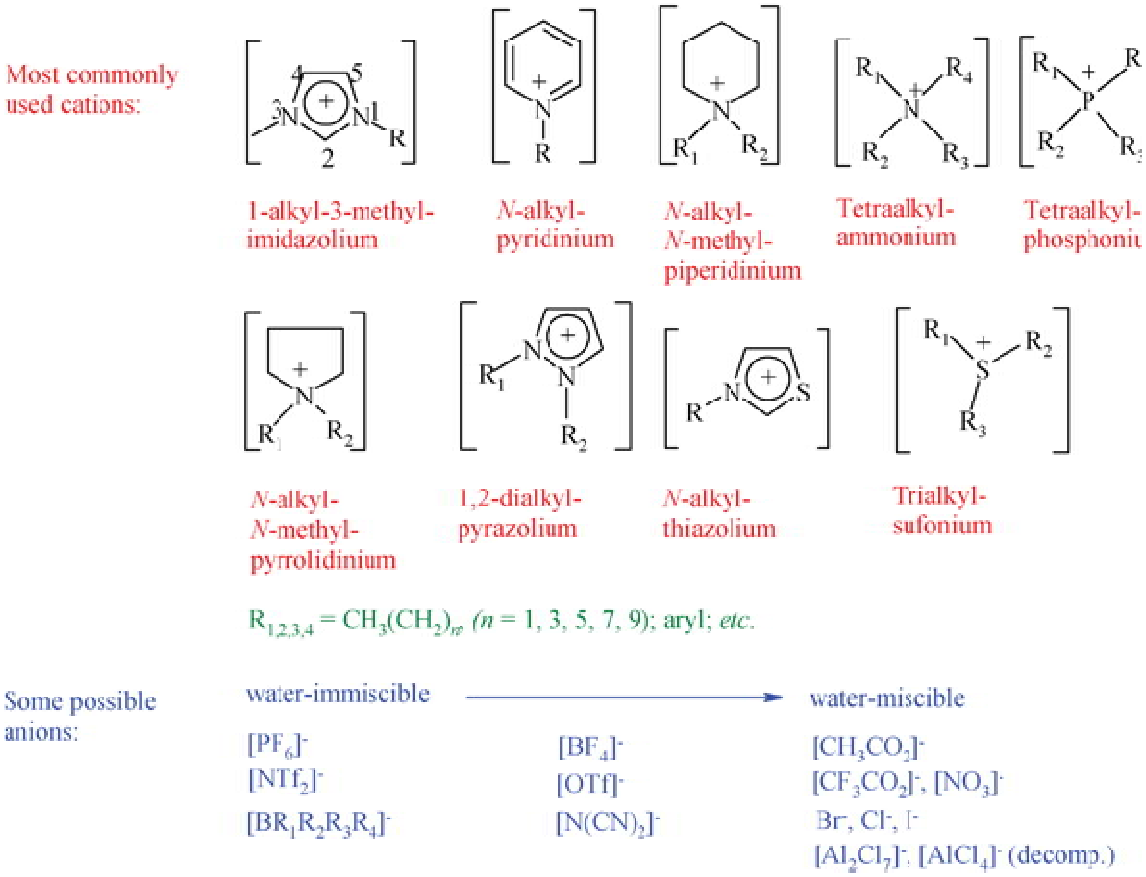

Figure 2.1: Ionic liquid structures (Plechkova and Seddon 2008)

2.3 Importance of Ionic Liquids

Ionic liquids are molten salts (Lehmann *et al.* 2010) that also act as "green solvents" (Welton 1999). ILs are composed of a large organic cation with a low degree of symmetry and a bulky inorganic/organic anion (Stark and Seddon 2007). ILs have properties such as low vapor pressure that practically makes them non-volatile, and they cannot enhance air contamination or cause health infection since they do not vaporise in the reaction vessel (Antony *et al.* 2004;

Barceló González 2010). ILs are used in green chemistry because of their advantageous physical properties (Table 2.1) ; it can replace volatile organic solvents (VOCs) in a chemical reaction (Berthod and Carda-Broch 2004); they are also environmental friendly because of non-toxicity, recyclability, wide liquid range and biodegradability. RTILs have interesting and tunable properties since both the thermodynamics and kinetics of reactions in ionic liquids are diverse to those in conventional molecular solvents.

Table 2.1: Physical properties of ionic liquids extracted from (Singh 2013)

Property	Value
Freezing point	< 373.15 K
Liquidus range	298.15 - 473.15 K
Thermal stability	High
Viscosity	< 100 Cp
Dielectric constant	< 30 ($F \cdot m^{-1}$)
Polarity	47 – 49
Specific conductivity	< 10 $mS \cdot cm^{-1}$
Molar conductivity	< 10 $Scm^2 \cdot mol^{-1}$
Electrochemical window	2V- 4.5 V
Solvent and/or catalyst	Excellent for many organic reactions
Vapor pressure	Usually negligible

2.4 Ionic Liquids Versus Organic Solvents

Table 2.2 underlines the benefits of ionic liquids over organic solvents whose attractiveness has increased tremendously.

Table 2.2: Contrast of organic solvents with ionic liquids (Plechkova and Seddon 2008)

Property	**Organic solvents**	**Ionic liquids**
Number of solvents	> 1000	>1 000 000
Applicability	Single function	Multifunction
Catalytic ability	Rare	Common tuneable
Chirality	Rare	Common tuneable
Vapour pressure	Obeys the Clausius-Claperyron equation	Negligible vapour pressure under normal condition
Flammability	Usually flammable	Usually non-flammable
Solvation	Weakly solvating	Strong solvating
Polarity	Conventional polarity concepts apply	Polarity concept questionable
Tuneability	Limited range of solvents available	Virtually unlimited range means "designer solvents"
Cost	Normal cheap	Typically between 2 and 100 times the cost of organic solvents
Recyclability	Green imperative	Economic imperative
Viscosity/cP	0.2-100	22-40 000
Density/$g \cdot cm^{-3}$	0.6-1.7	0.8-3.3
Refractive index	1.3-1.6	1.5-2.2

2.5 Probable Uses of Ionic Liquids Within the Chemical Industry

ILs have attracted the attention of chemists and engineers because of their properties and versatility for possible application in the petrochemical industry ((José-Alberto and Jorge 2011). The probable uses of ionic liquids within the chemical industry are given in Table 2.3.

Table 2.3: Probable uses of ionic liquids within the chemical industry (Plechkova and Seddon 2008)

Engineering	**Physical Chemistry**	**Electrochemistry**	**Analytics**	**Biochemistry**
Coatings	Refractive index	Metal plating	Matrices for mass spectrometry	biocides
Lubricants	Thermodynamics	Fuel cells	Gas chromatography columns	Biomass processing
Dispersing agents	Binary and ternary systems	Electrolyte in batteries	Stationary phase for HPLC	Drug delivery
Plasticisers		Solar panels		Personal care

2.6 Industrial Applications of Ionic Liquids

Plechkova and Seddon (2008) reported the different industrial uses of ILs and are described below.

2.6.1 Biphasic Acid Scavenging Utilizing Ionic Liquids (BASIL) Process

BASIL process is a principle case of an industrial procedure utilizing ionic liquid innovation. In 2002, BASF German introduced in the production of the generic photo initiator precursor alkoxy phenyl phosphines, 1-methylimidazolium chloride ionic liquid to scavenge the acid to separate out the reaction mixture as discrete phase, and the results were better than the triethylammonium that was original used (Plechkova and Seddon 2008).

2.6.2 Dimersol Process

IFP (Institut Français du Pétrole) uses chloroaluminate (III) ionic liquids for alkenes dimerization (Plechkova and Seddon 2008).

2.6.3 Isobutene Alkylation

Petro China performs isobutene alkylation with an ionic liquid. This is the biggest business using ionic liquids.

2.6.4 Gas Handling

Gas manufacturer Linde utilizes the low solubility of hydrogen in ILs to compress the gas up to 450 bars in filling stations by utilizing ionic liquid piston compressor. The IL 1-butyl-3-methylimidazolium chloride has been applied in separation of hydrogen from ammonia borane (Karkamkar, Aardahl and Autrey 2007). ILs and amines are exploited for capture of CO_2 and purification of natural gas (Barghi, Adibi and Rashtchian 2010; Mota-Martinez *et al.* 2014).

2.7 Further Viable Uses of ILs

The subsequent successful applications have been cited:

(a) manufacturing of lithium-ion rechargeable battery by Pionics in Japan (Plechkova and Seddon 2008)

(b) pharmaceutical intermediate manufacturing by Central Glass Co, Ltd in Japan (Plechkova and Seddon 2008)

(c) 2.5 dihydrofuran manufacturing by Eastman Chemical Company from 1996 to 2004 (Plechkova and Seddon 2008)

2.8 Pilot Plant Projects of ILs

The following pilot plant stage industrial processes using ILs have been established (Tumba 2010):

(a) Cellulose dissolution by BASF;

(b) Aluminum plating by BASF;

(c) Azeotrope-breaking for water-ethanol and water-tetrahydrofuran with minimized costs of solvent retrieval by BASF;

(d) Phosgene replacement by an ionic liquid in 1,4-dichlorobutane production, realised by BASF;

(e) Metathesis and olefin trimerization by SASOL in South Africa

2.9 Ionic Liquids and Separations

ILs can be used to make existing separation methods more efficient and environmentally friendly. However, the separation of ILs is the major challenge for the development of industrial processes that will use these new interesting solvents (Pereiro *et al.* 2012). Distillation is the most generally utilized separation strategy in the chemical process industry. When the components to be separated have comparative volatilities near 1.00 (i.e. close

boiling mixture), separation turns out to be challenging and costly since a huge amount of trays and a high reflux ratio are required.

Therefore, the following typical separation process is needed:

(a) Extractive or azeotropic distillation

(b) Liquid-liquid extraction

2.9.1 Extractive Distillation

Extractive distillation is the most popular method used in petrochemical or chemical industries for separating close boiling mixtures, low volatility mixtures and azeotropic mixtures. It is a partial evaporation procedure, a non-volatile and high boiling point separating agent (the entrainer), which is added to the azeotropic mixture to alter the relative volatility of the main constituent short of new azeotrope creation (Gil *et al.* 2008).

It uses an additional solvent to interact with the elements of different chemical structure within the mixture (Gutiérrez Hernández 2013). It works because the high boiling point entrainer is introduced close to the top of the extractive distillation column, to change the volatiles in such a way that the separation factor is greater than 1 (Gil *et al.* 2008). The extractive agent and less volatile component stream to the base of the distillation column, where the removed component is obtained by an ensuing distillation. Therefore, the non-extracted components are refined to the highest point of the extractive tower (Figure 2.2). The design of extractive distillation systems will similarly need substantial initial work as well as (i) selecting the solvent; (ii) experimental solubility studies; (iii) calculating essential data, such as azeotropic condition or residue curve; (iv) initial screening of solvent; (v) computer simulation; (vi) small scale testing.

Figure 2.2 is an illustration of the extractive distillation process, which is utilized for the separation of aliphatic and aromatic compounds. The existence of entrainers in the column through the separation course allows the aliphatic compounds to move to the top. The compounds with the lowest boiling point exit from the top of the column and the compounds with highest boiling points (aromatic hydrocarbons and the entrainer) remain at the bottom of the column exit.

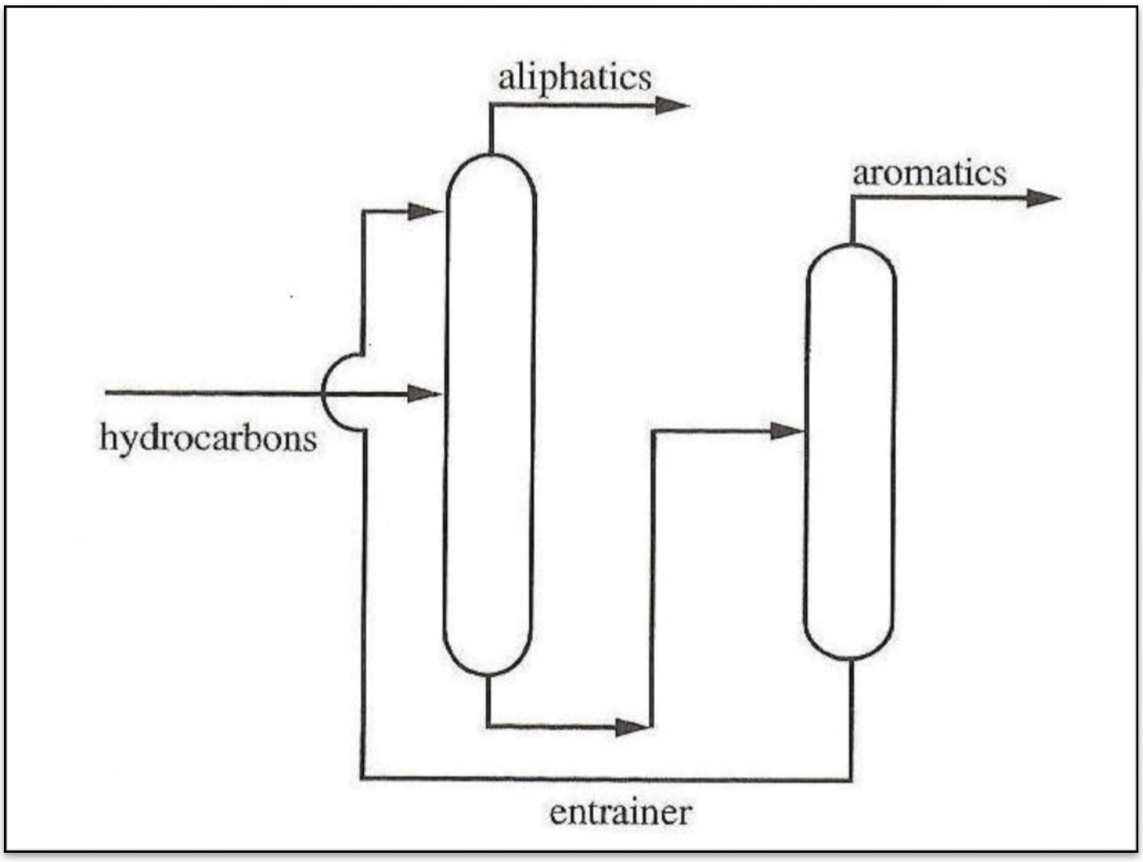

Figure 2.2: Schematic of an extractive distillation process (Letcher 2004)

2.9.2 Liquid-Liquid Extraction (LLE)

LLE has been recommended by the process engineers for the development of separation process (Lo and Schwietzer 1996). In LLE, extractants (selective solvents) are also required

which are slightly miscible with the liquid stream to be separated. In an example of this process, aliphatic compounds are separated from the aromatic compounds in the feed stream with the help of selective solvents (Huddleston *et al.* 1998; Gwala 2009).

This separation process is used in industry for the following separation processes (Gwala 2009):

(a) Separation of systems with similar boiling points (e.g., separation of aromatic compounds from aliphatic hydrocarbons;
(b) Separation of azeotropic mixtures (extraction of acetic or formic acid from aqueous media);
(c) Separation of temperature sensitive compounds;
(d) Separation of mixtures with high boiling points;
(e) Extraction of organic solutions.

2.9.3 Use of ILs for LLE

ILs are known as environmentally friendly solvents and are generally immiscible with aliphatic compounds. Aromatic compounds solubility in many IL is high and completely miscible, therefore this behavior allows the IL to separate aromatic/ aliphatic mixtures at any feed composition (Canales and Brennecke 2016). LLE performance of separation is determined by the selectivity as well as the solvent capacity. A selectivity and capacity analysis is needed to evaluate the economic feasibility of using IL for aliphatic-aromatic separations. Use of ILs ease the regeneration of extraction solvent due to the low vapor pressure. Loss of solvent should be avoided from the raffinate by its separation (Steltenpohl and Graczová 2014). The regeneration of IL from the final extract is done by distillation, which entails heating and cooling (Figure 2.3).

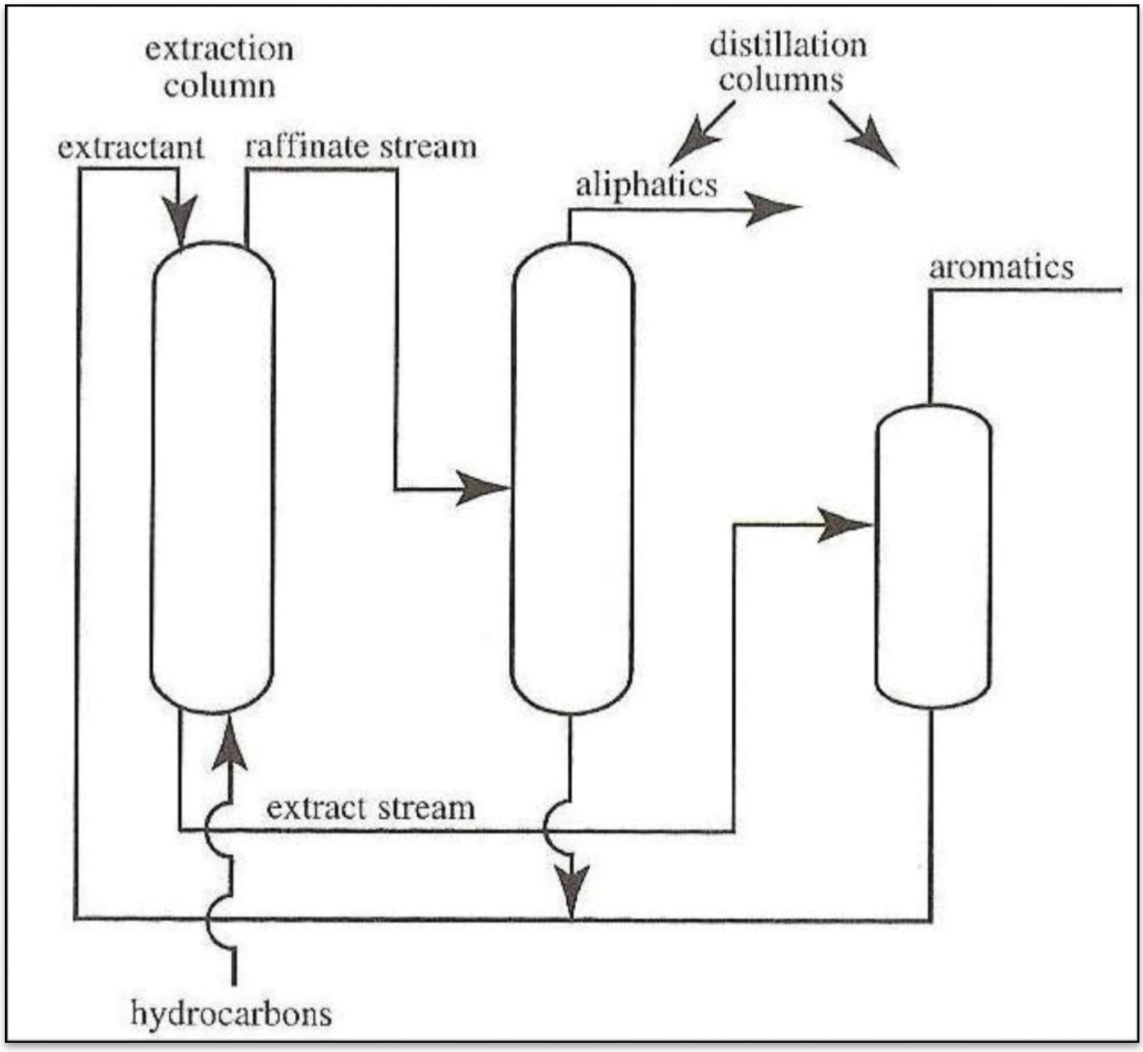

Figure 2.3: Schematic diagram of typical liquid-liquid extraction process (Letcher 2004)

2.10 Choice of Solvent in Separations

The selection of the solvent system is a critical step in the method of a separation. The exact composition of the solvent mixture will determine whether there will be complete separation of the components in the mixture.

Therefore, the solvent should:

(a) Enhance the ordinary relative volatility of the main component significantly;

(b) Not need an extreme proportion of solvent to non-solvent (due to operating cost of the column and supplementary equipment);

(c) Stay soluble in the feed components and culminate the creation of two phases;

(d) Effectively separate from the bottom product;

(e) Cheap and freely available;

(f) Steady at the temperature of the distillation and solvent separation;

(g) Nonreactive with the components in the feed mixture;

(h) Non-corrosive and non-hazardous;

(i) Have low latent heat of vaporization to assist separation and recovery after the extraction process.

2.11 Thermodynamic Properties Determined in this Work

In this work density, speed of sound and refractive index for the binary mixtures of ionic liquid: 1-butyl-3-methyimidazolium nitrate ([BMIM][NO_3] + pyridine), ([BMIM][NO_3] + acetonitrile), ([BMIM][NO_3] + thiophene) were measured at T = (298.15, 303.15, 308.15, 313.15, 318.15) K, and activity coefficients at infinite dilution for 28 polar and non-polar organic solutes in the IL:1-butyl-3-methylimidazolium hydrogen sulfate ([BMIM][HSO_4]) were calculated at T = (313.15, 323.15, 333.15) K.

2.11.1 Excess Molar Volumes, Change in Speed of Sound and Change in Isentropic Compressibility of Binary Mixtures

The thermodynamic properties: excess molar volumes, change of refractive indices, and change of isentropic compressibility are of keen interest for the adequate design of industrial processes and theoretical calculations for chemical processes (Orge *et al.* 1999).

It is reported that ([BMIM][NO_3]) is a halogen free and environmental friendly IL (Strechan *et al.* 2008).A halogen free ionic liquid is important because it does not have hidden problems including the hydrolytic instability of halogen containing anion, which can lead to halide waste (Wasserscheid, van Hal and Bösmann 2002).

The derived properties namely excess molar volume, deviation in isentropic compressibility and change in refractive index were computed based on density, the speed of sound and refractive index, respectively. The derived properties were computed over the mole fraction range of 0.1 – 0.9 and at different temperatures. The results are discussed in terms of molecular interactions (hydrogen bond, dipole-dipole interaction, ion-solvent or molecular interactions). Using the experimental data, excess molar volume, isentropic compressibility, molar refraction, *R*, and deviation in refractive index were computed from density.
The Redlich-Kister smoothing polynomial was utilized to fit the excess molar volume and deviation in isentropic compressibility data. The Lorentz-Lorenz equation was utilized in predictions the experimental density or refractive index and for correlation of excess molar volume.

Figure 2.4 is the structure of 1-butyl-3-methylimidazolium nitrate ([BMIM][NO_3]) used in this work and presented below.

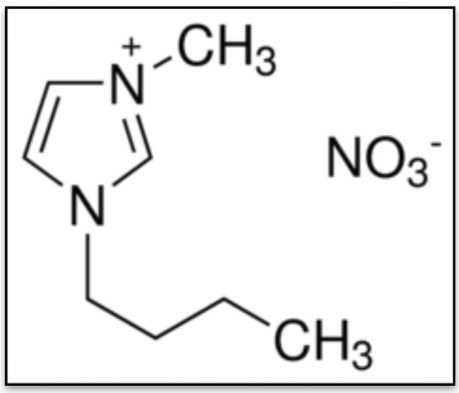

Figure 2.4: Structure of 1-Butyl-3-methylimidazolium nitrate ([BMIM][NO_3])

2.11.2 Activity Coefficients at Infinite Dilution

The activity coefficient at infinite dilution similarly known as limiting activity coefficient is the limiting value of the activity coefficient of a solute when its concentration tends towards zero in the solvent (in this study the IL). Activity coefficients at infinite dilution and (gas + liquid) partition coefficients (K_L) data gives a quantitative degree of interactions among unlike molecules when the (solute + solute) interactions are absent, and also provide information on the intermolecular interaction between ILs and organic solutes, and can be used to quantify the selectivity and solvent power of ILs (Ge, Xiong and Wang 2009; Sobota, Dohnal and Vrbka 2009; Domańska and Królikowska 2010; Marciniak 2010). This can be expected for mole fractions of 10^{-7} to 10^{-4} (usually 0.1 μL) of the solute.

Activity coefficients at infinite dilution are used to obtain other thermodynamic solution properties such as selectivity and excess molar enthalpy at infinite dilution. Selectivity values are used as a means of pre-screening different solvents for extractive distillation for a large range of solutes that have close boiling components (Schult *et al.* 2001). Thermophysical data of activity coefficients at infinite dilution is essential for the determination of the selectivity of the solvent for one solute over another and the capacity of the solvent for dissolution of a particular solute over another in a separation purposes.

The partial molar excess enthalpy at infinite dilution is an important thermodynamic property due to its relation to other functions of interest. For instance, knowing the excess partial molar enthalpy at infinite dilution, it is possible to calculate the temperature reliance of activity coefficient at infinite dilution from Gibbs-Helmholtz equation (Checoni and Francesconi 2006). This also works the other way round, i.e. activity coefficients at infinite dilution is utilized to compute the excess molar enthalpy at infinite dilution.

In this research gas liquid chromatography (GLC) was utilized to establish activity coefficients at infinite dilution. Activity coefficients at infinite dilution of organic solutes in the ionic liquid 1-butyl-3-methylimidazolium hydrogen sulfate were determined. The activity coefficients at infinite were measured by gas liquid chromatography from T = (313.15 to 333.15) K. The activity coefficients at infinite dilution values was utilized to calculate the selectivity values for different types of separation problems.

2.12 A: Literature Review: Excess Molar Volumes, Change in Refractive index and Change in Isentropic Compressibility of Binary Mixtures

Mokhtarani *et al.* (2009) studied density and viscosity of 1-butyl-3-methylimidazolium nitrate with ethanol, or 1-propanol, or 1- butanol at numerous temperatures. Experimental results reveal that the change of the density with respect to temperature is linear for both pure and binary systems. Experimentally determined excess molar volumes reveal negative deviation from the ideal solution. Therefore, experimental values of excess molar volumes and viscosity deviations were in good agreement with those computed from the third order Redlich-Kister equation.

Singh *et al.* (2014) measured density and speed of sound measurements of imidazolium-based ionic liquids with acetonitrile at different temperatures. The thermodynamically significant parameters such excess molar volumes, isentropic compressibility and the change in isentropic compressibility have been computed from the density and the speed of sound to check the intermolecular interactions that arise in the mixture. To examine the resultant parameters, the Redlich- Kister polynomial equation was utilized to fit excess molar volumes and change in isentropic compressibility and offers a worthy explanation of both systems.

Negative deviations were detected for both V_m^E and $\Delta \kappa_S$ for studied systems for all

temperatures, this point to a strong interaction amongst [EMIM][$EtSO_4$] or [BMIM][SCN] and acetonitrile. The $\rho, u,$ V_m^E and $\Delta\kappa_S$ show a detrimental effect while κ_S shows an incremental effect with temperature.

Strechan *et al.* (2008) determined thermochemical properties of 1-butyl-3 methylimidazolium nitrate. Heat capacity for 1-butyl-3-methylimidazolium nitrate [C_4MIM][NO_3] in the temperature range (5–370) K has been measured by adiabatic calorimetry. Temperatures and enthalpies of its phase transitions have been established. Thermodynamic functions have been computed for the crystalline and the liquid states. Phase transition temperatures for a group of nitrate salts have been compared. Enthalpy of combustion and enthalpy of formation for crystalline [C_4MIM][NO_3] have been established utilizing a static-bomb isoperibolic combustion calorimeter. A correlation scheme for the estimation of Cp of ionic liquids has been developed.

Huo, Xia and Ma (2007) studied densities of ionic liquids, 1-butyl-3-methylimidazolium hexafluorophosphate, and 1-butyl-3-methylimidazolium tetrafluoroborate, with benzene, acetonitrile and 1-propanol at T = (293.15 to 343.15) K. Density measurements were employed to compute the excess molar volumes. The excess molar volumes have been fitted to the Redlich-Kister equation. Excess molar volumes values are negative for all the mixtures over the miscible range and become more negative with increasing temperature.

Zafarani-Moattar and Shekaari (2006) reported experimental density for 1-butyl-3-methylimidazolium hexaflourophosphate [BMIM][PF_6] + acetonitrile or methanol at T = (298.15 to 318.15) K. V_m^E values were calculated from the experimental values of [BMIM][PF_6] + acetonitrile or methanol. The V_m^E values were negative for all the systems showing strong intermolecular interaction and packing effect.

Taib and Murugesan (2011) reported experimental data of 1-butyl-3-methylimidazolium tetraflouroborate ([BMIM][BF_4]) + water or monoethanolamine at a temperature range of (293.15 to 353.15) K over the entire mole fraction range. Excess molar volumes were computed from the experimental density and correlated utilizing Redlich-Kister polynomial equation. The densities of both systems decreased with increasing temperature and decreasing mole fraction of IL. At T = 298.15 K the $V_{m,\min}^{E}$ for ([BMIM][BF_4]+ water) at x_1= 0.8988 is 0.13027 $cm^3 \cdot mol^{-1}$, for ([BMIM][BF_4] + monoethanolamine) x_1 = 0.9002 is 0.82453 $cm^3 \cdot mol^{-1}$. The values of excess molar volumes were positive for both binary mixtures. This implies that there is a volume expansion on mixing and also the interaction between unlike molecules are weaker and insufficient to cause volume contraction.

Fan *et al.* (2009) reported experimental density for ([BMIM][PF_6] + methyl methacrylate) (MMA) over the whole concentration range in the temperature range from (283.15 to 353.15) K. The excess molar volumes were computed from the experimental density and Redlich-Kister polynomial equation was applied successfully. At 298.15 K the $V_{m,\min}^{E}$ for ([BMIM][PF_6] + MMA) at x_1 = 0.0986 is -0.4682 $cm^3 \cdot mol^{-1}$, indicating strong intermolecular interaction and packing effect.

Gadžurić *et al.* (2014) reported experimental density for 1-butyl-3-methylimidazolium tri-(pentaflouroethyl)triflourophosphate ([BMIM][FAP]) + n-methyl-formamide (NMF) or N-ethylformamide (NEF) or n,n-dimethylacetamide (DMA). Excess molar volumes were computed from the experimental densities and reported in the temperature range from (293.15 to 323.15) K and at atmospheric pressure (0.1MPa) across the entire mole composition range. The results were positive for both systems. This indicates that there is repulsive forces existing between the component which creates an increase in the mixture overall volume.

Zafarani-Moattar and Majdan-Cegincara (2007) measured experimental density for ([BMIM][PF_6]) + tetrahydrofuran (THF) or dimethylsulfoxide (DMSO) or methanol (MeOH)

or acetonitrile (MeCN) at T = 298 K. Excess molar volumes were computed from the experimental density, V_m^E for ([BMIM][PF_6] + tetrahydrofuran) (THF) is more negative than [BMIM][PF_6] + dimethylsulfoxide (DMSO) system. This indicates that more interaction occurred when IL and organic molecular liquids were mixed.

Pereiro and Rodríguez (2007) measured experimental density for ([BMIM][PF_6] + 2-propanol or 2-butanone or ethylacetate) binary systems at T = (293.15 to 303.15) K. At T = 298.15 K the $V_{m,\min}^E$ for ([BMIM][PF_6] + 2-butanone) at x_1 = 0.9491 is -0.165 $cm^3 \cdot mol^{-1}$, for ([BMIM][PF_6] + ethylacetate) x_1 = 0.9499 is -0.229 $cm^3 \cdot mol^{-1}$, and for ([BMIM][PF_6] + 2-propanol) x_1 = 0.9542 is -0.027 $cm^3 \cdot mol^{-1}$. The larger negative value for ([BMIM][PF_6] + ethylacetate) system indicates stronger intermolecular interaction and packing effect than ([BMIM][PF_6] + 2-butanone) and ([BMIM][PF_6] + 2-propanol).

Dikio *et al.* (2012) analysed density, dynamic viscosity and derived properties of binary mixtures of methanol, ethanol, *n*-propanol, and *n*-butanol with pyridine at T = (293.15, 303.15, 313.15 and 323.15) K. This study reported the intermolecular interaction among the components of the binary mixtures pointing to possible hydrogen bond formation of the type N···H─O between unlike molecules approving hydrogen bonding formation between pyridine and the alcohol mixtures. The deviations in viscosity, excess molar volume and excess Gibbs free energy of activation of viscous flow were correlated with Redlich-Kister polynomial equation.

Ali, Tariq and Nabi (2008) determined a study on density, viscosity, refractive index and speed of sound in binary mixtures of pyridine and 1-alkanols (C_6, C_7, C_8, and C_{10}) at T = 303.15 K and atmospheric pressure. The negative deviations in excess molar volumes, isentropic compressibility, and viscosity command the occurrence of strong interactions amongst pyridine and 1-alkanol molecules and that the strength of interaction follows the order of 1-hexanol > 1-heptanol > 1-octanol > 1-decanol. The positive molar refraction was

found to vary linearly with the chain length of 1-alkanols over the entire composition range. The noted decrease in the magnitude of molar refraction shows the strength of interactions between the component molecules increases in mixture. The derived parameter from thermodynamic properties which density, viscosity, refractive index and speed of sound were in good agreement with each other.

Nayak *et al.* (2003) reported density, viscosity, refractive index and speed of sound in the binary mixtures of (tri-n-butylamine + trimethylamine or tetrahydrofuran or tetradecane or tetrachloroethylene or pyridine or trichloroethylene) at T = (298.15, 303.15, and 308.15) K. The observed outcomes have been deliberated in relations of mixing behavior between the molecules. The measured properties have been fitted to a polynomial equation to derive the coefficients and approximate the standard errors.

Chen *et al.* (2015) reported a study on density, viscosity, the speed of sound, excess property and bulk modulus of binary mixtures of γ- butyrolactone (γ-GBL) + acetonitrile (ACN) or dimethyl carbonate (DMC) or tetrahydrofuran (THF) at temperatures (293.15 to 333.15) K. Excess molar volumes and excess viscosity of binary mixture solvents were computed and fitted with the Redlich-Kister equation. From the parameters, ideas about the actual interactions between the mixing components are mainly weak forces between different molecules (dipole-dipole interaction and dispersion force).

Table 2.4 shows the qualitative literature of V_m^E data for IL with common cation or anion or organic solute.

Table 2.4: Qualitative V_m^E data for the IL with common cation or anion or organic solute obtained from the literature

Author	Systems	V_m^E
(Zafarani-Moattar and Shekaari 2006)	([BMIM][PF_6] + acetonitrile or methanol)	negative
(Singh *et al.* 2014)	([BMIM][SCN] + acetonitrile)	negative
(Huo, Xia and Ma 2007)	([BMIM][PF_6] + benzene or acetonitrile or 1-propanol)	negative
(Mokhtarani *et al.* 2009)	([BMIM][NO_3] + ethanol or 1-propanol or 1- butanol)	negative
(Fan *et al.* 2009)	([BMIM][PF_6] + methyl methacrylate)	negative
(Pereiro and Rodríguez 2007)	([BMIM][PF_6] + 2-propanol or 2-butanone or ethylacetate)	negative
(Taib and Murugesan 2011)	([BMIM][BF_4] + water or monoethanolamine)	positive
(Gadžurić *et al.* 2014)	([BMIM][FAP] + N-methyl-formamide (NMF) or N-ethylformamide (NEF) or N,N-dimethylacetamide (DMA))	positive
(Zafarani-Moattar and Majdan-Cegincara 2007)	([BMIM][PF_6] + tetrahydrofuran (THF) or dimethylsulfoxide (DMSO) or methanol (MeOH) or acetonitrile (MeCN))	negative
(Zhou, Wang and Chen	([BMIM][BF_4] + water)	positive

2006)		
(Iloukhani and Almasi 2009)	(Acetonitrile + 2-propanol or 2-butanol or 2-pentanol or 2-hexanol or 2-heptanol)	positive
(Chen *et al.* 2015)	γ- butyrolactone (γ-GBL) or acetonitrile (ACN) or dimethyl carbonate (DMC) or tetrahydrofuran (THF)	negative
(Aznarez and Postigo 1998)	(Acetonitrile + methanol to decanol)	Positive and negative
(Aralaguppi, Jadar and Aminabhavi 1996)	(2-ethoxyethanol + dioxane or acetonitrile or tetrahydrofuran)	positive
(Alonso *et al.* 2011)	(2-pentanone + aniline or N-methylaniline or pyridine)	negative
(Ali, Tariq and Nabi 2008)	(Pyridine + 1-hexanol or 1-heptanol or 1-octanol or 1-decanol)	negative
(Nayak *et al.* 2003)	(Tri-n-butylamine + triethyamine or tetrahydrofuran or tetradecane or tetrachloroethylene or pyridine)	positive and negative

Table 2.5 shows the qualitative literature of κ_s data for the IL with common cation or anion or organic solute.

Table 2.5: Qualitative κ_s data for the IL with common cation or anion or organic solute obtained from the literature.

Author	Sytems	κ_s
(Singh *et al.* 2014)	([BMIM][SCN] + acetonitrile)	positive
(Saini *et al.* 2011)	(Tetrahydropyran + pyridine or picoline)	positive
(Pereiro and Rodríguez 2007)	([BMIM][PF_6] + 2-propanol or 2-butanone or ethylacetate)	positive
(Zafarani-Moattar and Majdan-Cegincara 2007)	([BMIM][PF_6] + tetrahydrofuran (THF) or dimethylsulfoxide (DMSO) or methanol (MeOH) or acetonitrile (MeCN))	positive

Singh *et al.* (2014) reported experimental data of pure components for speed of sound as well as the binary mixture ([BMIM][SCN] + acetonitrile) across the composition of their range at T = (293.15, 298.15, 303.15, 308.15, and 313.15) K. The $\kappa_{s,\min}$ at T = 298.15 at x_1 = is 30 Pa^{-1} for ([BMIM][SCN] + acetonitrile). The $\kappa_{s,\min}$ value for ([BMIM][SCN] + acetonitrile) is positive and this indicates that components of binary system is more compressible.

Zafarani-Moattar and Majdan-Cegincara (2007) reported pure components as well as an isentropic compressibility for binary mixtures of 1-n-butyl-3-methylimidazolium hexaflourophosphate ([BMIM][PF_6]) with THF, DMSO, methanol and acetonitrile as a function of composition under atmospheric pressure at T = 298.15 K. The values were positive for all binary mixtures indicating that the highly compressible mixtures of binary system are more compressible.

Pereiro and Rodríguez (2007) reported speed of sound of the binary mixtures of [BMIM][PF_6] + 2-propanol or 2-butanone or ethylacetate at T = (293.15 to 303.15) K. The isentropic compressibility of these binary mixtures were calculated. The $\kappa_{s,\min}$ value for ([BMIM][PF_6] + 2-propanol) at T = 298 K at x_1 = 1.0000 is 358 TPa^{-1}, ([BMIM][PF_6] + 2-butanone) T = 298 K at x_1 = 1.0000 is 351 TPa^{-1}, ([BMIM][PF_6] + ethylacetate) T = 298 K at x_1 = 1.0000 is 351 TPa^{-1}. The $\kappa_{s,\min}$ results indicate that the components of these binary systems are more compressible.

Saini *et al.* (2011) reported speed of sound and density of tetrahydropyran + pyridine or picoline binary mixtures at T = 298.15 K and 308.15 K. The results were used to calculate isentropic compressibility. The $\kappa_{s,\min}$ value for (tetrahydropyran + pyridine) at T = 298 K, x_1 = 0.0427 is 515.24 TPa^{-1}, (tetrahydropyran + picoline) T = 298 K at x_1 = 0.0367 is 562.71 TPa^{-1}. The results were positive and indicate that the components were more compressible.

Table 2.6 below shows Δn data for (ILs + organic solvent) with common anion or common organic solute obtained from the literature.

Table 2.6: Qualitative Δn data for the IL with common cation or anion or organic solute obtained from the literature

Author	Sytems	Δn
(Iloukhani and Almasi 2009)	(Acetonitrile + 2-propanol or 2-pentanol or 2-hexanol or 2-heptanol)	positive
(Iglesias-Otero *et al.* 2008)	([BMIM][PF_4]or [BMIM][$MeSO_4$] + ethanol or nitromethane or ethylene gycol or 1,3-dichloropropane)	positive
(Pereiro and Rodríguez 2007)	([BMIM][PF_6] + 2-propanol or 2-butanone or ethylacetate)	positive

Iloukhani and Almasi (2009) measured density and refractive indices of acetonitrile with 2-propanol, or 2-butanol, or 2-hexanol, and 2- heptanol as a function of composition at T = (298.15, 298.15, 303.15, 308.15) K and ambient pressure. At T = 298.15 K, the $\Delta n_{,\max}$ at x_1 = 0.4768 for (acetonitrile + 2-propanol) is 0.003, at x_1 = 0.5382 for (acetonitrile + 2-butanol) is 0.007, at x_1 = 0.53898 for (acetonitrile + 2-hexanol) is 0.013, at x_1 = 0.5436 for (acetonitrile + 2-heptanol) is 0.022.

Pereiro and Rodríguez (2007) measured density of ([BMIM][PF_6] + 2-propanol or 2-butanone or ethylacetate) at T = (298.15 to 303.15) K. The refractive indices of ([BMIM][PF_6] + 2-propanol or 2-butanone or ethylacetate) were computed from the experimental density. At T = 298.15 K, The $\Delta n_{,\max}$ at x_1 = 0.8175 for([BMIM][PF_6] + 2-propanol) is 0.0038, at x_1 = 0.7085 for ([BMIM][PF_6] + 2-butanone) is 0.0079, at x_1 = 0.7000 for ([BMIM][PF_6] + ethylacetate) is 0.0089.

Iglesias-Otero *et al.* (2008) measured experimental density of ([BMIM][BF_4] or [BMIM][$MeSO_4$] with ethanol or ethylene glycol or nitromethane or 1,3-dichloropropane) at atmospheric pressure and T = 298.15 K. The data was employed to compute refractive index deviation. Δn was positive in the whole range compositions and temperature.

2.13 B: Literature review: Activity Coefficients at Infinite Dilution

Ge *et al.* (2014) determined activity coefficients at infinite dilution of organic solutes in the ionic liquid 1-butyl-3-methyimidazolium methyl sulfate ([BMIM][CH_3SO_4]) through GLC measurements. The activity coefficient and the (gas + liquid) partition coefficients have been calculated for a series of polar and nonpolar organic solutes at T = (313.15 to 363.15) K. The results of the LFER prediction of log K_L of various solutes indicate in the IL and disclose molecular interactions operating amongst the IL and the discrete solutes. The highest selectivity value (24.05) was obtained for the separation of heptane/benzene.

Letcher *et al.* (2005a) determined activity coefficients at infinite dilution for different solutes (alkanes, alk-1-enes, alk-1-ynes, cycloalkanes, aromatic hydrocarbons, carbotetrachloride and methanol in the IL 1-butyl-3-methyl-imidazolium 2-(2-methoxyethoxy) ethyl sulfate using GLC at T = (298.15, 303.15, and 308.15) K. The results were used to estimate the solvent potential for the hexane/benzene separation from computed selectivity. The selectivity was 39.7. The data was compared to the literature in trying to comprehend the outcome nature of cation and anion has on solute-solvent interactions. The partial molar excess enthalpies at infinite dilution values, $\Delta H_1^{E,\infty}$ were computed from the experimental γ_{13}^{∞} values across the temperature range.

Kozlova *et al.* (2009) measured activity coefficient at infinite dilution of hydrocarbons, alkylbenzenes, and alcohols in the paramagnectic ionic liquid 1-butyl-3-methyl-imidazolium

tetrachloridoferrate (III) using gas liquid chromatography. The measurement were done at diverse temperatures amongst (305 and 403) K. The $\Delta H_1^{E,\infty}$ were derived from the temperature dependence experimental γ_{13}^{∞}. The $\Delta H_1^{E,\infty}$ for alkanes, alkenes, alcohols, butyl benzene and pentyl benzene was endothermic and alkylbenzene was exothermic.

Domańska and Laskowska (2009) determined activity coefficients at infinite dilution of aliphatic and aromatic hydrocarbons, alcohols, thiophene, tetrahydrofuran, MTBE, and water in ionic liquid 1-butyl-3-methyl-imidazolium thiocyanate ([BMIM][SCN]) using GLC. The measurements were done at various temperatures from 298 K to 368 K. The ratio for hexane/benzene, cyclohexane/benzene, hexane/thiophene, and other separations problems were computed from γ_{13}^{∞}. These selectivities were compared with other ionic liquids, sulfolane, and N-methyl-2pyrrolidinone, cited from current literature. This research confirms that the selected ionic liquid have the potential to separate different organic compounds with the highest selectivity, ever printed which was 106.1 for hexane/ benzene. The results reveals that IL ([BMIM][SCN]) has the potential to separate organic compounds and can be used in the desulphurization process.

Olivier *et al.* (2011) measured activity coefficients at infinite dilution of organic solutes in the ionic liquid 1-butyl-3-methyl-imidazolium hexaflouroantimonate [BMIM][SbF_6] using GLC at T = (313.15, 323.15, 333.15) K. The separation problems which is hexane/benzene, and methanol/benzene systems were compared to the temperature for related ILs, as well to the results on industrial molecular solvents. [BMIM][SbF_6] is noticeable to be a rational solvent for separation of aromatics from aliphatics. The highest selectivity value (62.1) was obtained for the separation of heptane/benzene.

Martins *et al.* (2015) determined activity coefficients at infinite dilution of organic solutes and water in three ionic liquids with common cation 1-butyl-3-methylimidazolium and the

polar anions $[Cl]^-$, $[CH_3SO_3]^-$, $[(CH_3)_2PO_4]^-$. The measurements were done using GLC at four temperatures in the range (358.15 to388.15) K for alcohols, and T = (398.15 – 428.15) K for organic solutes. The organic solutes includes alkane, cycloalkanes, alkenes,cycloalkenes, alkynes, ketones, ethers, cyclic ethers, aromatic hydrocarbons, esters, butylaldehyde, acetonitrile, pyridine, 1-nitropropane and thiophene. The partial molar excess Gibbs free energy, $G_m^{E\infty}$, enthalpy, $H_m^{E\infty}$, and entropy, $S_m^{E\infty}$ at infinite dilution were computed from γ_{13}^{∞}. The data were estimated to provide more knowledge about the interactions between the solutes and ILs. The ratio at infinite dilution for some separation problems such as octane/benzene, cyclohexane/benzene, cyclohexane/thiophene were calculated from γ_{13}^{∞}. The selctivities data were compared from N-methyl-2-pyrrolidinone (NMP), sulfolane, and other ILs with common cation or anion studied. From the selectivities and capacities obtained, the data revealed that ILs have the potential to replace conventional entrainers applied in separation process of aliphatic/aromatic hydrocarbons. The highest selectivity value (73.32) was obtained for the separation of octane/benzene.

Singh *et al.* (2016) determined an application of 1-butyl-3-methylimidazolium bis(triflouromethylsulfonyl) imide ionic liquids for the different types of separation problems.

The separation of alkane/aromatic, alkane/alk-1-ene, cyclohexane/aromatic, and water/alkan-1-ol were done using GLC at T = (323.15, 333.15, 343.15, 353.15, and 363.15) K. The separation potential of IL were compared with previous studied ILs and the industrial solvents such as N-methyl-2-pyrrolidinone (NMP), sulfolane, and N-formylmorpholine (NFM). The highest selectivity value (43.99) was obtained for the separation heptane/benzene

Domańska, Wlazło and Karpińska (2016) measured activity coefficients at infinite dilution of organic solvents and water in 1-butyl-3-methyl-imidazolium dicynamide [BMIM][DCA]. A literature review of hexane/hex-1-ene separation reports the experimental values for 64

solutes includes alkanes, cycloalkanes, alkenes, alkynes, aromatic hydrocarbons, alcohols, water, ethers, ketones, acetonitrile, pyridine, 1-nitropropane, thiophene, and esters in [BMIM][DCA]. All of these measurements were done using GLC at six temperatures over the range of (318.15 – 368.15) K. The results revealed that the proposed ILs may be utilized as an optional solvent in separation of alkenes from alkanes. The highest selectivity value (2.31) was obtained for the separation problem of hexane/hex-1-ene.

Letcher *et al.* (2005b) did analysis on determination of activity coefficients at infinite dilution of solutes in the ionic liquid 1-butyl-3-methlimidazolium octyl sulfate using GLC at T = (298.15, 313.15, 328.15) K. The results of γ_{13}^{∞} and $\Delta H_1^{E,\infty}$ obtained suggest not only the interaction between the solute and ionic liquid as hydrogen bonding, ion-induced dipole interaction but also the "free volume" and the interstitial effects in the solute and ionic liquid that may be expected. The highest selectivity value (5.1) was obtained for the separation of hexane/benzene.

Based on the on the literature survey the highest selectivity (106.1) for the common cation was obtained separation of hexane/benzene in [BMIM][SCN] (Domańska and Laskowska 2009).

Chapter 3

EXPERIMENTAL METHODS AND THEORETICAL FRAMEWORK

3.1 Excess Molar Volumes

3.1.1 Introduction

The excess molar volume is the difference between the actual molar volume and the ideal molar volume of a mixture (Shana'a and Canfield 1968) and is given by equation (3.1):

$$V_m^E = V_{mixture} - \sum_{i=1}^{N} x_i V_i^0 \tag{3.1}$$

V_m^E is the excess molar volume , x_i is the mole fraction of component i, and V_i^o the molar volume of the pure component *i* at the identical temperature and pressure as the mixture.

For a binary mixture the excess molar volume is given by the following equation:

$$V_m^E = V_{mixture} - (x_1 V_1^0 + x_2 V_2^0) \tag{3.2}$$

The change in volume on mixing of binary liquid mixtures, V_m^E , at constant pressure, is of concern to thermo-physical chemists and chemical engineers for two main reasons Battino (1971):

(i) Experiments are relatively easy to perform with great precision.

(ii) Serve as the sensitive indicator to the accuracy of theories of solution

V_m^E of a binary liquid mixture basically depends on (Patil *et al.* 2011)

(i) Its local structure

(ii) Stated in reference to the packing density

(iii) Free volume or radial distribution function

The volume change in a binary component mixture can be attributed to a number of processes: Ghafeli and Almasi (2016)

A) The loss of intermolecular interactions of the first component and second component that have a positive effect on volume.

B) The effect that the intermolecular forces between the species which leads to a reduction in the volume of the mixture

C) The cumulative effect caused by differences in size and shape of components. The effect may have negative or positive impact on the discussed solution.

The formation of an ideal binary liquid mixture occurs with no change in volume. However, because of molecular interactions amongst components of binary liquid mixtures in a real liquid mixture, this results in an increase or decrease in volume. The criterion and measure of molecular interaction can be based on this increase or decrease of the volume when mixing the liquids. The exhibited change in volume for the binary mixture is computed by using equation 3.1 (Patil *et al.* 2011).

3.1.2 Experimental Procedures for Measurement of Excess Molar Volumes

Volume changes for binary mixtures, V_m^E can be determined in one of two ways (Redhi 2003; Sibiya 2009):

(i) Direct measurements – by mixing the liquids and deducing the volume change (dilatometric method)

(ii) Indirect measurements by measuring the density of the mixture and the density of pure liquids (densitometer or hydrometer)

3.1.3 Direct Method

The direct method measures the change in volume which arises when the liquids are mixed. Direct methods of measurement of V_m^E, include batch dilatometer and continuous dilution dilatometer. The batch dilatometer is characterized by the determination of a single data point per loading of the apparatus, and continuous dilatometer is characterized by the identification of many data points per loading of the appliance. Apparatus for the direct measurement of volume change were designed along two fundamental lines: (a) one composition per loading of the apparatus at a single temperature or batch dilatometers; and (b) a number of compositions per loading at a single temperature or continuous dilution dilatometers (Handa and Benson 1979; Redhi 2003; Ghafeli and Almasi 2016).

3.1.4 Batch Dilatometer

The illustration of a batch dilatometer is presented in Figure 3.1. A known mass of pure liquids is used to fill the dilatometer which are separated from each other by mercury. The mercury height inside the calibrated graduated column is recorded. To mix the liquids, the dilatometer is rotated, and the change in volume is shown by the change in the mercury height inside the calibrated capillary. V_m^E, is calculated from the change in volume and the masses of the components. It was stated that a precision of $\pm$ 0.003 $cm^3 \cdot mol^{-1}$ in V_m^E, might be realised across the temperature range of (280 to 350) K when this technique is used. A drawback of this device lies in the difficulty in filling the dilatometer which is usually realized by means of a narrow needle. The main cause of error in this method is the determination of the composition as it is not possible to weigh the dilatometer since it

comprises mercury. This causes huge errors in the measured mass. The error related to taking a difference to great masses is usually significantly high (Keyes and Hildebrand 1917; Redhi 2003).

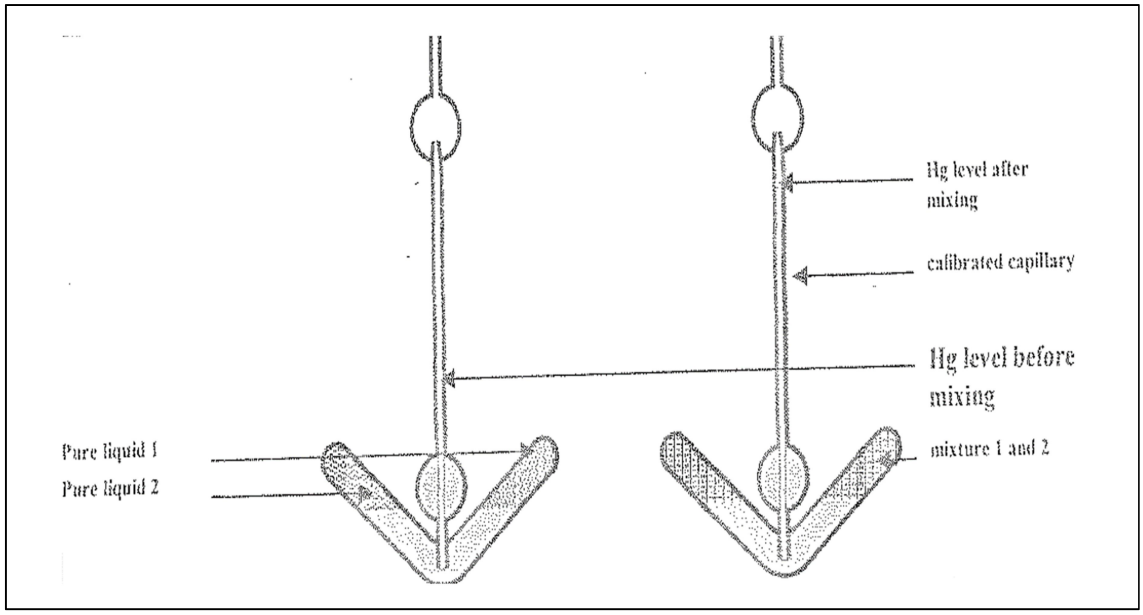

Figure 3.1: Schematic representation of a characteristic batch dilatometer (Redhi 2003; Sibiya 2009)

3.1.5 Continuous Dilatometer

Continuous dilatometer technique consumes less time and generates more data per loading, making it more popular than the batch technique. The method of operation comprises the successive addition of one liquid into the reservoir, which have the other liquid and noticing the change in volume that accompanies the addition. The instrument of Kumaran and McGlashan (1977) is considered an improvement on the one made by Bottomley and Scott (1974) since it is easier to load. Kumaran and McGlashan (1977) reported a precision of 0.0003 $cm^3 \cdot mol^{-1}$ in V_m^E, for their apparatus.

Figure 3.2 shows a schematic representation of a continuous dilatometer. To perform a measurement the burette (e) is filled with one of the pure liquids and the bulb (d) with the

other pure liquid. When the dilatometer is slanted, some of the displacement of mercury into the burette through a capillary (c) and collects at the bottom of the burette. The displacing of mercury pushes some of the pure liquid from the burette into the bulb through the higher capillary (b). After mixing the change in volume is registered as a change in the level of the mercury in the calibrated capillary (a). The quantity of pure liquid displaced is deduced from the height of the mercury in the burette. Since mercury is used, a capillary pressure effect is a possibility, and the compressibility of mercury has to be taken into account when determining the excess molar volume.

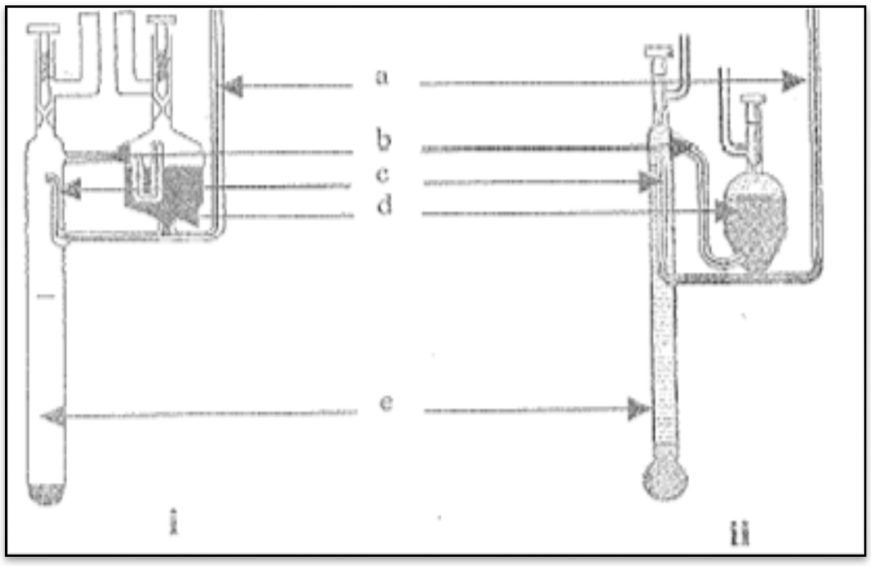

Figure 3.2: Schematic representation of a continuous dilatometer (i) design of Bottomley and Scott (1974) (ii) Kumaran and McGlashan (1977) a; calibrated capillary from which the volume change is determined, b; liquid capillary, c; mercury capillary, d; bulb that contains mercury, e; burette liquid 2**.** (Bottomley and Scott 1974; Kumaran and McGlashan 1977; Sibiya 2009; Singh 2013)

3.1.6 Indirect Method

Different methods were used to determine densities of liquids namely, pycnometer, magnetic float densitometer, and densitometer. The method is very simple.

3.1.7 Pycnometers

It is a device used to determine the density of the liquid. A single-arm pycnometer, showed in Figure 3.3, can be used to obtain 0.00001 $g \cdot cm^{-3}$ precision in density measurements. The bulb has an 11 cm^3 capacity and the 1 mm internal diameter precision capillary has 11 lines lightly etched around the stems, and spaced 1 mm apart. The bulb is filled using a hypodermic syringe and cannula. Corrections for buoyancy and vapor space are feasibly applied.

When determining densities using this technique, it is important to be able also to ascertain the composition of the mixtures with precision. However, careful measurements using this method can provide very precise density values. The pycnometer centred on the design of Wood and Brusie (1943) is shown in Figure 3.3.

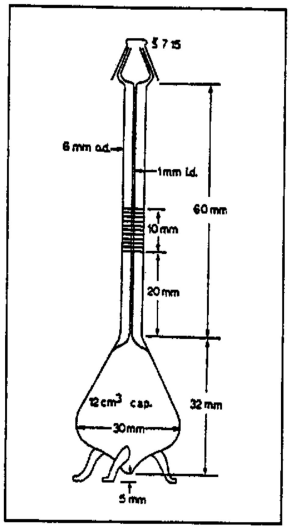

Figure 3.3: Schematic representation of a pycnometer based on the design of Wood and Brusie (1943)

3.1.8 Magnetic Float Densimeters

The operation method of a magnetic float densimeter depends on the determination of the height of a magnetic float in a liquid mixture. The height of the magnetic float in the presence of a recognized magnetic field is a function of the buoyancy of the fluid. The buoyancy of the liquid is linked to the density of the liquid. An instrument with a precision 3×10^{-6} g·cm^{-3} has been reported and this transforms to an accuracy of 0.0008 cm^{3}·mol^{-1} (Franks and Smith 1967) and is shown in Figure 3.4.

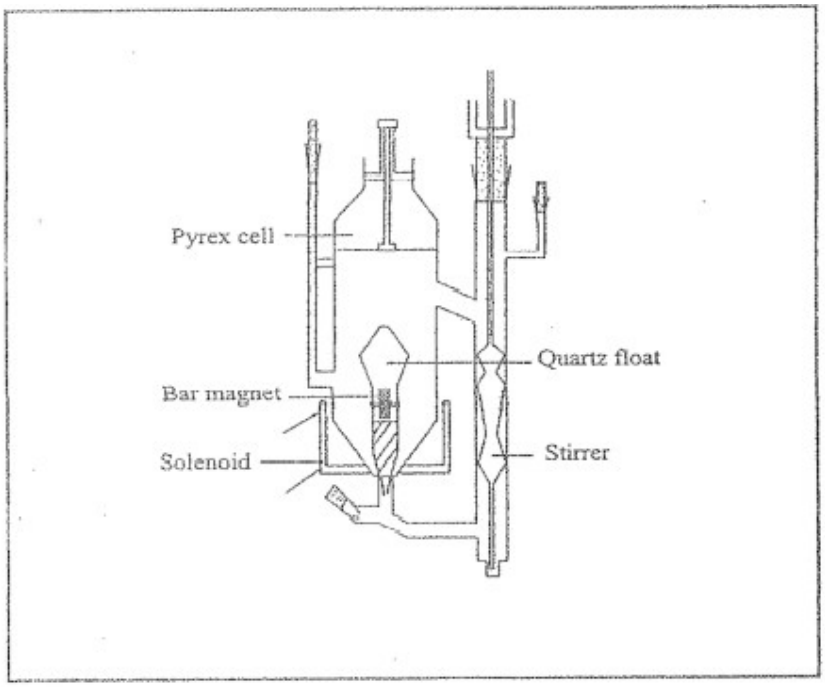

Figure 3.4: Schematic illustration of a magnetic float densimeter (Franks and Smith 1967).

3.1.9 Mechanical Oscillating Densitometer

Mechanical oscillating (vibrating tube) densimeters joined to digital output displays are extensively applied in the chemical industry and in research laboratories to measure densities

of pure liquids and liquid mixtures. The frequency of the vibrating tube having a liquid that is exposed to a constant electric stimulation is linked to the density of the liquid. According to (Handa and Benson 1979), the frequency of vibration of an undamped oscillator (e.g. tube containing a liquid) coupled by a spring with a constant elasticity, *c*, is linked to the mass of the oscillator and the liquid, *M*, by the following equation:

$$2\pi\nu = \left[\frac{c}{M}\right]^{\frac{1}{2}} \tag{3.3}$$

In which *M* is the mass of the contents of the tube and, c, is the constant elasticity. Since the oscillator is a hollow tube, if a liquid with density, ρ, fills the hollow tube occupying a volume *V*, then:

$$M = M_o + \rho V \tag{3.4}$$

M_o is the mass of the empty oscillator.

Substitution of equation (3.3) into equation (3.4) and solving for ρ, :

$$\rho = -\frac{M_o}{V} + \left[\frac{c}{4\pi^2}\right]\left[\frac{1}{V^2}\right] \tag{3.5}$$

Where $A = -\frac{M_o}{V}$ and $B = \left[\frac{c}{4\pi^2}\right]$ are constants. Consequently, this validates the equation that follows:

$$\rho = A + B\left(\frac{1}{v}\right)^2 \tag{3.6}$$

The constants *A* and *B* are characteristics of the oscillator, *v* is the volume, τ is the period, and density is given by the symbol ρ, hence:

$$\rho = A + B\left(\frac{1}{v}\right)^2 \tag{3.7}$$

In which *A* and *B* are determined by calibration. This involves determining the period for two pure substances of known density.

As densities are measured in connection to a reference material:

$$\rho - \rho_0 = B\left(\tau - \tau_0^2\right) \tag{3.8}$$

Commercially obtainable vibrating tube densimeters with a precision of 0.001 % are in existence. This indicates an accuracy of 0.003 $cm^3 \cdot mol^{-1}$ in the measurement of V_m^E (Singh 2013).

In this work, an Anton Paar DSA 5000 M instrument was used to measure the density and speed of sound the densities of mixtures at different temperatures.

The density, ρ, of a sample, is defined as the mass, (m) divided by the volume, (v):

$$\rho = \frac{m}{v} \tag{3.9}$$

Density is used to calculate excess molar volume.

3.2 Speed of Sound and Isentropic Compressibility

The speed of sound is important in some technical applications such as flow measurements, and production monitoring. It employed in the development of an equation of state that describes the fluid and consequently can be used to derive several thermo-physical properties, such as the reduced isobaric thermal expansion coefficient, isentropic and isothermal compressibility, bulk modulus, thermal pressure coefficient, isobaric and isochoric heat capacities (Fortin *et al.* 2013).

Measurement of the speed of sound, u, in fluids is a great source of information (e.g. to sense slight variations in gas composition or the effects of slight concentrations variations) about the thermo-physical properties of chemical constituents and their mixtures (Azevedo *et al.* 2004).

The speed of sound and density, are employed in computation of isentropic compressibility by means of the Newton-Laplace equation:

$$\kappa_s = \frac{1}{\rho u^2} \tag{3.10}$$

3.2.1 Ultrasonic Interferometer

It is the device used to deduce the high velocity in liquids with great accuracy, and it comprises of the following:

(i) High-frequency generator that is intended to energize the quartz plate fixed at the base of the measuring cell at its resonant frequency to generate ultrasonic waves in the experimental liquid in the measuring cell.

(ii) A micro-ammeter used to observe the variations in the current and two controls for regulating the sensitivity and preliminary tunings of micro-ammeter are present on the high-frequency generator.

(iii) Measuring cell which is a particularly designed double-walled cell for keeping the temperature of the liquid constant throughout the experiment.

(iv) A fine micro-meter screw is made available at the top, which can lower or raise the reflector plate in the cell over a set distance. It has a quartz plate fixed at the bottom.

A diagram illustrating an ultrasonic interferometer is shown in Figure 3.5.

Figure 3.5: Photograph of an Ultrasonic Interferometer M-81G.
(Taken from Instruction Manual of Mittal Enterprises Ultrasonic Interferometer for Liquids)

The principle applied during measurement of velocity, (u), is founded on the precise determination of the wavelength, (λ), in the medium. Ultrasonic waves with a known frequency (f) are generated by a quartz plate cell. A portable plate held parallel with respect to quartz plate reflects the waves. If the displacement between these plates is precisely a whole multiple of the sound wavelength, standing waves are generated in the medium. There is an electrical reaction present on the generator driving the quartz plate due to acoustic resonance, this drives the generator anode current to maximum. When the separation between the reflector and crystal is increased or decreased and the disparity is precisely one-half wavelength (λ / 2) or multiple of it, the anode current becomes maximum. From the knowledge of wavelength, (λ) , the velocity, (u), can be obtained by the relation:

$$Velocity = Wavelength \times frequency \tag{3.11}$$

3.3 Refractive Index

The refractive index, n, is a constant for a pure solvent. It can be defined as:

$$n = \frac{speed\ of\ light\ in\ material\ 2}{speed\ of\ light\ in\ material\ 1} \tag{3.12}$$

It is commonly expressed as $n_{1,2}$ and is the refractive index in material 2 in relation to material 1. The incident light is in material 1, and the refracted light is in material 2. If we let material 1 to be a vacuum then the value is referred to as absolute refractive index of material 2. Normally, the refractive index is taken to be 1 in a vacuum. For practical purposes, the refractive index of air is taken to be 1.0008 which has little impact on refraction of light occasioning the use of absolute refractive index when the incident light is in the air.

The refractive index is also expressed as the ratio of the speed of a wave (light or sound) in a reference medium to a second medium. It is most commonly used in the context of the rate of the wave of light with a vacuum as a reference medium, even though other reference media (e.g. air at a regulated pressure and temperature) have been assumed historically.

Another common definition of the refractive index is the ratio of the sine of the angle of incidence (medium 1) θ_1 and the angle of refraction of (medium 2) θ_2 and is given by (Iglesias-Otero *et al.* 2008):

$$n = \frac{\sin\theta_1}{\sin\theta_2} \tag{3.13}$$

The angles are measured perpendicular to the surface. This expression is founded on Snell's law (Iglesias-Otero *et al.* 2008). Moreover, it is comparable to the expression above if the light come in from the reference medium (a vacuum).

3.3.1 Instruments Used for the Determination of Refractive Index

3.3.1.1 Atago RX 5000 Refractometer

The RX-5000 digital refractometer gives quick and precise measurements. The RX-5000 measures refractive index with an accuracy and resolutions of ± 0.00004 and 0.00001 respectively, in four seconds. The range of the instrument is from 1.32420-1.58000. The entire data, comprising date, time, current temperature, measurement result, and temperature are electronically displayed. It is used in testing and developing medicines, chemical products, or processed foods, by examining the refractive index and concentration of materials as a supporting way of analysis. Figure 3.6 shows the photograph of an ATAGO RX 5000 Refractometer.

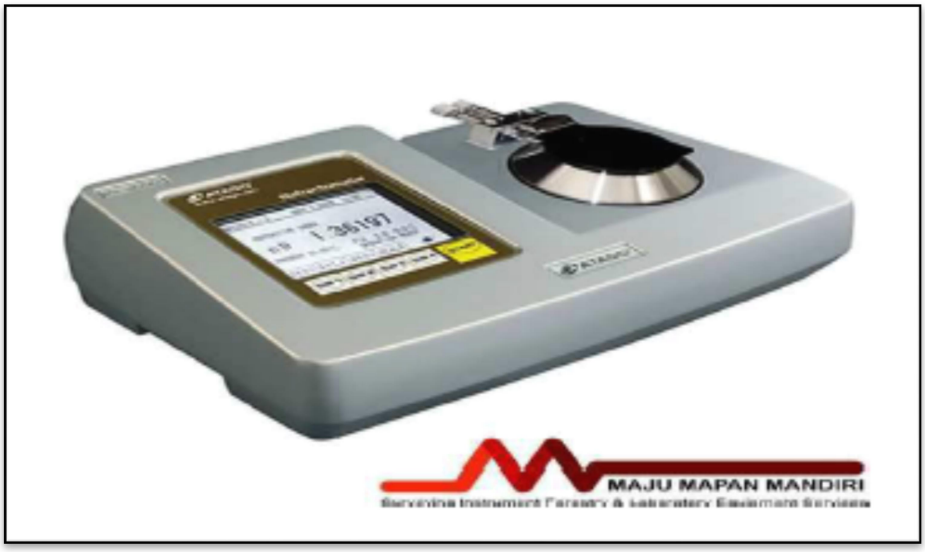

Figure 3.6: Photograph of an ATAGO RX 5000 Refractometer

3.3.1.2 Abbemat Digital Refractometer

Abbemat digital refractometers permit for quick but less accurate refractive index measurements. Normally, they are calibrated in the factory using official standards from the

Physikalisch-Technische Bundesanstalt (PTB, National Metrology Institute of Germany). Refractive index values obtained by Abbemat 300/350 are correct to ± 0.0001 n_D and for an Abbemat 500/550 ± 0.00002. Abbemat 350/550 refractometers are set up suitably with a touchscreen. The instrument has a colored liquid crystal display (LCD) screen and membrane keys which are impervious to spillage and dirt. Instrument generates a spontaneous caution if the sample is not adequate. There is a rapid wipe system which wipes the prism after every measurement. Abbemat 350/550 measures turbid, colored or opaque samples and all samples from liquids to pastes and polymers to solids. There is no humidity impact, temperature or vibrations. A varied range of scales is kept in the Abbemat for adapting the refractive index into concentrations.

Figure 3.7 is the photograph of an Abbemat Digital Refractometer 350/550

Figure 3.7: Photograph of an Abbemat Digital Refractometer 350/550.

In this work for the measurement of refractive index the instrument Anton Paar refractive index analyzer RXA 156 was used.

3.4 Correlations

3.4.1 Redlich-Kister Polynomial

The V_m^E and Δn data were fitted by the Redlich–Kister polynomial (Redlich and Kister, 1948) at the T = (298.15, 303.15, 308.15, 313.15 and 318.15) K. The Redlich–Kister equation for binary mixtures can be expressed as follows:

$$Z = x_1 x_2 \sum_{i=0}^{N} A_i (2x-1)^i \tag{3.14}$$

Where Z is V_m^E or Δn; x_1 is the mole fraction of the pyridine, acetonitrile or thiophene x_2 is the mole fraction of [BMIM][NO_3]; N is the degree of the polynomial expansion; and A_i is the Redlich–Kister parameters obtained for the system. The standard deviation, σ, was calculated using equation (3.15) below:

$$\sigma = \left(\frac{\sum_{i}^{m} (Z_{\exp} - Z_{cal})}{M-k} \right)^{1/2} \tag{3.15}$$

where Z_{exp}, Z_{cal}, are the values of the experimental and computed V_m^E or Δn and M represents the number of experimental data points and k is the number of coefficients employed in the Redlich-Kister correlation, respectively.

3.4.2 Lorentz-Lorenz Equation

The Lorentz-Lorenz relationship amongst the refractive index at zero frequency and mean molecular polarizability, α, of a nonpolar, nonmagnetic material results in the following expression (Brocos *et al.* 2003) of molar refraction R,

$$R = \left(\frac{n^2 - 1}{n^2 + 2} \right) V_m \tag{3.16}$$

where V_m is the molar volume and n is the refractive index of the mixture.

The molar refraction is also given by:

$$R = \frac{N_A \alpha}{3\varepsilon_0} \tag{3.17}$$

Where N_A is the Avogadro constant and ε_o is the permittivity of free space.

3.4.3 Prediction of Density by the Lorentz-Lorenz (L-L) Approximation

The Lorentz–Lorenz equation is applied in predicting the density ρ that is linked with the refractive index n, by:

$$\rho = \frac{\left(\frac{n^2 - 1}{n^2 + 2} \right) \left(x_1 M_1 + x_2 M_2 \right)}{\left(\frac{n_1^2 - 1}{n_1^2 + 2} \right) x_1 \frac{M_1}{\rho_1} + x_2 \left(\frac{n_2^2 - 1}{n_2^2 + 2} \right) \frac{M_2}{\rho_2}} \tag{3.18}$$

Equation (3.18) was used to predict the density of the binary mixture, ρ, hence, if ρ_1 and n_1 for the pure components, and n for the mixture, are known, the density of the mixture can be estimated.

3.4.4 Correlation of refractive index by the Lorentz-Lorenz Approximation

From equation (3.17) n can be obtained and allows one to get the inverse prediction, i.e., to predict n from the pure solvent density and refractive index data and the experimental density of the mixture. The Lorentz-Lorenz expression for the prediction of n is given below:

$$n = \left(\frac{2\left[\left(\frac{n_1^2 - 1}{n_2^2 + 2} \right) x_1 \rho \frac{M_1}{M_1} + x_2 \left(\frac{n_1^2 - 1}{n_2^2 + 2} \right) \rho \frac{M_2}{M_2} \right] + \left[x_1 M_1 + x_2 M_2 \right]}{\left[x_1 M_1 + x_2 M_2 \right] - \left[\left(\frac{n_1^2 - 1}{n_2^2 + 2} \right) x_1 \rho \frac{M_1}{\rho_1} + x_2 \left(\frac{n_1^2 - 1}{n_2^2 + 2} \right) \rho \frac{M_2}{\rho_2} \right]} \right)^{1/2} \tag{3.19}$$

On simplifying equation (3.18) equation (3.19) is obtained. The derivation is given below:

$$\rho = \frac{\left(\frac{n^2 - 1}{n^2 + 2} \right) \left(x_1 M_1 + x_2 M_2 \right)}{\left(\frac{n_1^2 - 1}{n_1^2 + 2} \right) x_1 \frac{M_1}{\rho_1} + x_2 \left(\frac{n_2^2 - 1}{n_2^2 + 2} \right) \frac{M_2}{\rho_2}} \tag{3.20}$$

$$1 = \frac{\left(\frac{n^2 - 1}{n^2 + 2} \right) \left(x_1 M_1 + x_2 M_2 \right)}{\left(\frac{n_1^2 - 1}{n_1^2 + 2} \right) x_1 \rho \frac{M_1}{\rho_1} + x_2 \rho \left(\frac{n_2^2 - 1}{n_2^2 + 2} \right) \frac{M_2}{\rho_2}} \tag{3.21}$$

Assume:

$$a = x_1 M_1 + x_2 M_2 \text{ and} \tag{3.22}$$

$$b = \left(\frac{n_1^2 - 1}{n_1^2 + 2} \right) x_1 \frac{M_1}{\rho_1} + x_2 \left(\frac{n_2^2 - 1}{n_2^2 + 2} \right) \frac{M_2}{\rho_2} \tag{3.23}$$

Equation (3.19) becomes

$$1 = \frac{\left(\frac{n^2 - 1}{n^2 + 2}\right)a}{b} \tag{3.24}$$

$$\frac{b}{a} = \left(\frac{n^2 - 1}{n^2 + 2}\right) \tag{3.25}$$

$$B(n^2 + 2) = a(n^2 - 1) \tag{3.26}$$

$$n^2 = \frac{2b + a}{a - b} \tag{3.27}$$

$$n = \sqrt{\frac{2b + a}{a - b}} \tag{3.28}$$

After substituting the values of *a* and *b* from equations (3.22) and (3.23) in equation (3.28) the Lorentz- Lorenz predictive equation (3.19) for n is obtained.

3.4.5 Correlation of Excess Molar Volume by the Lorentz-Lorenz Approximation

Correlation of the excess molar volume can be obtained using the refractive index obtained from the binary mixtures by the Lorentz-Lorenz approximation. Inside the framework of the Lorentz-Lorenz approximation, V_m^E can be correlated via the change in reduced free volume, namely:

$$\Delta\left(\frac{V_{m,f}}{R}\right) = \frac{V_{m,f}}{R} - \left(\frac{V_{m,f}}{R}\right)^{id} \tag{3.29}$$

Application of the Lorentz-Lorenz equation allows this expression to be reduced to:

$$\Delta\left(\frac{V_{\mathrm{m,f}}}{R}\right)=\frac{3}{n^2-1}-\frac{3}{\left(n^{\mathrm{id}}\right)^2-1} \tag{3.30}$$

The assumption $R = R^{\mathrm{id}}$, is most often a highly accurate approximation. The following expression can then be obtained from equation (3.28).

$$\Delta\left(\frac{V_{\mathrm{m,f}}}{R}\right)=\frac{V_m^E}{R} \tag{3.31}$$

where

$$V_{\mathrm{m}}^{\mathrm{f}}-V_{\mathrm{m,f}}^{\mathrm{id}}=V_{\mathrm{m,f}}=V_m^E \tag{3.32}$$

Therefore,

$$V_m^E=\left(-n\right)\frac{3R(n^{\mathrm{id}}+n)}{\left(n^2-1\right)\left(\left(n^{\mathrm{id}}\right)^2-1\right)} \tag{3.33}$$

3.5 Activity Coefficients at Infinite Dilution

Activity coefficients at infinite dilution can be deduced experimentally or can be generated using models for Gibbs excess energy as was done by (Van Dyk and Nieuwoudt 2000).

The method of infinite dilution from chromatography have been commonly used. This approach was developed by Everett (1965) and expanded by Cruickshank, Windsor and Young (1966), is employed to obtain activity coefficients at infinite dilution of a volatile solute in an involatile solvent from gas liquid chromatography results. This method was also only applied when ideal gas was assumed but was shown by Cruickshank, Windsor and Young (1966) to extend to non-ideal carrier gasses with a fair degree of accuracy and also

made use of virial coefficients to estimate the molar vapor molar volumes on the assumption of an imperfect gas mixture.

In this work, the solute will be referred to as component 1, the carrier gas as component 2 and the solvent as component 3. The activity coefficient at infinite dilution is obtained in equation (3.34).

$$ln\gamma_{13}^{\infty} = ln\frac{n_3 RT}{V_N P_1^*} - \frac{(B_{11} - V_1^*)P_1^*}{RT} + \frac{P_o J_2^3 (2B_{12} - V_1^{\infty})}{RT} \quad (3.34)$$

where V_N is the net retention volume of the solute, P_o the column outlet pressure, J_2^3 the pressure correction term, n_3 number of moles of solvent in the column packing, T the column temperature, P_1^* the saturated vapour pressure of the solute at the column temperature, V_1^* the molar volume of the solute, V_1^{∞} the partial molar volume at infinite dilution of the solute in the solvent, B_{11} the second virial coefficient of the pure solute and B_{12} the mixed second virial coefficient of the solute and the carrier gas. The saturated vapour pressure in equation (1) was computed based on Antoine modified equation (Poling, Prausnitz and O'Connell 2000; Lide 2009).

The solute retention volume was calculated using the equation given by Letcher *et al.* (2001).

$$V_N = (J_2^3)^{-1} U_o (t_R - t_G) \quad (3.35)$$

t_R is the retention time of the solutes, t_G is the retention time for the unretained gas, and U_o the carrier gas flow rate at the column temperature and the outlet pressure.

The use of a soapy solution in a graduated column for the measurement of the flow rate of the carrier gas meant that the volumetric flow rate of the carrier had to be corrected for the vapor pressure exerted by the water that was present in the soap solution (Heintz, Kulikov and Verevkin 2002). This correction was given by Heintz, Kulikov and Verevkin (2002) and Letcher *et al.* (2001).

$$U_O = U\left(1 - \frac{P_W}{P_O}\right)\frac{T}{T_f} \tag{3.36}$$

P_W is the saturated vapour pressure of water at a temperature T, U_O is the flow rate of the carrier gas measured with the bubble soap flow meter at the column outlet.

The pressure correction term, J_2^3 was proposed by Everett (1965) and was calculated as follows:

$$J_2^3 = \frac{2}{3}\left[\frac{(P_i/P_o)^3 - 1}{(P_i/P_o)^2 - 1}\right] \tag{3.37}$$

P_i is the inlet pressure drops and P_O is the outlet pressure of the gas chromatography column.

3.5.1 Gas Liquid Chromatography

Martin and Synge (1941) reported a theory on chromatography that it would be possible to use gas as a mobile phase and stationary phase. They related the equilibrium partition coefficient, *K*, to retention properties using a plate theory. Their general equation, when considered in relation to gas liquid chromatography (for zero pressure difference across the column) relates the retention volume of the solute, V_R to the gas hold-up volume, V_G, and net retention volume of solute KV_3 according to:

$$V_R = V_G + KV_3 \tag{3.38}$$

3.5.2 Correlations between Physical Properties

The procedure for calculating the dilution activity coefficients at infinite dilution needed a significant amount of physical data such as critical properties and pure component properties.

Not all this data was readily available at times, correlations and approximations had to be made.

3.5.2.1 Second Virial Coefficients

Second virial coefficients were determined by using correlations. The correlations were also approximated for the second virial coefficients based on the critical properties of the solutes. The two correlations equation used were proposed by McGlashan and Potter (1962).

3.5.2.2 McGlashan and Potter Equation

The second virial coefficient of the pure solute B_{11} is computed based on McGlashan and Potter (1962)

$$B/V^C = 0.43 - 0.886(T^c/T) - 0.694(T^c/T)^2 - 0.0375(n-1)(T^c/T)^{4.5} \quad (3.39)$$

where n denotes the number of carbon atoms of the solute, T^c is the critical temperature and V^c is the critical volume. Equation 3.39 was suitable for non-polar alkanes, alkenes, alkynes and aromatics compounds. The mixed virial coefficients, B_{12} were calculated by means of mixing rules as follows in equations 3.40 to 3.43.

3.5.3 Mixing Rules for Cross Coefficients

The mixed virial coefficients B_{12} were deduced based on Hudson and McCoubrey (1960) mixing rules which is expressed as below:

$$T_{12}^c = (T_{11}^c T_{22}^c)^{\frac{1}{2}} \frac{2(\mathrm{I}_1 I_2)^{\frac{1}{2}}}{I_1 + I_2} \frac{2^6 V_{11}^c V_{22}^c}{\left[(V_{11}^c)^{\frac{1}{3}} + (V_{22}^c)^{\frac{1}{3}}\right]^6} \quad (3.40)$$

$$I_{c,12} \cdot V_{c,12}^2 = \left(I_{c,11} + I_{c,22}\right)\left(V_{c,11}^{\frac{1}{3}} + V_{c,22}^{\frac{1}{3}}\right)^6 \tag{3.41}$$

$$V_{12}^c = \frac{1}{8}\left[(V_{22}^c)^{\frac{1}{3}} + (V_{22}^c)^{\frac{1}{3}}\right]^3 \tag{3.42}$$

$$n = \frac{1}{2}(n_1 + n_2) \tag{3.43}$$

In equations 3.40 – 3.43, the subscripts '1', '2', and '12', refers to the solute, the carrier gas and the mixture of the two components, *n* is the number of carbon atoms and for a compound with no carbon is equivalent to one. Critical points T_C, V_C were found in the literature (Poling, Prausnitz and O'Connell 2000) and the ionization energies, I_C were found in (Lide 2009).

3.5.4 Molar Volumes

Molar volumes are a function of temperature and the modified Rackett equation was used to calculate the molar volumes as follows (Poling, Prausnitz and O'Connell 2000):

$$v = V_c(0.29056 - 0.08775\omega)^{\left(1-\frac{T}{T_c}\right)^{\frac{2}{7}}} \tag{3.44}$$

The acentric factors, ω were taken from the literature (Van Dyk and Nieuwoudt 2000).
The partial molar excess enthalpies at infinite dilution were determined from the Gibbs-Helmholtz equation below (Deenadayalu, Letcher and Reddy 2005):

$$\left[\frac{\partial In\gamma_i^{\infty}}{\partial(1/T)}\right] = \frac{\Delta H_1^{E,\infty}}{R} \tag{3.45}$$

where R is the Universal Gas constant.

The selectivity S_{ij}^{∞} is defined as the ratio of activity coefficients at infinite dilution for the two solutes that are to be separated and is given by the equation below:

$$S_{ij,s}^{\infty} = \frac{\gamma_i^{\infty}}{\gamma_j^{\infty}} \tag{3.46}$$

where i and j refers to the two solutes to be separated. If the selectivity is greater than 1 it indicates that a solvent is suitable as an entrainer in extractive distillation and in this work it refers to the IL (Tiegs *et al.* 1986).

The capacity of the solvent for a solute, k_j^{∞} gives a measure of the amount of the solute which dissolves in the solvent and is given by equation 3.47.

$$k_j^{\infty} = \frac{1}{\gamma_j^{\infty}} \tag{3.47}$$

Chapter 4

EXPERIMENTAL METHODS

4.1 Experimental

Two instruments namely an Anton Paar DSA 5000 M coupled with a refractometer (RXA 156) and a gas liquid chromatograph (Shimadzu GC-2014) were employed in this research. The materials utilized, the experimental setup and experimental procedures are discussed in this chapter. For both the Anton Paar DSA 5000 M and GLC measurements, the experimental procedures have been validated by comparing measured values with literature.

4.2 Apparatus for Density and Speed of Sound Measurements

4.2.1 Density and Sound Velocity Meter (DSA 5000 M)

In this work ρ and u were determined using the Anton Paar oscillating U-tube DSA 5000 M. DSA 5000 M concurrently determines two independent physical properties using a single sample. The instrument is fitted with a density cell and a sound velocity cell hence merging the Anton Paar oscillating U-tube method with an extremely precise instrument for the measurement of sound velocity. Both cells are temperature-controlled by a built-in Peltier thermostat. The temperature is controlled to ± 0.02 K.

V_m^E, for a binary mixture is determined from density measurements utilizing the expression given below:

$$V_m^E = \frac{x_1 M_1 + x_2 M_2}{\rho} - \frac{x_1 M_1}{\rho_1} - \frac{x_2 M_2}{\rho_2} \quad (4.1)$$

where x_1 and x_2 are mole fractions, M_1 and M_2 are the molecular masses ρ_1 and ρ_2 are the densities of pure components 1 and 2, respectively (Govender *et al.* 1996; Redhi 2003). Density values are highly temperature dependent.

4.2.2 Oscillating U-tube

The operation of an oscillation-type density meter is founded on the principle of harmonic oscillation, where a U-tube is packed with the sample to be analyzed and exposed to an electromagnetic force. The measurement of the frequency and period of vibration of the tube packed with the sample permits the determination of the density value of the sample. The U-tube vibrates at its fundamental frequency, that is a function of the system mass (Furtado *et al.* 2009). This method gives highly accurate measurements for the density.

4.2.3 Sound Velocity Analyzer

The equipment is fitted with a stainless steel cell and employs the method of pulse-echo that infers to the transmission of a short pulse of ultrasound through the middle of the sample. The sound velocity was measured at a frequency of approximately 3 MHz. This technique provides extremely precise measurements of the density. In the event that an impediment is met, a portion of the pulse is reflected, and the other portion is transmitted (Luning Prak and Lee 2016).

Therefore, the equipment records the time amid the emission of the pulse and getting the echo, changing it into the distance (Cunha *et al.* 2013).

The density, ρ, is computed based on the quotient of the period of oscillation of the U-tube and the reference oscillator:

$$\rho = KA \times Q^2 \times f_1 - KB \times f_2 \quad (4.2)$$

KA, KB are the apparatus constants

Q is the quotient of the period of oscillation of the U-tube divided by the period of oscillation of the reference oscillator

f_1, f_2 are the correction terms for temperature, viscosity, and non-linearity

The value of the density is displayed on the LCD screen. The DSA 5000 M is coupled to a computer which is loaded with software that stores all the measured density values. A photograph of the Density and Sound Velocity Meter (DSA 5000 M) is given in Figure 4.1. below.

Figure 4.1: Photograph of the Density and Sound Velocity Meter (DSA 5000 M)
(Taken from Instruction Manual of Anton Paar DSA 5000 M)

For the measurement of the sound velocity, the sample is put into the sound velocity measuring cell which is bounded by an ultrasonic transmitter on one side, and a receiver on

the other side. The transmitter transmits sound waves of a recognized duration through the sample. The velocity of sound, u, is computed by using the period of the sound waves and the distance between the transmitter and receiver.

$$u = \frac{l \text{ x } (1 + 1.6 \text{ x } 10^{-5} \text{ x } \Delta T)}{\frac{Ps}{512} - A \text{ x } f_3} \tag{4.3}$$

where l is the original path length of the sound waves, ΔT is the temperature deviation to 278.15 K, P_S is the oscillation period of the received sound waves, A is apparatus constant for sound velocity, and f_3 is the correction term for temperature. The frequency of the measurement was done at 3 MHz.

As a result of high-temperature dependency of the density and velocity of sound, the measuring cells are thermostated, using the Peltier elements.

The key features of the DSA 5000M are the high accuracy of the density measurements. The DSA 5000 M instrument is equipped with the world's most advanced digital density and sound velocity measurement technology were:

(i) The period of oscillation of the U-tube is measured by optical pickups.

(ii) Two integrated Pt 100 platinum thermometers together with the Peltier elements provide a highly accurate thermosetting of the sample.

(iii) There is a thermobalance which is an additional reference oscillator that provides long-term stability and enables precise measurements over the whole temperature range of the instrument with only one adjustment at T = 293.15 K.

(iv) Viscosity- related errors are naturally remedied over the full viscosity run by measuring the damping effect of the viscous sample followed by a mathematical rectification for the density value.

(v) Special adjustments to standards of high viscosity and high density lead to an enhanced precision when samples with high viscosity and high density are used.

A primary source of measuring errors when using a density and sound velocity meter are gas bubbles in the measuring cells. To reduce the formation of gas bubbles, Anton Paar introduced two new features:

(i) Filling Check: The instrument automatically senses gas bubbles in the density measuring cell by an advanced analysis of its oscillation pattern and gives a cautionary message.

(ii) U-View: Using a real-time camera with zoom function the U-tube can be visually inspected for gas bubbles in the density measuring cell.

The specifications for the DSA 5000 M are given in Table 4.1.

Table 4.1: Specifications of the DSA 5000 M

Measuring range density	0 to 3 g/cm^3
Measuring range sound velocity	1000 to 2000 m/s
Measuring range temperature	273.15 to 343.15 K (32 to 158 °F)
Pressure range	0 to 3 bar (0 to 44 psi)
Repeatability density	0.000001 g/cm^3
Repeatability sound velocity	0.1 m/s
Repeatability temperatures	273.151 K (0.002 °F)
Measuring time per sample	1 to 4 minutes
Sample volume	approx. 3 ml
Ambient air pressure sensor	yes
Reference oscillator	yes
Automatic bubble detection	yes
Visual check of the density measuring cell	camera

4.3 Apparatus for Refractive Index

In this work, Δn was determined using the Anton Paar refractive index analyzer RXA 156.

The DSA 5000 M was coupled with the RXA 156 and Xsample 452.

A photograph of the DSA 5000 M and the RXA 156 and Xsample 452 is given in Figure 4.2.

Figure 4.2: Photograph of the DSA 5000 M and the RXA 156 and Xsample 452
(Taken from Instruction Manual of Anton Paar DSA 5000 M)

An overview of the Anton Paar refractive index analyzer RXA 156 is given briefly in the description below.

The RXA 156 module is fitted with a micro flow cell, and an integrated Peltier thermostat to ensure:

- correct and automatic temperature control;
- Quick and non-destructive measurements;
- needing only small sample volume.

The Anton Paar refractive index analyzer RXA 156 consists of the following characteristics:

- Simple adjustment of the DSA 5000 M and RXA 156 using air and water in a single method.

- Automatic filling and cleaning of the DSA 5000 M and RXA 156 sample changer. Single measuring cycle, three sample parameters
- It saves time by concurrently determining the density, sound velocity, and refractive index.
- It is quick and gives consistent outcomes.
- Initiated U-tube technique for measuring density.
- It is an extremely correct measurement of the angle of total reflection for deducing the refractive index.

Table 4.2 shows the specifications lists of the refractometer RXA 156.

Table 4.2: Specifications of the refractometer RXA 156

Refractive index	
Measuring range	1.32 – 1.56 n_D
Resolution	0.000001
Accuracy	0.00002
Temperature	
Measuring temperature	283.15 - 343.15 K
Resolution	273.16 K
Accuracy	273.18 K
Stability	273.152 K
Speed of temperature change from	20 s
ambient temperature	288 K – 308 K

4.4 Chemicals

The chemical 1-butyl-3-methylimidazolium nitrate was obtained from Fluka, and the purity was > 95% (mass by mass %) (Table 4.3). Thiophene, pyridine, and acetonitrile were purchased from Sigma-Aldrich. The purity of these substances were > 99% (mass by mass %) (Table 4.3). All the purified chemicals were stored in molecular sieves to reduce the moisture content if any, before use. All of these solvents were used without further purification. The Metrohm 831 Karl- Fischer coulometric titrator was used for the determination of water content. The mole fraction of water content for 1-butyl-3-methylimidazolium nitrate, pyridine, acetonitrile, and thiophene were determined to be 0.01656, 0.00139, 0.00052 and 0.000078, respectively (Table 4.3). The purity of these solvents was ascertained by comparing the measured density, refractive indices, and speed of sound with the available literature values, as illustrated in Table 4.3.

Table 4.3: Suppliers, purity, and water content of chemicals

chemical name	source	CAS number	purity	purification method	water content (mole fraction)
1-butyl-3-methy-limidazolium nitrate	Fulka	179075-88-8	>95%	Used as procured	0.01656
pyridine	Sigma Adrich	110-86-1	>99%	Used as procured	0.00139
acetonitrile	Sigma Adrich	75-05-8	>99%	Used as procured	0.00052
thiophene	Sigma Adrich	110-02-1	>99%	Used as procured	0.00078

Table 4.4 shows the comparison of experimental data and literature density, ρ, speed of sound, u, and refractive index, n, of pure components at T = (298.15, 303.15, 308.15, 313.15 and 318.15) K.

Table 4.4: Comparison of experimental and literature density, ρ, speed of sound, u, and refractive index, n, of pure components at T = (298.15, 303.15, 308.15, 313.15 and 318.15) K

T (K)	ρ (kg·m^{-3})		n_D		u (m·s^{-1})	
	expt	lit	expt	lit	expt	lit
[BMIM][NO_3]						
298.15	1151.66	1156.50[a]	1.493611	-	1743.77	-
303.15	1148.44	1153.40[a]	1.492273	-	1731.89	-
		1149.00[b]		-		-
308.15	1145.24	1150.20[a]	1.490743	-	1720.07	-
		1143.50[b]		-		-
313.15	1142.06	1147.00[a]	1.489157	-	1708.49	-
		1143.50[b]		-		-
318.15	1138.90	1143.90[a]	1.487556	-	1698.16	-
Pyridine						
298.15	978.27	978.24[c]	1.505654	1.5062[d]	1417.67	1416.42[c]
				1.5074[e]		
303.15	973.23	973.20[d]	1.502731	1.5025[e]	1397.65	1398.60[e]
308.15	968.19	968.20[d]	1.499886	1.5016[d]	1377.60	-
313.15	963.12	963.10[d]	1.497089	-	1358.97	-
318.15	958.05	958.10[d]	1.494251	-	1342.53	-

Table 4.4 continued

Acetonitrile						
298.15	776.75	776.50[f]	1.341422	1.3416[i]	1279.75	1279.00[g]
303.15	771.33	771.48[g]	1.339058	1.3391[i]	1259.82	1258.73[g]
308.15	765.87	765.78[g]	1.336594	1.3366[i]	1241.01	1238.66[g]
313.15	760.38	760.29[g]	1.334103	-	1226.05	1218.52[g]
318.15	754.85	750.15[h]	1.331552	-	1216.75	1209.00[h]
Thiophene						
298.15	1059.68	1058.56[d]	1.524470	1.5252[j]	1277.37	-
303.15	1053.70	1052.50[d]	1.521326	-	1256.75	1258.65[j]
308.15	1047.70	1046.50[d]	1.518089	-	1236.20	-
313.15	1041.67	1040.50[d]	1.514815	-	1216.77	-
318.15	1035.61	1034.40[d]	1.511558	-	1198.48	-

[a](Mokhtarani *et al.* 2009), [b]Ref (Micaelo, Baptista and Soares 2006), [c], [d](Anantharaj and Banerjee 2011), [e](Ali, Tariq and Nabi 2008), [f](Zafarani-Moattar and Shekaari 2006), [g](Singh *et al.* 2014), [h](Chen *et al.* 2015), [i](Aralaguppi, Jadar and Aminabhavi 1996), [j](Shekaari, Zafarani-Moattar and Behrooz 2015).

There is good correlation between the physical properties from this work and the literature data.

4.5 Preparation of Binary Mixtures

The binary mixtures were prepared to ensure that the entire mole fraction range was covered. An OHAUS (Pine Brook, NJ, USA) analytical balance with a precision of ±0.0001 g was employed to measure the masses of the components of the binary mixtures. The binary

mixtures were prepared by putting the pure liquids into vials to reduced evaporation, and the mixtures were shaken to ensure total mixing of the samples and sample homogeneity. Each mixture was prepared immediately before performing the density, speed of sound or refractive index measurements to avoid disparities in composition as a result of evaporation of the solvent.

4.6 Experimental Procedures for Measurement of Density, Speed of Sound and Refractive Index

4.6.1 Density and Speed of Sound

The density and speed of sound were measured using an Anton Paar DSA 5000M vibrating U-tube densimeter, set at the experimental temperatures with precision of ±0.02 K for temperature, ±0.000005 $g \cdot cm^{-3}$ for density, and ± 0.01 $m \cdot s^{-1}$ for the speed of sound.

For each experimental run, the cell was initialy cleaned with ethanol (liquid 1) and then dried with acetone (liquid 2) using a fully automatic Xsample 452 Module. Xsample 452 performs a cleaning routine after each measurement. Rinsing ethanol (liquid 1) dissolves sample remains in the measuring cell of the DSA 5000 M. Rinsing acetone (liquid 2) is highly volatile and soluble in rinsing liquid 1. Rinsing removes cleaning liquid 1 and is easily evaporated under a stream of dry air to accelerate drying of the cell. Acetone is a good solvent for removing ethanol. After rinsing and cleaning the instrument was calibrated by ultra-pure water and ambient air. The goal of a calibration is to validate the accuracy of the density measurement. Each binary mixture is placed in a vial and sealed with a cap. Each vial is placed onto the Xsample 452 with a 48-position magazine. The DSA 5000 M automatically detects the connected Xsample 452. The sample changer automatically fills the binary solutions from each sample vial into the measuring cell of the DSA 5000 M. The binary

mixtures are filled easily and safely without evaporation losses or the formation of bubbles. The instrument automatically senses gas bubbles in the measuring cell by an innovative analysis of its oscillations pattern and produces a cautionary message. The instrument software also allows visual inspection for gas bubbles on an external PC using a real-time camera with zoom function. After each measurement, the measuring cell is automatically rinsed and cleaned with two rinsing liquids and subsequently dried. Density and speed of sound results are shown together on the LED display, and the computer using the pre-installed software. The projected error in temperature, density, and sound velocity was less than ± 0.02 K, ±

$5x10^{-5}$ $g \cdot cm^{-3}$ and ± 2 $m \cdot s^{-1}$, respectively.

4.6.2 Refractive Index

Measurement of the refractive index of pure components and binary mixtures were gotten by a digital automatic refractometer (Anton Paar RXA 156) with a precision of ±0.03 K in temperature. The RXA 156 measuring module is operated in combination with the density and sound velocity analyzer DSA 5000 M. The measuring results of the RXA 156 are transmitted to the DSA 5000 M instrument where refractive indices are displayed, saved and can be exported or printed. The LED screen shows the result of all three properties namely, density, the speed of sound and refractive index. The instrument was standardized by measuring the refractive index of ultra-pure water before each series of measurements.

4.6.3 Validation of Experimental Technique

The experimental method was evaluated by measuring density, speed of sound sound and refractive index and then determining the excess molar volume, isentropic compressibility and change in refractive index on mixing for the test system (ethanol + heptane) at T =

303.15 K and comparing it with literature data (Orge *et al.* 1999). The maximum variations amid the experimental and literature values for the excess molar volume, deviation in isentropic compressibility and deviation in refractive index was ± 0.0004 $cm^3 \cdot mol^{-1}$, ± 0.11 x 10^{12} Pa^{-1}, and ± 0.00031, respectively for the test system. The table for the literature and experimental data for V_m^E, κ_s and Δn for the test system at T = 303 K is given below in Table 4.5.

Table 4.5: The literature and experimental data for V_m^E, κ_s and Δn for the test system {ethanol (x_1) + heptane (x_2)} at T = 303 K

x_1	ρ / (g·cm^{-3})	V_m^E /(cm^3·mol^{-1})	Δn	κ_s /(10^{12} Pa^{-1})
		Experimental		
		T = 303.15 K		
0.0000	0.67538	0.000	0.00000	1202.6
0.0530	0.67677	0.197	0.00015	1212.8
0.1270	0.67958	0.326	0.00084	1216.6
0.2186	0.68377	0.425	0.00166	1216.6
0.3037	0.68836	0.482	0.00235	1213.6
0.4002	0.69450	0.514	0.00295	1206.0
0.4678	0.69947	0.524	0.00328	1198.9
0.5398	0.70551	0.523	0.00350	1189.0
0.6342	0.71482	0.506	0.00354	1171.6
0.7652	0.73144	0.434	0.00294	1137.6
0.8298	0.74187	0.367	0.00239	1112.9
0.9572	0.76918	0.149	0.00052	1041.1
		Literature		
0.1191	0.67830	0.280	0.00056	1217.6
0.2042	0.68260	0.411	0.00123	1219.3
0.3024	0.68850	0.476	0.00203	1215.0

Table 4.4 continued

0.4031	0.69480	0.507	0.00274	1207.8
0.4887	0.70260	0.500	0.00317	1196.1
0.5972	0.71090	0.483	0.00335	1182.0
0.7027	0.72410	0.436	0.00308	1155.8
0.7956	0.73260	0.373	0.00250	1129.0
0.8890	0.75490	0.222	0.00145	1082.7

The graphs of the literature and experimental data together with a polynomial fit for V_m^E, κ_s and Δn are given in Figures 4.3, 4.4 and 4.5, respectively.

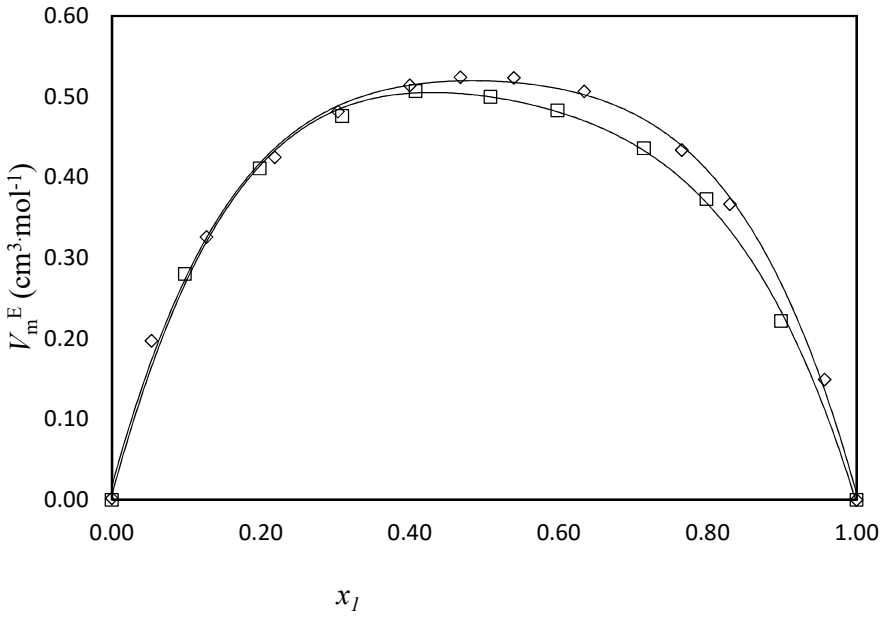

Figure 4.3: V_m^E plot for the binary mixture (ethanol + heptane) at T = 303.15 K, □, literature data (Orge *et al.* 1999); ◊, this work.

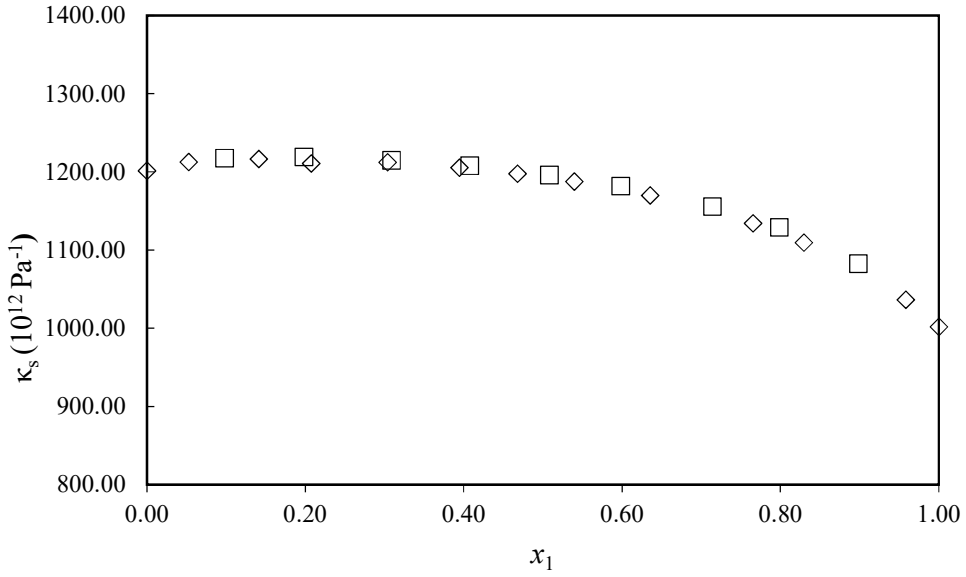

Figure 4.4: Comparison of the calculated κ_s from this work with the literature data for the binary mixture (ethanol + heptane) at T = 303.15 K, □, literature data (Orge *et al.* 1999); ◊, this work.

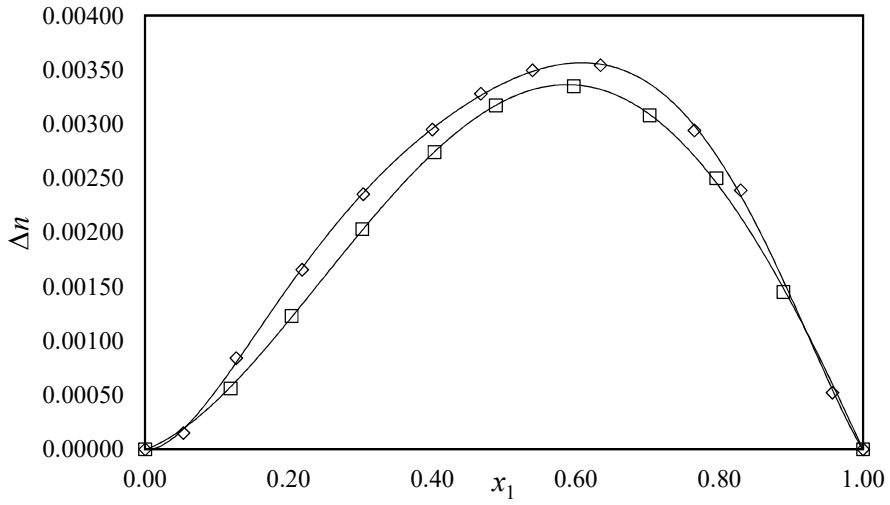

Figure 4.5: Comparison of the calculated Δn from this work with the literature data for the binary mixture (ethanol + heptane) at T = 303.15 K, □, literature data (Orge *et al.* 1999); ◊, this work.

4.7 Gas Liquid Chromatography (GLC)

In the gas liquid chromatography (GLC) technique, the IL is used as the stationary phase and it is coated onto the solid support before being loaded into the column. The solute, which is a mobile phase, is injected into the head of the chromatographic column. Helium is used as the carrier gas. The solute is carried through the column by the carrier gas and detected as a peak (retention times) by a thermal conductivity detector. GLC can be used for activity coefficients at infinite dilution, γ_{13}^{∞} volatile solutes in low volatility solvents. Everett (1965) and Cruickshank, Windsor and Young (1966), developed this method.

Table 4.6 summarizes the advantages and disadvantages of GLC technique (Tumba 2010).

Table 4.6: Advantages and disadvantages of the GLC method

Advantages	**Disadvantages**
Sample purity is not needed	The method is only suited to low volatility solvents only.
It has fast method because many solutes can be injected at once	The activity coefficient at infinite dilution of the solvent in the solute cannot be determined.
Reactive systems can be investigated	

Figure 4.6 is the schematic diagram of the GLC equipment used in this work.

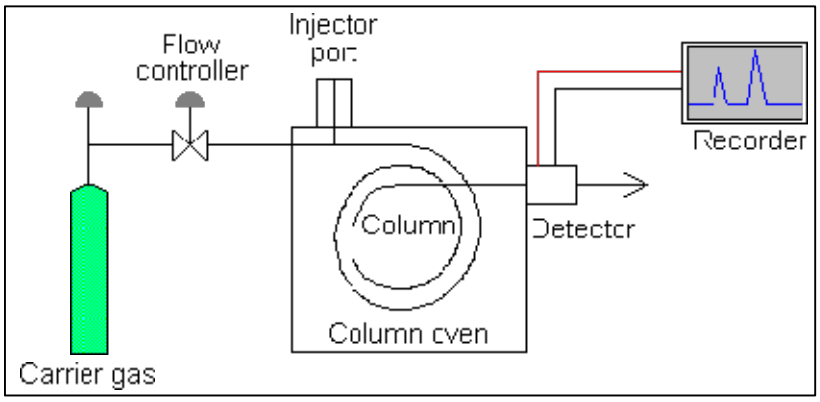

Figure 4.6: Schematic diagram of the GLC equipment (Skoog, Holler and Crouch 2007)

4.7.1 Thermal Conductivity Detector

The thermal conductivity detector (TCD) contains a filament that is heated electrically so that it is hotter than the detector body. The filament temperature is kept constant while alternate streams of reference gas and column effluent pass over it. When the sample is injected, the power required to maintain the filament temperature constant changes. When helium (or hydrogen) is used as carrier gas, the sample causes conductivity to fall (Skoog, Holler and Crouch 2007). When the sample (analyte) elutes from the column, it reaches the detector, and a change of conductivity is shown as peak. Retention time is related to temperature and flow, conductivity does not affect it.

This work used helium as the the carrier gas, which was supplied by Afrox. Knoop, Tiegs and Gmehling (1989) reported that helium has superior measurements for GLC when using TCD compared to nitrogen. Helium is the most popular carrier gas for gas chromatograph because it produces a reasonable chromatographic efficiency, is highly inert and non-explosive. The schematic of the Shimadzu TCD is given in Figure 4.7.

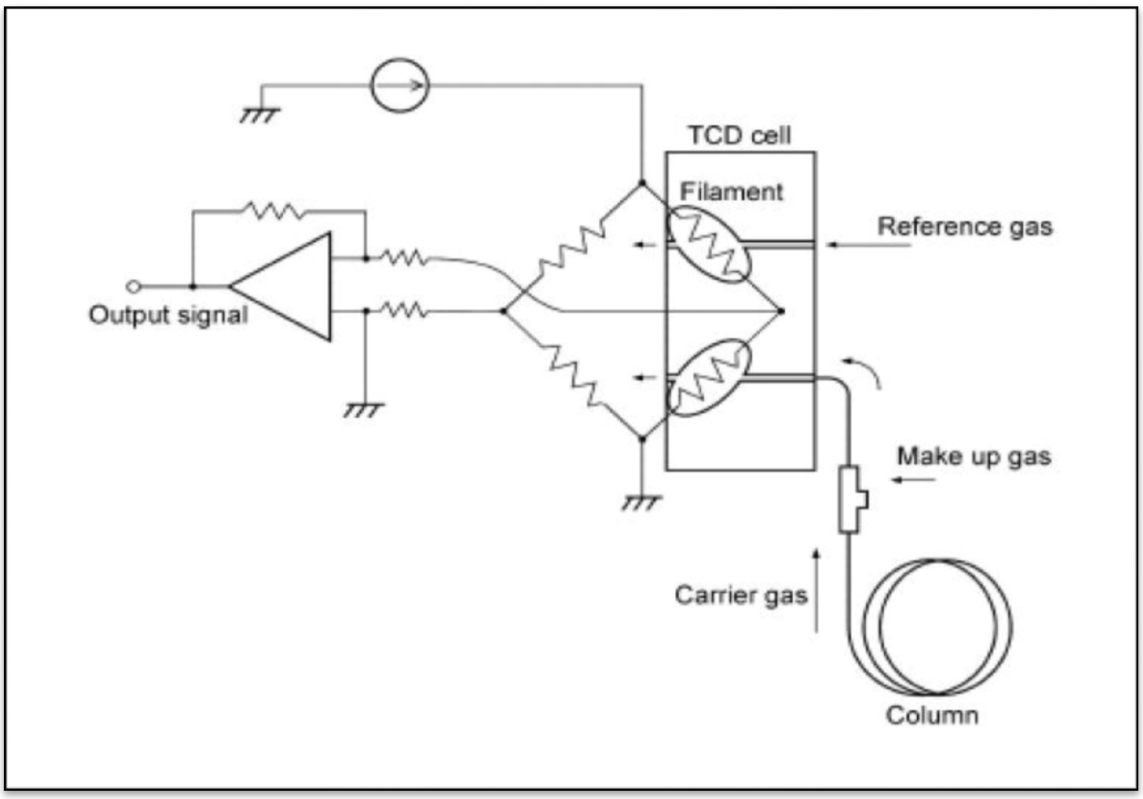

Figure 4.7: Schematic of a Shimadzu TCD provided by (Shimadzu Asia Pacific Pty. Ltd., 2006) (Williams-Wynn 2012).

4.7.2 Advantages of TCD

The TCD detector has the following advantages (Gwala 2009)

(a) Responds to most compounds;

(b) Adequate sensitive for many compuonds;

(c) Good linear range;

(d) Simple construction;

(e) Nondestructive detection;

(f) Signal quite stable if carrier gas flow rate, block temperature, and filament power are effectively controlled.

4.7.3 Rotary Evaporator

Rotary evaporator is the device used to remove the homogeneousing solvent namely methanol from the column packing by evaporation under vacuum. The evaporator comprises of a heated water bath with a rotating flask, in which the homogenising solvent is spread as a thin film across the hot wall surfaces and can evaporate effortlessly while the column packing is coated with IL. The evaporation is controlled by the temperature of the heated water ,as well as, the speed of rotation, the pressure of distillation and the size of the flask.

Figure 4.8 is the photograph of rotary evaporator.

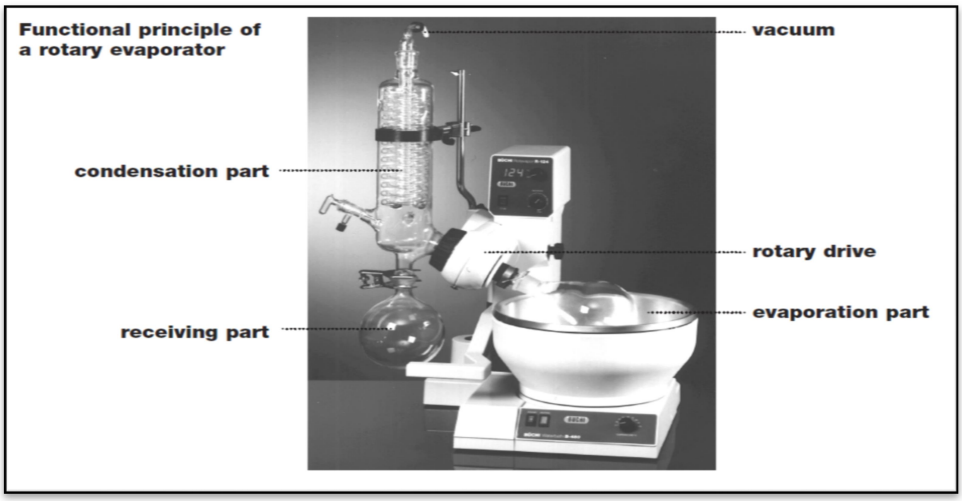

Figure 4.8: Photograph of rotary evaporator (Williams-Wynn 2012)

4.8 Experimental Method for Measuring Activity Coefficient at Infinite Dilution Using GLC

4.8.1 Chemicals and Materials

The solutes were purchased from Sigma-Aldrich and Fluka with a purity that ranged from 98.5-99.8 (mass by mass %). The solutes were utilized without further purification because the chromatographic column separates all the impurities, leaving the major solute-free of impurities. The IL: 1-butyl-3-methylimidazolium sulfate was also purchased from Sigma-Aldrich with a purity ranges from (95-98) % (mass by mass %). The solutes were n-pentane, n-hexane, n-heptane, n-octane, cyclopentane, cyclohexane, cyclooctane, benzene, toluene, o-xylene, m-xylene, p-xylene, methanol, ethanol, 1-propanol, hex-1-ene, non-1-ene, dec-1-ene, hex-1-yne, hept-1-yne, oct-1-yne, pyridine, thiophene, acetonitrile, dichloromethane, acetone, 3-pentanone and ethyl acetate.

The mass percentage of water content in the ionic liquid was determined using a Karl-Fischer Coulometer {Metrohm 831] and was found to be 0.93 % (mass by mass %).

4.8.2 Experimental Setup

Experiments were done using a Shimadzu GC-2014 gas chromatograph apparatus, fitted with a thermal detector, an auto-sampler, and auto-injector. Retention times and chromatograms linked to each run were obtained on computer using a GC solution workstation software. The experimental set up is shown in figure 4.9 and the software is programmed so as to carry out injections of samples from 125 diverse vials with minimum human intervention required in the sample injections.

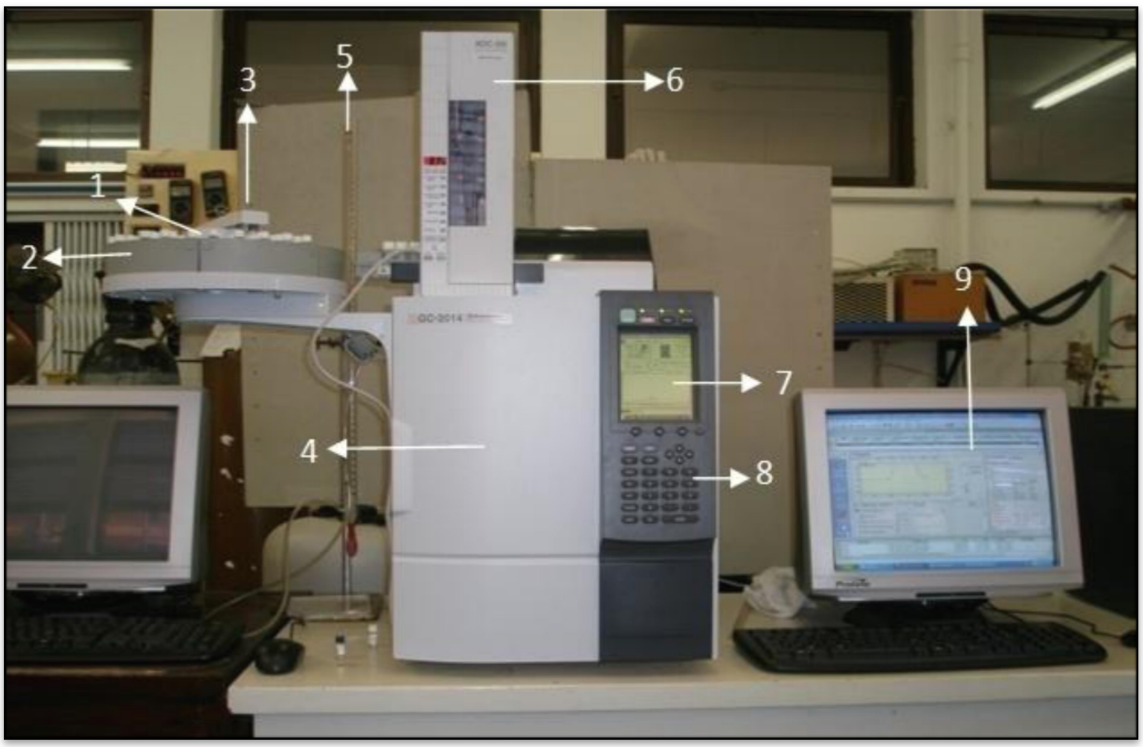

Figure 4.9: Experimental setup for the gas liquid chromatography equipment (Tumba 2010)

1. Vials, 2. Tray, 3. Auto-sampler (arm); 4. Column oven; 5. Soap bubble flow meter; 6. Auto-injector; 7. GC screen; 8. Operation panel; 9. Software program displayed on PC Monitor

4.8.3 Experimental Procedure

The experimental procedure for the measurement of retention times for the calculation of activity coefficients at infinite dilutions using the GLC method was reported by (Tumba 2010; Bahadur *et al.* 2014) as well as by (Deenadayalu, Letcher and Reddy 2005). The GLC column was packed with the solid support coated with the IL. It was made of stainless steel (304 grade) of 1.0 m length and 4.1 mm diameter and supplied by Swagelok. The column was thoroughly cleaned before use by rinsing it several times with hot soapy water, followed by hot water distilled water and then flushed with acetone to reduce the drying time. A vacuum

flask containing the IL was immersed into an ultrasonic bath and degassed for at least 2 weeks to remove any absorbed water, volatile impurities and dissolved air from the IL. The degassing was performed with an Ilmvac ROdist digital rotary vacuum evaporator capable of a vacuum of up to 95 kPa (guage). The solvent was held at 40 ^{o}C while being degassed.

Chromosorb W-HP (100/120 mesh) was used as solid support for the column. A rotary evaporator was used to dry the chromosorb for at least 8 hours (at a temperature 313.15 K) before the latter was coated with the IL. For the preparation of the stationary phase, the IL was carefully weighed, using a Mettler Toledo AB204S electronic balance with a stated accuracy of 0.1 mg, dissolved in methanol and quantitatively transferred to a pre-weighed amount of chromosorb in a round bottom flask. The percentage of ionic liquid packed on the solid support was ±40% (mass by mass %). The large ratio of IL to support solid support was used to avoid solute adsorption effects (Domańska, Królikowski and Acree 2011). The mixing of IL and chromosorb was done in a rotatory evaporator at a medium rotation speed for at least 12 hours to ensure complete mixing. The temperature of the mixture of IL and chromosorb was slowly increased from 313.15 to 323.15 K to prevent entrainment of the IL with volatile of methanol. To ensure that all the methanol was removed from the packing, the drying was continued until a mass of IL and inert support (chromosorb) was in agreement within 0.0005 g to the mass measured before adding methanol. The prepared column packing material was slowly inserted into the column using a funnel and tapping of the column to ensure tight packing and elimination of dead volumes. The prepared column was inserted into the Shimadzu GC-2014 GC equipped with a TCD detector. The column packing was conditioned was conditioned for 24 hours by passing dry helium, which was the carrier gas, through the column at flow rates between (20 and 30) $cm^{3}.min^{-1}$ and at a temperature of 313.15 K, to eliminate all traces of volatile materials remaining in the packing and to pre-

saturate the packing with the carrier gas. The solutes were injected into the column immediately after packing and conditioning, and the retention times recorded.

The injector and detector were both maintained at T = 573 K for all measurements. Thermogreen LB-2 septa (Supelco, USA) were used in the injection port to reduce any contamination in the column through the failure of the septum. The instrumental temperature accuracy is ± 0.1 K with a temperature stability of ± 0.1 K. Solute samples (0.2 μL) were injected individually by the Shimadzu AOC-20i/s Autoinjector /Autosampler that ensure of the excellent reproducibility. Reproducibility was checked by injecting in triplicate for all the experimental temperatures. The retention time of the non-retainable component (air) was obtained by injecting dry air into the column.

The flow rate and the inlet pressure of the helium carrier gas were controlled by the automatic flow controller on the GC. A 0.0001 m^3 graduated soap bubble flow meter placed at the outlet of the detector was used to measure the carrier gas flow rates and was corrected for the vapor pressure generated by the water present in the soap solution. The outlet pressure was equal to the atmospheric pressure which was measured using a WIKA CPH 6000 digital sensor.

4.8.4 Determination of Number of Moles

The subsequent method was used to calculate the no of moles of 1-butyl-3-methylimidazolium hydrogen sulfate.

- The mass of empty flask was measured by means of a digital balance;
- The chromosorp was added to flask and weighed;
- The flask with chromosorp was weighed before and after drying;
- The mass of solvent to be added was approximately calculated by using the percentage loading of the solvent;

- The solvent was added and its mass found accurately;
- The mass of flask with chromosorp and solvent was weighed before and after drying;
- After packing the column, the flask with the remaining mixture plus mixture was weighed;
- Mass of packing in column is equal to the mass of flask plus chromosorp and solvent minus the mass of flask plus mixture remaining after packing;
- Mass of solvent in column is equal to mass of contents filled multiply by percentage loading;
- No of moles of solvent is equal to mass of solvent in column divided by molar mass of ionic liquid.

The validity of the experimental procedure was checked by a comparison of the calculated activity coefficients at infinite dilution for pentane, hexane, heptane, cyclohexane, benzene and 1-hexene in hexadecane with those available in literature and given in Table 4.7. The maximum percentage error in γ_{13}^{∞} was ± 3 %.

Table 4.7: Activity coefficients at infinite dilution of selected organic solutes in n-hexadecane together with the literature values and the present relative deviation (% R.D)

Solutes	*T*/ K	$\gamma_{13}^{\infty,exp}$	$\gamma_{13}^{\infty,lit}$	R.D*./ %
n-pentane	313.15	0.818	0.833[abc]	-1.8
n-hexane	313.15	0.876	0.87-0.911[abc]	0.7
n-heptane	313.15	0.916	0.898-0.920[ab]	-0.5
cyclohexane	313.15	0.787	0.776-0.778[ab]	1.2
Benzene	313.15	1.026	0.995-1.01[ab]	1.6
1-Hexene	313.15	0.878	0.862[a]	-3.2

[a](Schult *et al.* 2001); [b](Cheong 2002); [c](Lehmann *et al.* 2010)

*Relative deviation, R.D., is given by:

$$\frac{\left(\gamma_{13}^{\infty,exp} - \gamma_{13}^{\infty,lit}\right)}{\gamma_{13}^{\infty,lit}} \times 100 \tag{4.4}$$

In this work the γ_{13}^{∞} values were calculated from gas liquid chromatography measurements for different solutes at the three temperatures (313.15, 323.15 and 333) K using 1-butyl-3-methylimidazolium hydrogen sulfate [BMIM][HSO_4] (Figure 4.10).

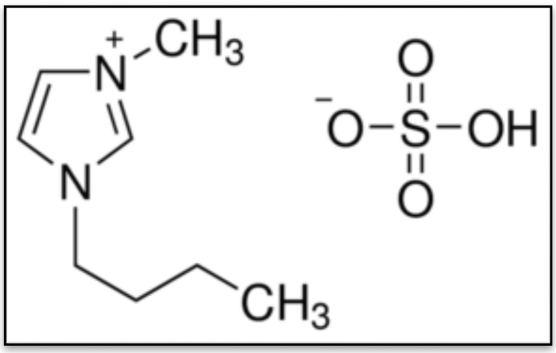

Figure 4.10: Structure of 1-butyl-3-methylimidazolium hydrogen sulfate [BMIM][HSO_4].

The partial molar excess enthalpies at infinite dilution value $\Delta H_1^{E,\infty}$ were computed from the γ_{13}^{∞} obtained at the three temperatures using the Gibbs-Helmholz equation (equation 3.44). The activity coefficients at infinite dilution values were used to calculate the selectivities (equation 3.45) and capacity (equation 3.46) values for different types of separation problems.

Chapter 5

RESULTS

5.1 Excess Molar Volume, V_m^E, Isentropic Compressibility, κ_s, Change in Refractive Index, Δn and Molar Refraction, R

The results of excess molar volume, isentropic compressibility, change in refractive index, and molar refraction, for all binary systems at the five temperatures are given in this chapter.

The V_m^E, for binary mixtures ([BMIM][NO_3] + pyridine) or ([BMIM][NO_3] + acetonitrile) and ([BMIM][NO_3] + thiophene) across the whole composition range was computed from density data at temperatures ranging from 298.15 K to 318.15 K in increments of 5 K steps utilising the equation given in 4.1 and is repeated here for convenience:

$$V_m^E = \frac{x_1 M_1 + x_2 M_2}{\rho} - \frac{x_1 M_1}{\rho_1} - \frac{x_2 M_2}{\rho_2} \qquad (4.1)$$

where x_1 and x_2 are mole fractions, M_1 and M_2 are the molecular masses, ρ_1 and ρ_2 are the densities of pure components 1 and 2, respectively, where '1' refers to pyridine or acetonitrile or thiophene, and '2' refers to [BMIM][NO_3] and ρ, is the density of the mixture.

The density, ρ, and excess molar volume, V_m^E, for the binary systems {[BMIM][NO_3] (x_2) + pyridine (x_1) or [BMIM][NO_3] (x_2) + acetonitrile (x_1) and [BMIM][NO_3] (x_2) + thiophene (x_1) at T = (298.15, 303.15, 308.15, 313.15 and 318.15) K are presented in Tables 5.1, 5.2, and 5.3.

The isentropic compressibilities, κ_s, was computed using Newton–Laplace expression given in 3.10:

$$\kappa_s = \frac{1}{\rho u^2} \tag{3.10}$$

where ρ, is the density and u is the speed of sound of the binary mixtures.

The speed of sound, u, and isentropic compressibility, κ_s, for the binary systems {[BMIM][NO_3] (x_2) + pyridine (x_1)} or {[BMIM][NO_3] (x_2) + acetonitrile (x_1)} and {[BMIM][NO_3] (x_2) +thiophene (x_1)} at T = (298.15, 303.15, 308.15, 313.15 and 318.15) K are also given in Tables 5.1, 5.2 and 5.3 .

The change in refractive index, Δn, was computed using equation (5.1):

$$\Delta n = n - x_1 n_1 - x_2 n_2 \tag{5.1}$$

where n_1 and n_2 are the refractive index of pure components and n is the refractive index of the mixtures. The change in refractive index, Δn , for the binary systems {[BMIM][NO_3](x_2) + pyridine (x_1)} or {[BMIM][NO_3] (x_2) + acetonitrile (x_1) }and {[BMIM][NO_3] (x_2) + thiophene (x_1)} at T = (298.15, 303.15, 308.15, 313.15 and 318.15) K are presented in Tables 5.4, 5.5, and 5.6 .

The molar refraction, R, was computed using Lorentz–Lorenz equation shown as follows:

$$R = \left(\frac{n^2 - 1}{n^2 + 2}\right) V_m \tag{5.2}$$

where V_m is the molar volume and n is the refractive index of the mixture. The molar refraction, R, for the binary systems {[BMIM][NO_3] (x_2) + pyridine (x_1)} or {[BMIM][NO_3] (x_2) + acetonitrile (x_1)} and {[BMIM][NO_3] (x_2) + thiophene (x_1)} at T = (298.15, 303.15, 308.15, 313.15 and 318.15) K are presented in Tables 5.4, 5.5, and 5.6.

Table 5.1: Density, ρ , excess molar volume, V_m^E , speed of sound, *u*, and isentropic compressibility, κ_s , for the binary mixture {[BMIM][NO_3] (x_2) + pyridine (x_1)} at T = (298.15, 303.15, 308.15, 313.15 and 318.15) K

x_1	ρ /(g ·cm^{-3})	V_m^E /(cm^3·mol^{-1})	u /(m·s^{-1})	κ_s / (10^{10} Pa^{-1})
		T = 298.15 K		
0.0000	1.15166	0.000	1743.8	2.86
0.1203	1.14598	-0.661	1735.1	2.90
0.2068	1.14027	-0.991	1721.4	2.96
0.3047	1.13145	-1.166	1703.0	3.05
0.4033	1.12126	-1.332	1681.2	3.16
0.7008	1.07292	-1.162	1585.6	3.71
0.7844	1.05469	-1.132	1574.0	3.96
0.8210	1.04579	-1.121	1529.6	4.09
0.8584	1.03394	-0.920	1506.8	4.26
0.8918	1.02319	-0.793	1487.5	4.42
0.9146	1.01510	-0.675	1473.8	4.54
0.9419	1.00477	-0.524	1456.7	4.69
0.9562	0.99893	-0.429	1441.5	4.78
0.9780	0.98929	-0.250	1433.2	4.92
1.0000	0.97827	0.000	1417.7	5.09
		T = 303.15 K		
0.0000	1.14844	0.000	1731.9	2.90
0.1203	1.14276	-0.684	1723.8	2.94
0.2068	1.13698	-1.020	1709.2	3.01

Table 5.1 continued

0.3047	1.12814	-1.209	1690.4	3.10
0.4033	1.11785	-1.379	1668.1	3.22
0.7008	1.06837	-1.119	1570.1	3.80
0.7844	1.05066	-1.156	1530.5	4.02
0.8210	1.04166	-1.071	1512.6	4.20
0.8584	1.02966	-0.961	1489.2	4.38
0.8918	1.01878	-0.828	1469.2	4.55
0.9146	1.01066	-0.712	1455.3	4.67
0.9419	1.00011	-0.547	1437.3	4.84
0.9562	0.99420	-0.447	1428.5	4.93
0.9780	0.98442	-0.261	1413.8	5.08
1.0000	0.97323	0.000	1397.7	5.26
		T = 308.15 K		
0.0000	1.14524	0.000	1720.1	2.95
0.1203	1.13959	-0.712	1711.8	2.99
0.2068	1.13372	-1.050	1696.9	3.06
0.3047	1.12419	-1.167	1677.8	3.16
0.4033	1.12419	-1.427	1654.9	3.28
0.7008	1.11445	-1.172	1554.4	3.89
0.7844	1.04663	-1.208	1513.9	4.17
0.8210	1.03753	-1.119	1495.6	4.31
0.8584	1.02538	-1.003	1471.5	4.50
0.8918	1.01436	-0.864	1451.1	4.68
0.9146	1.00614	-0.743	1436.7	4.82

Table 5.1 continued

0.9419	0.99545	-0.571	1418.8	4.99
0.9562	0.98945	-0.467	1409.1	5.09
0.9780	0.97954	-0.273	1394.1	5.25
1.0000	0.96819	0.000	1377.6	5.55
		T = 313.15 K		
0.0000	1.14206	0.000	1708.5	3.00
0.1203	1.13645	-0.741	1699.9	3.05
0.2068	1.13046	-1.080	1684.7	3.12
0.3047	1.12151	-1.290	1641.8	3.22
0.4033	1.11107	-1.477	1538.9	3.34
0.7844	1.04261	-1.261	1480.0	4.28
0.8210	1.03340	-1.168	1454.4	4.42
0.8584	1.02110	-1.047	1432.8	4.63
0.8918	1.00994	-0.902	1418.0	4.82
0.9146	1.00161	-0.775	1399.6	4.97
0.9419	0.99078	-0.596	1389.7	5.15
0.9562	0.98470	-0.487	1389.7	5.26
0.9780	0.97465	-0.285	1374.4	5.43
1.0000	0.96312	0.000	1065	5.62
		T = 318.15 K		
0.0000	1.13890	0.000	1698.2	3.04
0.1203	1.13333	-0.773	1688.0	3.10
0.2068	1.12723	-1.112	1678.6	3.15
0.3047	1.11821	-1.332	1652.6	3.27
0.4033	1.10769	-1.528	1629.0	3.40

Table 5.1 continued

0.7008	1.05687	-1.284	1523.7	4.08
0.7844	1.03859	-1.316	1481.3	4.39
0.8210	1.02927	-1.219	1469.1	4.50
0.8584	1.01681	-1.092	1438.0	4.76
0.8918	1.00550	-0.940	1414.4	4.97
0.9146	0.99707	-0.808	1398.8	5.13
0.9419	0.98610	-0.621	1380.1	5.32
0.9562	0.97994	-0.508	1369.9	5.44
0.9780	0.96975	-0.297	1354.5	5.62
1.0000	0.95805	0.000	1342.5	5.79

Table 5.2: Density, ρ , excess molar volume, V_m^E , speed of sound, *u*, and isentropic compressibility, κ_s , for the binary mixture {[BMIM][NO_3] (x_2) + acetonitrile (x_1)} at *T* = (298.15, 303.15, 308.15, 313.15 and 318.15) K

x_1	ρ /(g ·cm^{-3})	V_m^E /(cm^3·mol^{-1})	*u* /(m·s^{-1})	κ_s /(10^{10} Pa^{-1})
		T = 298.15 K		
0.0000	1.15166	0.000	1743.8	2.86
0.1237	1.13806	-0.246	1699.2	3.04
0.2754	1.11974	-0.849	1660.5	3.24
0.3576	1.10685	-1.093	1639.6	3.36
0.5881	1.05233	-1.345	1597.6	3.72
0.6609	1.02812	-1.420	1561.6	3.99
0.7144	1.00701	-1.464	1530.2	4.24
0.7930	0.96770	-1.394	1476.0	4.74
0.8650	0.92071	-1.230	1417.3	5.41
0.9241	086967	-0.917	1361.4	6.20
0.9653	0.82450	-0.552	1319.8	6.96
0.9835	0.80097	-0.313	1299.6	7.39
1.0000	0.77675	0.000	1279.8	7.86
		T = 303.15 K		
0.0000	1.14844	0.000	1731.9	2.90
0.1237	1.13481	-0.264	1694.2	3.07
0.2754	1.11635	-0.880	1659.5	3.25
0.3576	1.10340	-1.134	1629.9	3.41
0.5881	1.04865	-1.408	1583.3	3.80
0.6609	1.02430	-1.485	1546.7	4.08

Table 5.2 continued

0.7144	1.00308	-1.531	1515.0	4.34
0.7930	0.96353	-1.458	1459.8	4.87
0.8650	0.91626	-1.286	1400.0	5.57
0.9241	0.86490	-0.959	1343.3	6.41
0.9653	0.81943	-0.577	1300.7	7.21
0.9835	0.79574	-0.327	1280.3	7.67
1.0000	0.77133	0.000	1259.8	8.17
		T = 308.15 K		
0.0000	1.14524	0.000	1720.1	2.95
0.1237	1.13164	-0.294	1681.4	3.13
0.2754	1.11298	-0.913	1646.2	3.32
0.3576	1.09997	-1.176	1611.0	3.50
0.5881	1.04496	-1.473	1568.8	3.89
0.6609	1.02048	-1.554	1531.8	4.18
0.7144	0.99914	-1.601	1499.5	4.45
0.7930	0.95936	-1.525	1443.6	5.00
0.8650	0.91180	-1.346	1382.7	5.74
0.9241	0.86011	-1.004	1325.0	6.62
0.9653	0.81434	-0.605	1281.6	7.48
0.9835	0.79047	-0.343	1260.7	7.96
1.0000	0.76587	0.000	1241.0	8.48
		T = 313.15 K		
0.0000	1.14206	0.000	1708.5	3.00
0.1237	1.12843	-0.314	1668.5	3.18

Table 5.2 continued

0.2754	1.10962	-0.947	1630.8	3.39
0.3576	1.09654	-1.221	1603.2	3.55
0.5881	1.04129	-1.541	1554.5	3.97
0.6609	1.01667	-1.626	1516.8	4.28
0.7144	0.99521	-1.674	1484.0	4.56
0.7930	0.95520	-1.597	1427.3	5.14
0.8650	0.90734	-1.410	1365.5	5.91
0.9241	0.85532	-1.053	1306.7	6.85
0.9653	0.80923	-0.634	1262.5	7.75
0.9835	0.78519	-0.360	1241.2	8.27
1.0000	0.76037	0.000	1226.1	8.75
		T = 318.15 K		
0.0000	1.13890	0.000	1698.2	3.04
0.1237	1.12520	-0.331	1686.7	3.12
0.2754	1.10627	-0.982	1654.9	3.30
0.3576	1.09313	-1.267	1616.3	3.50
0.5881	1.03762	-1.612	1539.1	4.07
0.6609	1.01287	-1.700	1501.5	4.38
0.7144	0.99129	-1.752	1468.3	4.68
0.7930	0.95103	-1.671	1411.0	5.28
0.8650	0.90287	-1.475	1348.3	6.09
0.9241	0.85051	-1.103	1288.5	7.08
0.9653	0.80409	-0.665	1243.5	8.04
0.9835	0.77987	-0.378	1221.7	8.59

Table 5.2 continued

1.0000	0.75485	0.000	1216.8	8.95

Table 5.3: Density, ρ , excess molar volume, V_m^E , speed of sound, *u*, and isentropic compressibility, κ_s , for the binary mixture {[BMIM][NO_3] (x_2) + thiophene (x_1)} at T = (298.15, 303.15, 308.15, 313.15 and 318.15) K

x_1	ρ /(g ·cm^{-3})	V_m^E /(cm^3·mol^{-1})	u /(m·s^{-1})	κ_s /(10^{10} Pa^{-1})
		T = 298.15 K		
0.0000	1.15166	0.000	1743.8	2.86
0.2309	1.14450	-0.470	1697.4	3.03
0.3039	1.14314	-0.792	1671.1	3.13
0.4176	1.14059	-1.280	1624.7	3.32
0.4989	1.13829	-1.610	1624.7	3.47
0.5621	1.13387	-1.615	1572.0	3.57
0.6658	1.12575	-1.648	1526.7	3.81
0.7669	1.11189	-1.301	1486.3	4.07
0.8596	1.09146	-0.560	1456.0	4.32
0.9713	1.06006	0.406	1351.3	5.17
1.0000	1.05968	0.000	1277.4	5.78
		T = 303.15 K		
0.0000	1.14844	0.000	1731.9	2.90
0.2309	1.14117	-0.503	1684.1	3.09
0.3039	1.13974	-0.835	1666.2	3.16
0.4176	1.13703	-1.332	1618.4	3.36
0.4989	1.13461	-1.669	1580.6	3.53
0.5621	1.13008	-1.679	1552.7	3.67
0.6658	1.12170	-1.713	1511.0	3.90
0.7669	1.10730	-1.341	1520.2	3.91

Table 5.3 continued

0.8596	1.08594	-0.546	1507.4	4.05
0.9713	1.05409	0.422	1383.8	4.95
1.0000	1.05370	0.000	1253.7	6.01
		T = 308.15 K		
0.0000	1.14524	0.000	1720.1	2.95
0.2309	1.13784	-0.537	1664.4	3.17
0.3039	1.113634	-0.878	1628.7	3.32
0.4176	1.13347	-1.384	1582.9	3.52
0.4989	1.13093	-1.729	1547.2	3.69
0.5621	1.12631	-1.745	1521.5	3.84
0.6658	1.11766	-1.778	1495.0	4.00
0.7669	1.10259	-1.373	1462.3	4.24
0.8596	1.08026	-0.518	1423.6	4.57
0.9713	1.04810	0.438	1315.3	5.51
1.0000	1.04770	0.000	1236.2	6.25
		T = 313.15 K		
0.0000	1.14206	0.000	1708.5	3.00
0.2309	1.13453	-0.572	1625.6	3.34
0.3039	1.13297	-0.924	1592.7	3.48
0.4176	1.12993	-1.439	1560.9	3.63
0.4989	1.12725	-1.790	1527.0	3.80
0.5621	1.12254	-1.813	1519.1	3.86
0.6658	1.11362	-1.847	1480.9	4.09
0.7669	1.09720	-1.345	1449.3	4.34
0.8596	1.07512	-0.539	1416.0	4.64

Table 5.3 continued

0.9713	1.04208	0.455	1309.3	5.60
1.0000	1.04167	0.000	1216.8	6.48
		T = 318.15 K		
0.0000	1.13890	0.000	1698.2	3.04
0.2309	1.13124	-0.610	1605.3	3.43
0.3039	1.12639	-0.554	1592.5	3.50
0.4176	1.12639	-1.495	1579.7	3.56
0.4989	1.12359	-1.855	1536.9	3.77
0.5621	1.11879	-1.883	1499.1	3.98
0.6658	1.10956	-1.916	1472.3	4.16
0.7669	1.09245	-1.375	1436.3	4.44
0.8596	1.06953	-0.523	1385.0	4.87
0.9713	1.03602	0.473	1278.5	5.91
1.0000	1.03561	0.000	1198.5	6.72

Table 5.4: Refractive index, n, change in refractive index, Δn, molar refraction, R, for the binary mixture {[BMIM][NO_3] (x_2) + pyridine (x_1)} at T = (298.15, 303.15, 308.15, 313.15 and 318.15) K

x_1	n	Δn	R /($cm^3 \cdot mol^{-1}$)
	T = 298.15 K		
0.0000	1.49361	0.00000	0.00
0.1203	1.49695	0.00189	0.06
0.2068	1.49833	0.00223	0.06
0.3047	1.49984	0.00255	0.08
0.4033	1.50155	0.00308	0.09
0.7008	1.50581	0.00376	0.20
0.7844	1.50800	0.00494	0.29
0.8210	1.50763	0.00413	0.35
0.8584	1.50872	0.00477	0.45
0.8918	1.50882	0.00477	0.60
0.9146	1.50870	0.00407	0.78
0.9419	1.50837	0.00342	1.16
0.9562	1.50812	0.00299	1.56
0.9780	1.50760	0.00221	3.13
1.0000	1.50565	0.00000	0.00
	T = 303.15 K		
0.0000	1.49227	0.00000	0.00
0.1203	1.49551	0.00080	53.37
0.2068	1.49685	0.00135	57.73
0.3047	1.49999	0.00196	62.86
0.4033	1.50329	0.00271	68.69
0.7008	1.50639	0.00282	95.28
0.7844	1.50534	0.00317	106.34
0.8210	1.50625	0.00428	112.06
0.8584	1.50639	0.00495	119.03
0.8918	1.50644	0.00469	125.84

Table 5.4 continued

0.9146	1.50625	0.00430	130.98
0.9419	1.50585	0.00365	137.78
0.9562	1.50554	0.00321	141.65
0.9780	1.50492	0.00239	148.08
1.0000	1.50273	0.00000	0.00
	T = 308.15 K		
0.0000	1.49074	0.00000	0.00
0.1203	1.49409	0.00225	53.22
0.2068	1.49536	0.00273	57.58
0.3047	1.49683	0.00330	62.79
0.4033	1.49847	0.00403	68.54
0.7008	1.50184	0.00470	95.12
0.7844	1.50385	0.00595	106.18
0.8210	1.50318	0.00497	111.91
0.8584	1.50411	0.00552	118.90
0.8918	1.50406	0.00516	125.73
0.9146	1.50381	0.00471	130.89
0.9419	1.50332	0.00397	137.73
0.9562	1.50294	0.00345	141.62
0.9780	1.50224	0.00256	148.09
1.0000	1.49989	0.00000	0.00
	T = 313.15 K		
0.0000	1.48916	0.00000	0.00
0.1203	1.49265	0.00307	53.12
0.2068	149392	0.00377	57.48
0.3047	1.49530	0.00427	62.60
0.4033	1.49687	0.00452	68.47
0.7008	1.49985	0.00514	95.02
0.7844	1.50178	0.00641	106.08
0.8210	1.50096	0.00533	111.81
0.8584	1.50185	0.00589	118.82
0.8918	1.50174	0.00548	125.65

Table 5.4 continued

0.9146	1.50139	0.00498	130.84
0.9419	1.50077	0.00415	137.70
0.9562	1.50032	0.00358	141.61
0.9780	1.49952	0.00261	148.11
1.0000	1.49709	0.00000	0.00
	T = 318.15 K		
0.0000	1.48916	0.00000	0.00
0.1203	1.49265	0.00277	53.12
0.2068	1.49392	0.00352	57.47
0.3047	1.49530	0.00417	62.61
0.4033	1.49687	0.00495	68.40
0.7008	1.49985	0.00564	94.91
0.7844	1.50178	0.00686	105.96
0.8210	1.50096	0.00570	111.70
0.8584	1.50185	0.00625	118.72
0.8918	1.50171	0.00581	125.59
0.9146	1.50139	0.00527	130.78
0.9419	1.50077	0.00442	137.66
0.9562	1.50032	0.00383	141.59
0.9780	1.49952	0.00276	148.13
1.0000	1.49709	0.00000	0.000

Table 5.5: Refractive index, n, change in refractive index, Δn, molar refraction, R, for the binary mixture {[BMIM][NO_3] (x_2) + acetonitrile (x_1)} at T = (298.15, 303.15, 308.15, 313.15 and 318.15) K

x_1	n	Δn	R /($cm^3 \cdot mol^{-1}$)
	T = 298.15 K		
0.0000	1.49361	0.00000	0.00
0.1237	1.48821	0.01343	0.05
0.2754	1.48071	0.02901	0.06
0.3576	1.47556	0.03637	0.07
0.5881	1.45617	0.05206	0.12
0.6609	1.44626	0.05323	0.15
0.7144	1.43766	0.05277	0.19
0.7930	1.42149	0.04857	0.27
0.8650	1.40203	0.04006	0.45
0.9241	1.38074	0.02776	0.87
0.9653	1.36190	0.01520	2.08
0.9835	1.35183	0.00790	4.56
1.0000	1.34142	0.00000	0.00
	T = 303.15 K		
0.0000	1.49227	0.00000	0.00
0.1237	1.48613	0.01281	45.44
0.2754	1.47917	0.02909	57.99
0.3576	1.47398	0.03650	63.56
0.5881	1.45445	0.05228	85.25
0.6609	1.44445	0.05343	95.75
0.7144	1.43584	0.05302	105.52
0.7930	1.41955	0.04878	125.15
0.8650	1.39995	0.04020	152.07
0.9241	1.37861	0.02792	186.38
0.9653	1.35977	0.01540	222.40
0.9835	1.34959	0.00801	243.64
1.0000	1.33906	0.00000	0.000

Table 5.5 continued

	T = 308.15 K		
0.0000	1.49074	0.00000	0.00
0.1237	1.48449	0.01282	46.31
0.2754	1.47767	0.02938	57.90
0.3576	1.47246	0.03685	63.47
0.5881	1.45277	0.05268	85.09
0.6609	1.44272	0.05386	95.56
0.7144	1.43405	0.05343	105.30
0.7930	1.41768	0.04918	124.89
0.8650	1.39800	0.04059	151.79
0.9241	1.37647	0.02817	186.14
0.9653	1.35758	0.01564	222.26
0.9835	1.34722	0.00809	243.61
1.0000	1.33659	0.00000	0.00
	T = 313.15 K		
0.0000	1.48916	0.00000	0.00
0.1237	1.48283	0.01286	46.18
0.2754	147616	0.02970	57.81
0.3576	1.47092	0.03722	63.36
0.5881	1.45112	0.05315	84.92
0.6609	1.44102	0.05434	95.35
0.7144	1.43230	0.05391	105.07
0.7930	1.41585	0.04965	124.62
0.8650	1.39601	0.04097	151.50
0.9241	1.37432	0.02845	185.87
0.9653	1.35524	0.01576	222.11
0.9835	1.34483	0.00818	243.56
1.0000	1.33410	0.00000	0.00
	T = 318.15 K		
0.0000	1.48756	0.00000	0.00
0.1237	1.48124	0.01299	46.05
0.2754	147464	0.03004	57.71

Table 5.5 continued

0.3576	1.46961	0.03785	63.26
0.5881	1.44947	0.05366	84.73
0.6609	1.43934	0.05488	95.13
0.7144	1.43054	0.05443	104.82
0.7930	1.41398	0.05013	124.33
0.8650	1.39400	0.04138	151.17
0.9241	1.37218	0.02878	185.58
0.9653	1.35300	0.01604	221.92
0.9835	1.34239	0.00827	243.47
1.0000	1.33155	0.00000	0.00

Table 5.6: Refractive index, n, change in refractive index, Δn, molar refraction, R, for the binary mixture {[BMIM][NO_3] (x_2) + thiophene (x_1)} at T = (298.15, 303.15, 308.15, 313.15 and 318.15) K

x_1	n	Δn	R /($cm^3 \cdot mol^{-1}$)
	T = 298.15 K		
0.0000	1.49361	0.00000	0.00
0.2309	1.50190	0.00117	0.07
0.3039	1.50530	0.00231	0.07
0.4176	1.50968	0.00319	0.09
0.4989	1.51281	0.00381	0.11
0.5621	1.51587	0.00493	0.12
0.6658	1.51909	0.00495	0.16
0.7669	1.52191	0.00465	0.24
0.8596	1.52314	0.00303	0.42
0.9713	1.52482	0.00126	2.17
1.0000	1.52445	0.00000	0.00
	T = 303.15 K		
0.0000	1.49227	0.00000	0.00
0.2309	1.50053	0.00155	58.25
0.3039	1.50388	0.00278	62.57
0.4176	1.50794	0.00353	68.71
0.4989	1.51091	0.00414	73.94
0.5621	1.51260	0.00400	78.69
0.6658	1.51560	0.00398	87.76
0.7669	1.51800	0.00344	99.56
0.8596	1.52001	0.00277	114.39
0.9713	1.52257	0.00208	138.90
1.0000	1.52133	0.00000	0.00
	T = 308.15 K		
0.0000	1.49074	0.00000	0.00
0.2309	1.49803	0.00097	58.16

Table 5.6 continued

0.3039	1.50160	0.00200	62.50
0.4176	1.50498	0.00282	68.63
0.4989	1.50835	0.00396	73.58
0.5621	1.51045	0.00434	78.58
0.6658	1.51434	0.00539	87.64
0.7669	1.51625	0.00454	99.49
0.8596	1.51737	0.00313	114.47
0.9713	1.51940	0.00210	139.00
1.0000	1.51809	0.00000	0.00
	T = 313.15 K		
0.0000	1.48916	0.00000	0.00
0.2309	1.49690	0.00182	58.06
0.3039	149900	0.00204	62.42
0.4176	1.50351	0.00364	68.54
0.4989	1.50570	0.00374	73.75
0.5621	1.50789	0.00431	78.47
0.6658	1.51070	0.00446	87.51
0.7669	1.51200	0.00317	99.54
0.8596	1.51417	0.00297	114.42
0.9713	1.51613	0.00205	139.09
1.0000	1.51482	0.00000	0.00
	T = 318.15 K		
0.0000	1.48756	0.00000	0.00
0.2309	1.49460	0.00150	57.96
0.3039	1.49699	0.00214	62.72
0.4176	1.50088	0.00330	68.45
0.4989	1.50400	0.00447	73.65
0.5621	1.50581	0.00447	78.35
0.6658	1.50835	0.00481	87.39
0.7669	1.51024	0.00428	99.47
0.8596	1.51196	0.00377	114.47
0.9713	1.51188	0.00101	139.20

Table 5.6 continued

1.0000	1.51156	0.00000	0.00

The calculated of excess molar volumes was plotted against mole fraction for all the binary systems studied at T = (298.15, 303.15, 308.15, 313.15 and 318.15) K and are are given in Figures 5.1 to 5.3 together with the Redlich-Kister polynomial fit.

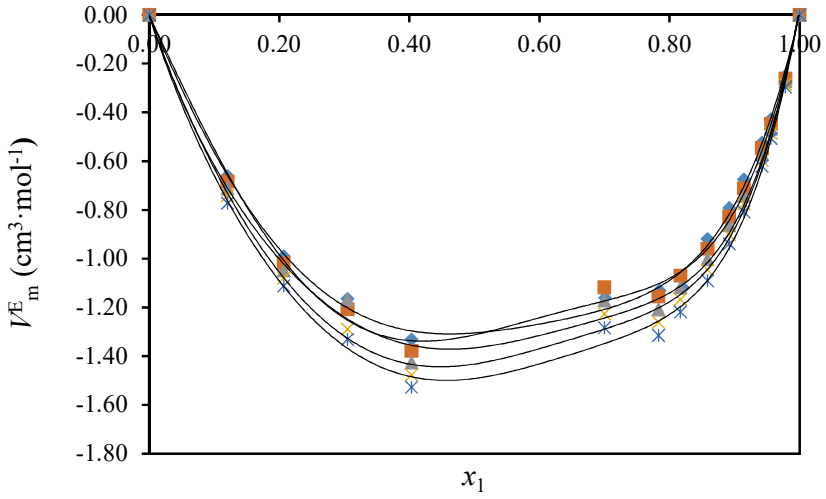

Figure 5.1: Plot of excess molar volumes, V_m^E, binary mixture of {[BMIM][NO_3] (x_2) + pyridine (x_1)} versus mole fraction x_1 of pyridine at T = 298.15 K; ◊, T = 303.15 K; □, T = 308.15 K;△, T = 313.15 K; X and, ✳ T = 318.15 K. The solid lines were produced utilizing the Redlich-Kister smoothing polynomial

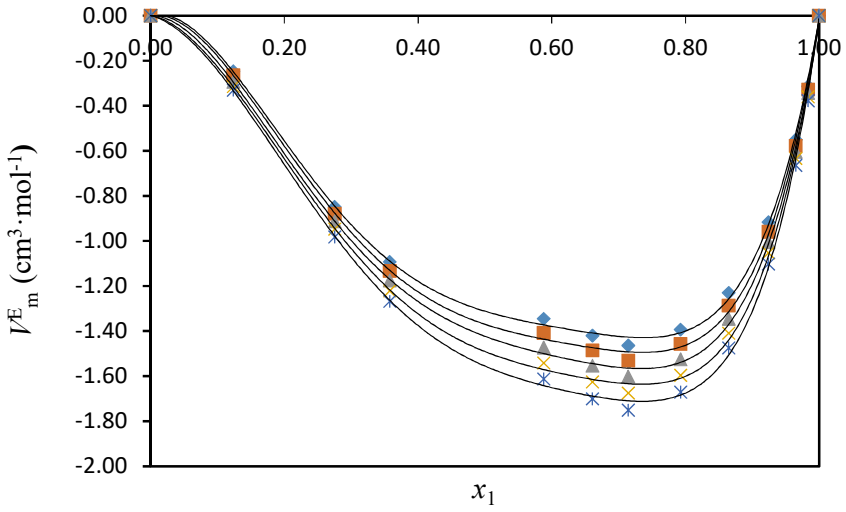

Figure 5.2: Graph of excess molar volumes, V_m^E, binary mixture of {[BMIM][NO_3] (x_2) + acetonitrile (x_1)} versus mole fraction x_1 of acetonitrile at T = 298.15 K; ◊, T = 303.15 K;□, T = 308.15 K;△, T = 313.15 K; X and, ✳ T = 318.15 K. The solid lines were produced utilizing the Redlich-Kister smoothing polynomial

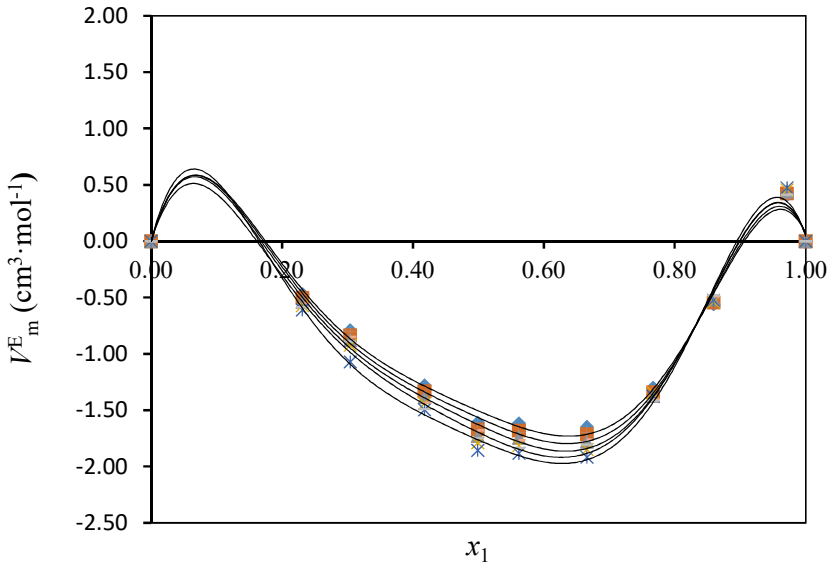

Figure 5.3: Graph of excess molar volumes, V_m^E, binary mixture of {[BMIM][NO_3] (x_2) + thiophene (x_1)} versus mole fraction x_1 of thiophene at T = 298.15 K; ◊, T = 303.15 K;□ , T = 308.15 K;△ , T = 313.15 K; X and , ✳ T = 318.15 K. The solid lines were produced utilizing the Redlich-Kister smoothing polynomial

The graphs of isentropic compressibility versus mole fraction for all the binary systems studied at T = (298.15, 303.15, 308.15, 313.15 and 318.15) K are given in Figures 5.4 to 5.6.

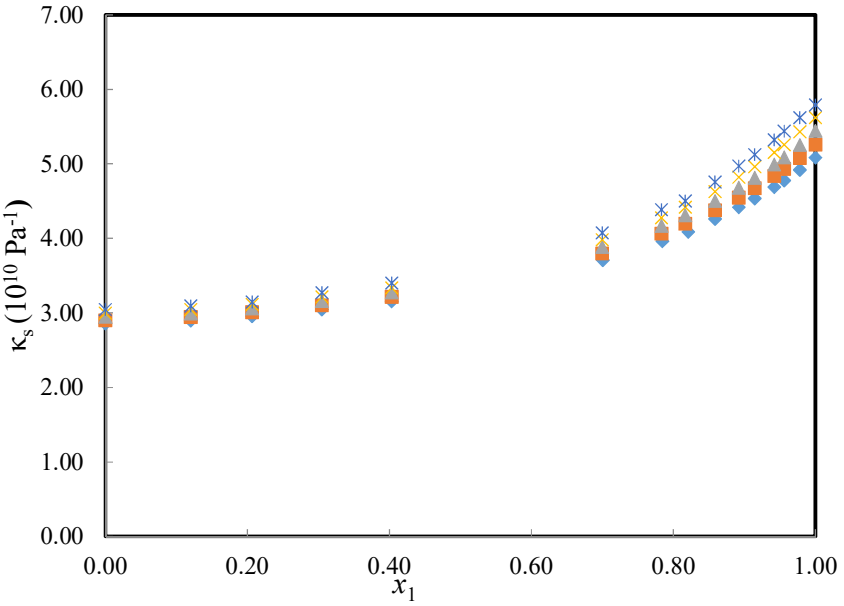

Figure 5.4: Plot of isentropic compressibility, κ_s, of the binary mixture of {[BMIM][NO_3] (x_2) + pyridine (x_1)} versus mole fraction x_1 of pyridine at T = 298.15 K; ◊, T = 303.15 K; □, T = 308.15 K;Δ , T = 313.15 K; X and , ✳ T = 318.15 K

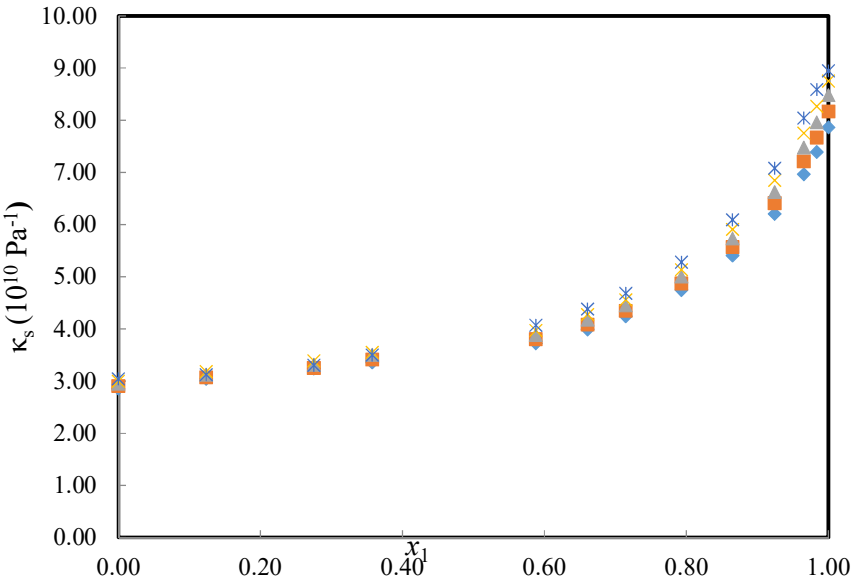

Figure 5.5: Plot of isentropic compressibility, κ_s, of the binary mixture of {[BMIM][NO_3] (x_2) +acetonitrile (x_1)} versus mole fraction x_1 of acetonitrile at T = 298.15 K; ◊, T = 303.15 K; □, T = 308.15 K;Δ , T = 313.15 K; X and , ✳ T = 318.15 K

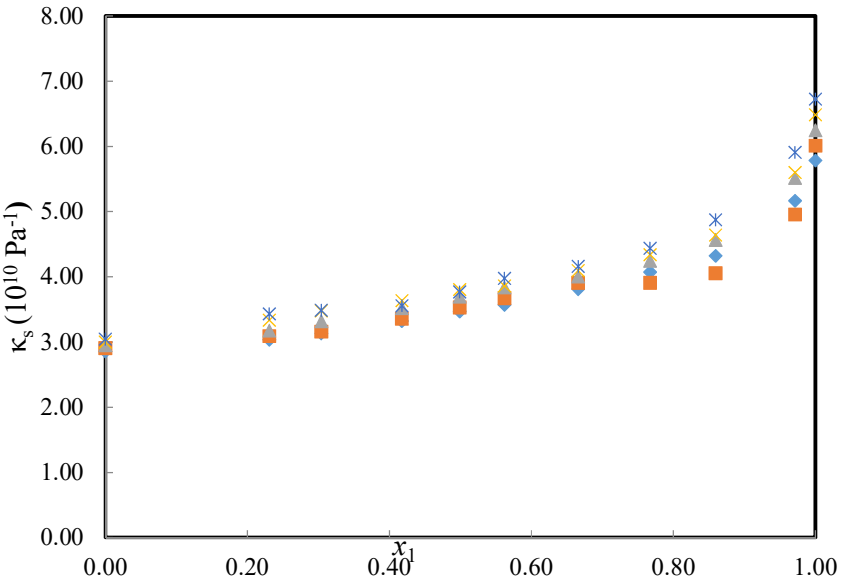

Figure 5.6: Plot of isentropic compressibility, κ_s, of the binary mixture of {[BMIM][NO_3] (x_2) + thiophene (x_1)} versus mole fraction x_1 of thiophene at T = 298.15 K; ◊, T = 303.15 K; □, T = 308.15 K; Δ, T = 313.15 K; X and , ✳ T = 318.15 K

The calculated change in refractive index was plotted against mole fraction for all the binary systems studied at T = (298.15, 303.15, 308.15, 313.15 and 318.15) K and are given in Figure 5.7 to 5.9 together with the Redlich-Kister polynomial fit.

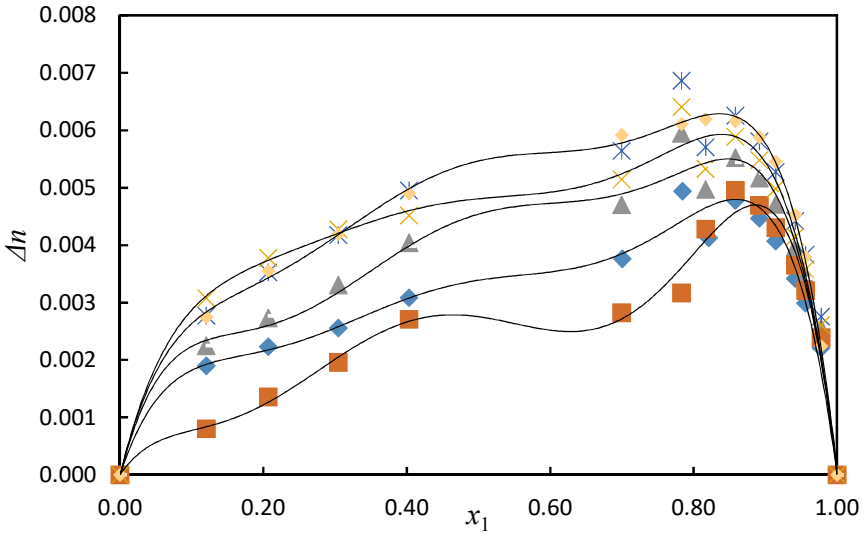

Figure 5.7: Graph of change in refractive index, Δn, of the binary mixture of {[BMIM][NO_3] (x_2) + pyridine (x_1)} versus mole fraction x_1 of pyridine at T = 298.15 K;◊, T = 303.15 K;□ , T = 308.15 K;△ , T = 313.15 K; X and , ✳ T = 318.15 K. The solid lines were produced utilizing the Redlich-Kister smoothing polynomial

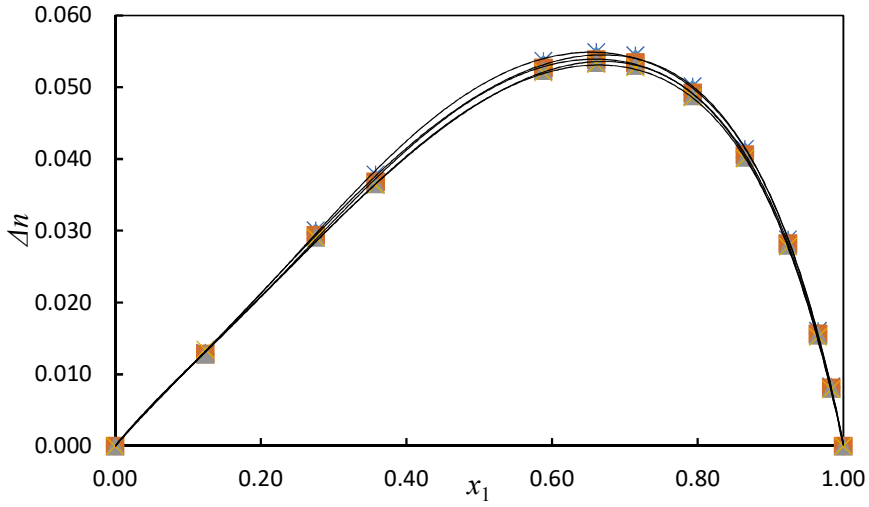

Figure 5.8: Graph of change in refractive index, Δn, of the binary mixture of {[BMIM][NO_3] (x_2) + acetonitrile (x_1)} versus mole fraction x_1 of acetonitrile at T = 298.15 K;◊, T = 303.15 K; □, T = 308.15 K; Δ, T = 313.15 K; X and, ✳ T = 318.15 K. The solid lines were produced utilizing the Redlich-Kister smoothing polynomial

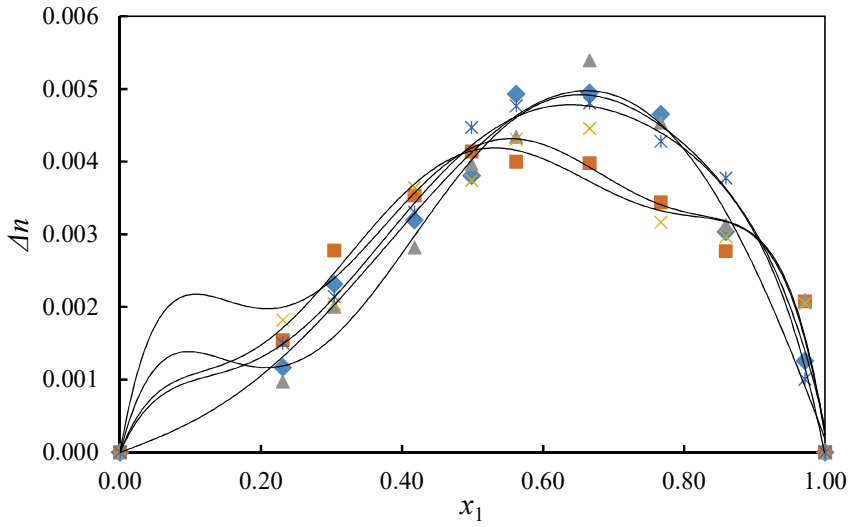

Figure 5.9: Graph of change in refractive index, Δ*n,* of the binary mixture of {[BMIM][NO_3] (x_2) + thiophene (x_1)} versus mole fraction x_1 of thiophene at T = 298.15 K;◊, T = 303.15 K; □, T = 308.15 K;△ , T = 313.15 K; X and , ✳ T = 318.15 K. The solid lines were produced utilizing the Redlich-Kister smoothing polynomial

The Redlich- Kister fitting parameters were calculated from equation (3.14):

$$Z = x_1 x_2 \sum_{i=0}^{N} A_i (2x-1)^i , \qquad (3.12)$$

where Z is the V_m^E or Δn; x_1 is the mole fraction of the pyridine or acetonitrile or thiophene; x_2 is the mole fraction of [BMIM][NO_3]; N is the degree of the polynomial expansion; and A_i is the Redlich–Kister parameters obtained for the system.

The root mean square deviation was calculated from equation (3.15)

$$\sigma = \left(\frac{\sum_{i}^{m} (Z_{\exp} - Z_{cal})}{M-k} \right)^{1/2} \qquad (3.13)$$

where Z_{exp}, Z_{cal}, are the values of the experimental and computed V_m^E or Δn and M is the number of experimental data points and k is the number of coefficients used in the Redlich-Kister correlation, respectively.

The Redlich-Kister parameters and the root mean square deviation for all binary systems are given in Table 5.7.

Table 5.7: Redlich- Kister fitting parameters and root-mean-square deviation, σ, for the binary mixtures at T = (298.15, 303.15, 308.15, 313.15 and 318.15) K

	T/K	A_0	A_1	A_2	A_3	A_4	A_5	σ
				{[BMIM][NO_3] (x_2) + pyridine (x_1)}				
V_m^E/($cm^3 \cdot mol^{-1}$)	298.15	-5.201	-0.898	-2.725	6.189	-1.560	-4.205	0.0356
	303.15	-5.250	-1.793	-2.311	9.032	-2.844	-6.395	0.0303
	308.15	-5.493	-1.282	-1.298	8.471	-4.960	-7.000	0.0446
	313.15	-5.695	-1.651	-2.178	9.434	-3.674	-7.063	0.0311
	318.15	-5.929	-1.568	-2.098	9.625	-4.151	-7.451	0.0315
Δn	298.15	0.014	-0.006	0.004	-0.009	0.045	-0.017	0.00031
	303.15	0.011	0.003	-0.008	-0.046	0.060	-0.002	0.00027
	308.15	0.018	-0.009	0.001	-0.004	0.052	-0.052	0.00035
	313.15	0.019	-0.007	0.015	-0.003	0.039	-0.035	0.00035
	318.15	0.022	-0.010	0.004	0.001	0.051	-0.034	0.00037
				{[BMIM][NO_3] (x_2) + acetonitrile (x_1)				
V_m^E ($cm^3 \cdot mol^{-1}$)	298.15	-5.116	2.392	-3.538	2.360	1.440	6.724	0.0258
	303.15	-5.342	2.583	-3.570	2.335	1.157	6.876	0.0265
	308.15	-5.575	2.805	-3.587	2.179	0.645	7.006	0.0276
	313.15	-5.821	3.010	-3.635	2.179	0.307	7.186	0.0284
	318.15	-6.071	3.249	-3.743	2.010	0.115	7.645	0.0298
Δn	298.15	0.190	-0.130	0.062	0.018	0.041	-0.099	0.00014
	303.15	0.190	-0.131	0.066	0.026	0.025	-0.125	0.00016
	308.15	0.192	-0.132	0.068	0.027	0.023	-0.131	0.00017
	313.15	0.194	-0.133	0.070	0.026	0.019	-0.134	0.00017
	318.15	0.196	-0.132	0.067	0.017	0.026	-0.127	0.00019
				{[BMIM][NO_3] (x_2) + thiophene (x_1)}				

Table 5.7 continued

V_m^E/(cm^3·mol^{-1})	298.15	-6.257	3.402	5.286	17.964	-4.519	-49.579	0.0472
	303.15	-6.490	3.656	4.879	16.717	-2.580	-48.152	0.0421
	308.15	-6.727	3.977	4.468	14.753	-0.281	-45.679	0.0421
	313.15	-7.000	4.114	5.238	13.515	-1.261	-44.831	0.0597
	318.15	-7.467	6.086	19.623	19.008	-45.987	-87.458	0.0658
Δn	298.15	0.016	-0.023	0.023	-0.058	-0.082	-0.132	0.00021
	303.15	0.016	-0.010	0.009	-0.055	-0.059	-0.174	0.00020
	308.15	0.015	-0.030	0.032	0.113	-0.114	-0.244	0.00024
	313.15	0.016	-0.018	0.011	-0.074	0.012	-0.134	0.00030
	318.15	0.017	-0.015	-0.016	-0.012	0.050	0.037	0.00017

5.2 Correlations and Predictions

The Lorentz–Lorenz expression (3.20) was used in calculating the density ρ that is associated with the refractive index *n*, by:

$$\rho = \frac{\left(\frac{n^2-1}{n^2+2}\right)(x_1M_1 + x_2M_2)}{\left(\frac{n_1^2-1}{n_1^2+2}\right)x_1\frac{M_1}{\rho_1} + x_2\left(\frac{n_2^2-1}{n_2^2+2}\right)\frac{M_2}{\rho_2}} \tag{3.20}$$

By utilizing expression (3.19), *n* can be predicted from pure component density and refractive index data and from the experimental density of the mixture. The expression for *n* is presented as follows:

$$n = \left(\frac{2\left[\left(\frac{n_1^2-1}{n_2^2-1}+\right)x_1\rho\frac{M_1}{M_1} + x_2\left(\frac{n_1^2-1}{n_2^2-1}+\right)\rho\frac{M_2}{M_2}\right] + \left[x_1M_1 + x_2M_2\right]}{\left[x_1M_1 + x_2M_2\right] - \left[\left(\frac{n_1^2-1}{n_2^2-1}+\right)x_1\rho\frac{M_1}{\rho_1} + x_2\left(\frac{n_1^2-1}{n_2^2-1}+\right)\rho\frac{M_2}{\rho_2}\right]}\right)^{1/2} \tag{3.19}$$

Table 5.8 enumerates the root mean square deviation, σ for excess molar volume, density and refractive index for the binary mixtures at T = (298.15, 303.15, 308.15, 313.15 and 318.15) K obtained by using the Lorentz-Lorenz equations.

Root square mean equation can be expressed mathematically as follows:

$$\sigma = \sqrt{\frac{1}{n}\sum_{i=1}^{n}(x_i - \bar{x}_i)^2} \tag{5.4}$$

where x_i is the set of n random variables, and $\bar{x}_i$ the corresponding set of accepted values.

Table 5.8: Root mean square deviation, σ, obtained from the Lorentz-Lorenz expression, for V_m^E, ρ and n for the binary mixtures at T = (298.15, 303.15, 308.15, 313.15 and 318.15) K

	σ				
Properties	T/K				
	298.15	303.15	308.15	313.15	318.15
	{[BMIM][NO_3] (x_2) + pyridine (x_1)}				
V_m^E /($cm^3 \cdot mol^{-1}$)	0.745	0.738	0.717	0.670	0.681
ρ /($g \cdot cm^{-3}$)	0.00088	0.00457	0.00810	0.01205	0.01616
n	0.01201	0.01110	0.011197	0.01195	0.01193
	{[BMIM][NO_3] (x_2) + acetonitrile (x_1)				
V_m^E /($cm^3 \cdot mol^{-1}$)	0.584	0.551	0.522	0.492	0.512
ρ /($g \cdot cm^{-3}$)	0.11537	0.11908	0.12271	0.12638	0.13527
n	0.00207	0.00197	0.00201	0.00207	0.00217
	{[BMIM][NO_3] (x_2) + thiophene (x_1)}				
V_m^E /($cm^3 \cdot mol^{-1}$)	0.763	0.685	0.710	0.431	0.510
ρ /($g \cdot cm^{-3}$)	0.00427	0.00422	0.00438	0.00447	0.00509
n	0.00292	0.00251	0.00277	0.00240	0.00230

5.3 Activity Coefficients at Infinite Dilution

The results for activity coefficients at infinite dilution for selected solutes in 1-butyl-3-methylimidazolium hydrogen sulphate are given in Table 5.9. The activity coefficients at infinite dilution were calculated equation using equation 3.34 and is given below for convenience. Figures 5.10 to 5.17 are the graphs of $\ln\gamma_{13}^{\infty}$ versus $1/T$ for IL: 1-butyl-3-methylimdazolium hydrogen sulfate which was used for the computation of partial molar enthalpy at infinite dilution using the Gibbs-Helmoltz equation (equation 3.44).

$$ln\gamma_{13}^{\infty} = ln\frac{n_3RT}{V_N P_1^*} - \frac{(B_{11} - V_1^*)P^*}{RT} + \frac{P_0 J_2^3(2B_{12} - V_1^{\infty})}{RT}$$

The partial molar enthalpies at infinite dilution were computed using the following equation and were given in Table 5.10.

$$\left[\frac{\partial In\gamma_i^{\infty}}{\partial(1/T)}\right] = \frac{\Delta H_1^{E\infty}}{R}$$

The selectivity and capacity at infinite dilution, were computed using equations for different solutes separation problems and is given in Table 5.11 and 5.12, respectively. The equations are given in 3.46 and 3.47 repeated below for convenience.

$$S_{ij,s}^{\infty} = \frac{\gamma_i^{\infty}}{\gamma_j^{\infty}}$$

$$k_j^{\infty} = \frac{1}{\gamma_j^{\infty}}$$

Table 5.9: Activity coefficients at infinite dilution for selected solutes (1) in 1-butyl-3-methylimidazolium hydrogen sulfate (3) at T = (313.15, 323.15 and 333.15) K and n_3 = 0.0127 mol (40.0%)

Solutes	n_3/mol	T = 313,15 K	T = 323,15 K	T = 333,15 K
		γ_{13}^{∞}		
n-Pentane	0.0127	354.049	782.150	1697.065
n-Hexane	0.0127	582.826	791.079	809.259
n-Heptane	0.0127	868.564	675.474	987.426
n-Octane	0.0127	1279.319	1267.843	1035.184
Cyclopentane	0.0127	187.112	195.625	144.798
Cyclohexane	0.0127	305.742	230.432	154.564
Cyclooctane	0.0127	451.857	372.679	322.115
Benzene	0.0127	7.077	6.497	6.336
Toluene	0.0127	13.102	12.909	12.516
o-Xylene	0.0127	21.025	21.298	20.578
m-Xylene	0.0127	28.144	27.531	26.072
p-Xylene	0.0127	26.270	26.203	24.895
Methanol	0.0127	3.630	4.959	4.743
Ethanol	0.0127	1.132	1.133	1.106
1-Propanol	0.0127	1.899	1.822	1.759
Hex-1-ene	0.0127	296.700	246.050	268.450
Non-1-ene	0.0127	582.790	589.690	777.160
Dec-1-ene	0.0127	590.230	597.490	887.660
Hex-1-yne	0.0127	29.481	22.051	28.809

Table 5.9 continued

Hept-1-yne	0.0127	41.415	43.218	43.965
Octy-1-yne	0.0127	20.990	23.342	35.394
Pyridine	0.0127	33.429	22.677	20.947
Thiophene	0.0127	3.181	3.333	3.308
Acetonitrile	0.0127	3.171	3.176	3.288
Dichloromethane	0.0127	0.221	0.261	0.311
Acetone	0.0127	7.686	3.619	3.519
3-Pentanone	0.0127	12.333	12.363	11.853
Ethylacetate	0.0127	13.715	13.733	12.942

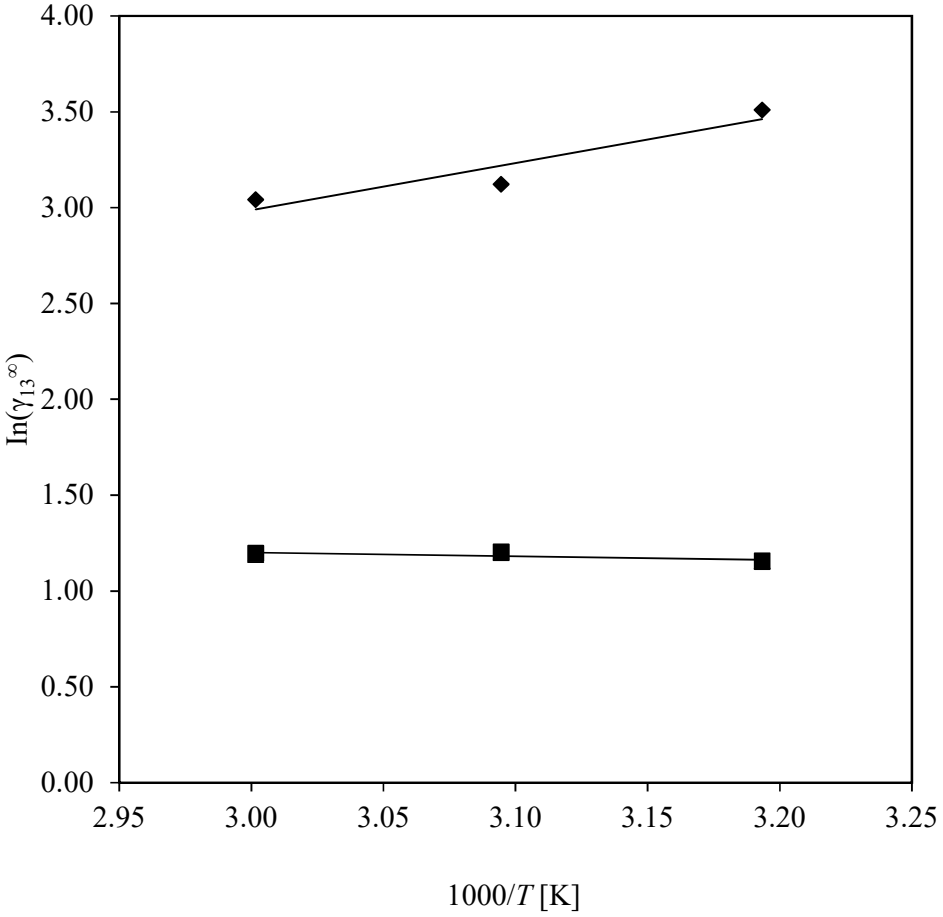

Figure 5.10: Graph of $\mathbf{ln\gamma_{13}^{\infty}}$ against $1/T$ of various solutes (1); acetonitrile (Δ), thiophene (■) and pyridine (♦) in IL: 1-butyl-3-methyimidazolium hydrogen sulfate (3)

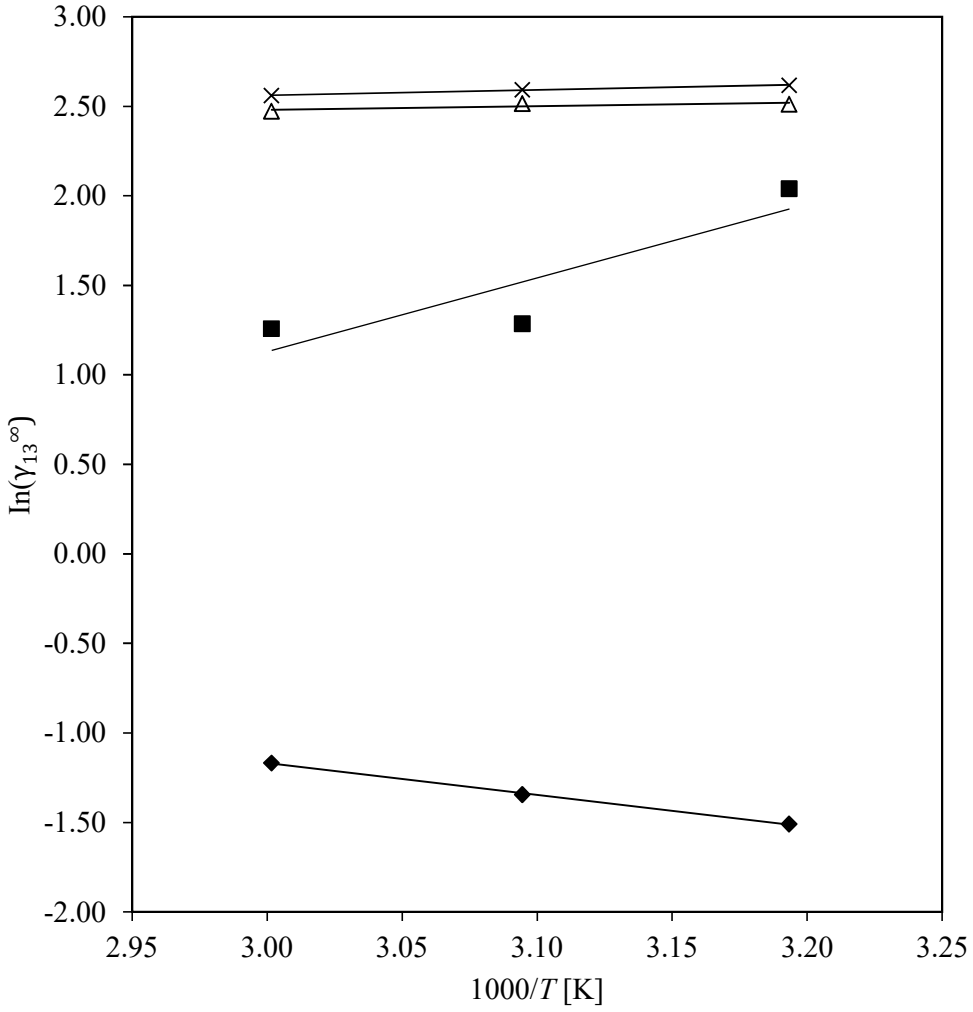

Figure 5.11: Graph of $\mathbf{ln\gamma_{13}^{\infty}}$ against 1/T of various solutes (1); 3-pentanone (Δ), acetone (■), ethylacetate (×) and dichloromethane (♦) in IL: 1-butyl-3-methyimidazolium hydrogen sulfate (3)

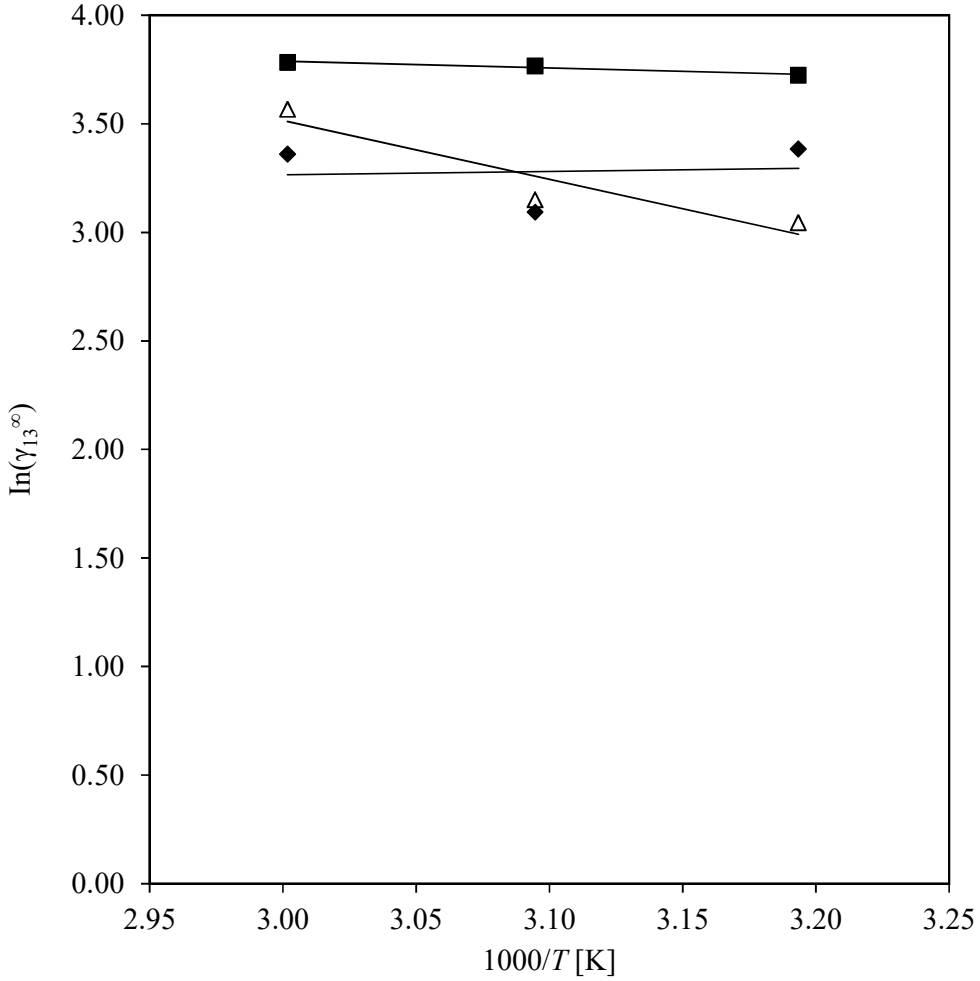

Figure 5.12: Graph of $\mathbf{ln\gamma_{13}^{\infty}}$ against 1/*T* of various solutes (1); octy-1-yne (Δ), hept-1-yne (■) and hex-1-yne (♦) in IL: 1-butyl-3-methyimidazolium hydrogen sulfate (3)

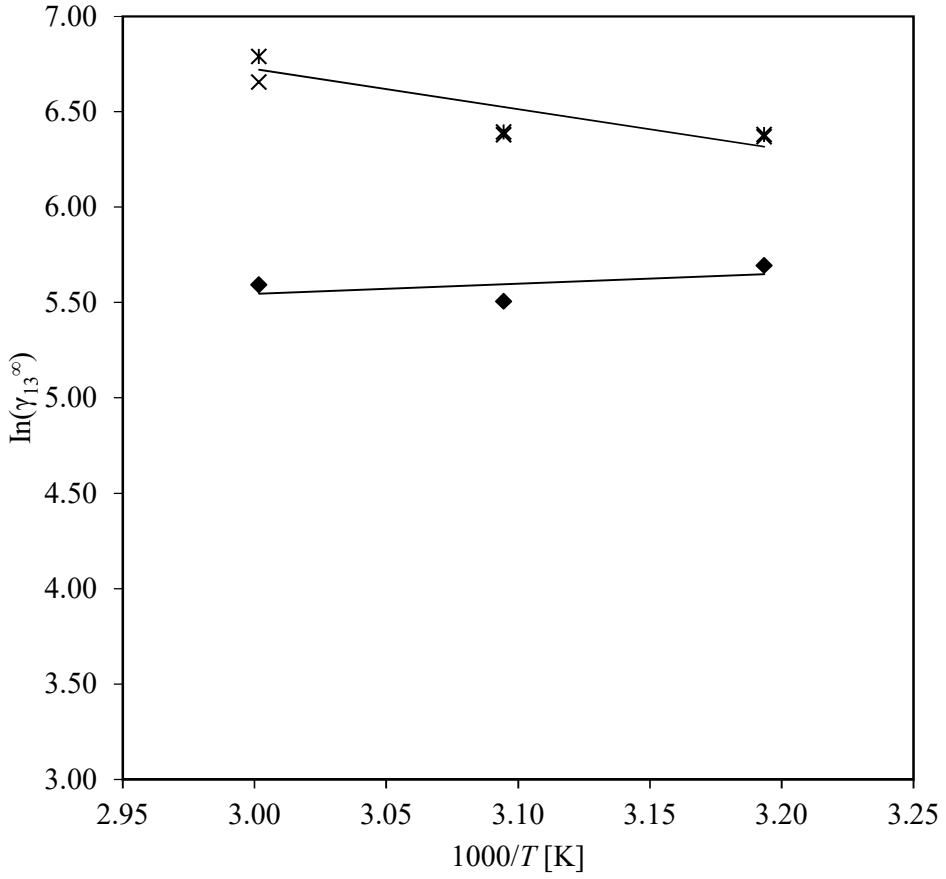

Figure 5.13: Graph of $\mathbf{ln\gamma_{13}^{\infty}}$ against $1/T$ of various solutes (1); non-1-ene (×), dec-1-ene (∗) and hex-1-ene (♦) in IL: 1-butyl-3-methyimidazolium hydrogen sulfate (3)

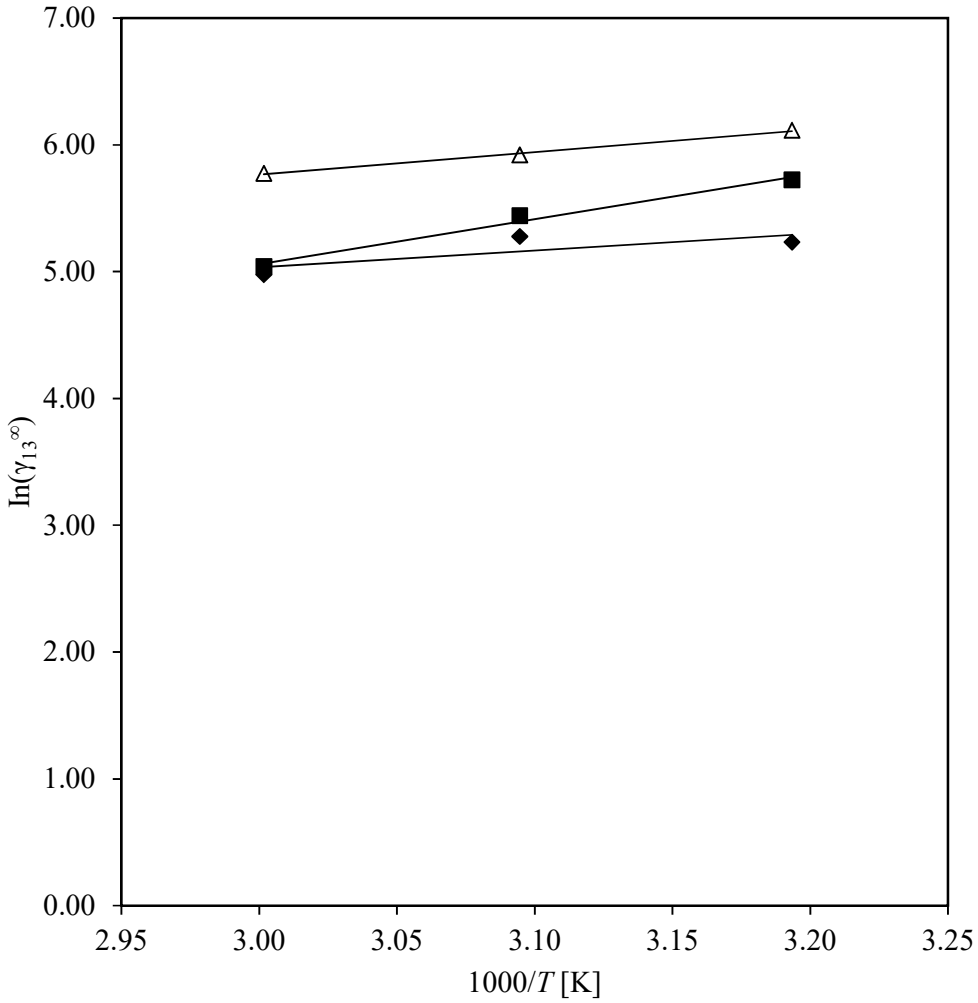

Figure 5.14: Graph of $\mathbf{ln\gamma_{13}^{\infty}}$ against 1/*T* of various solutes (1); cyclooctane (Δ), cyclohexane (■) and cyclopentane (♦) in IL: 1-butyl-3-methyimidazolium hydrogen sulfate (3)

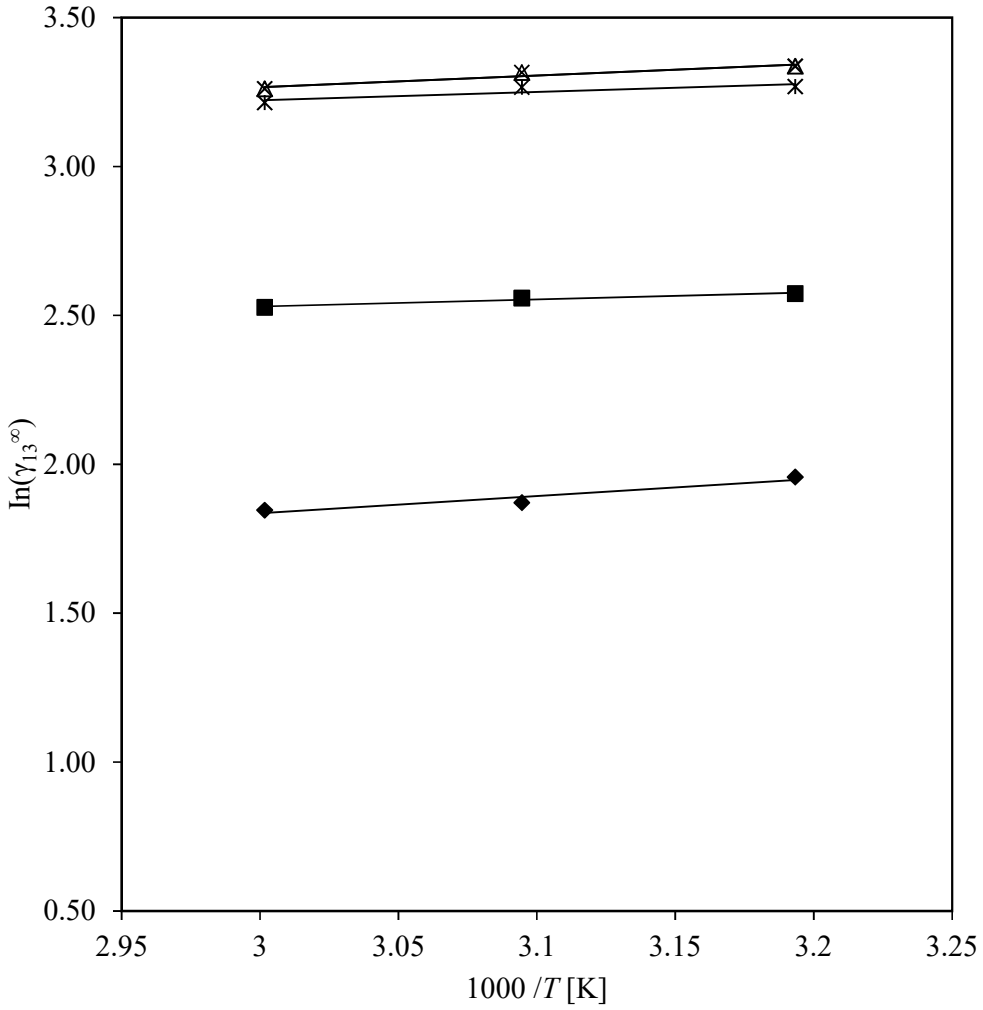

Figure 5.15: Graph of $\mathbf{ln\gamma_{13}^{\infty}}$ against 1/T of various solutes (1); o-xylene (Δ), toluene (■), m-xylene (×), p-xylene (∗) and benzene (♦) in IL: 1-butyl-3-methyimidazolium hydrogen sulfate (3)

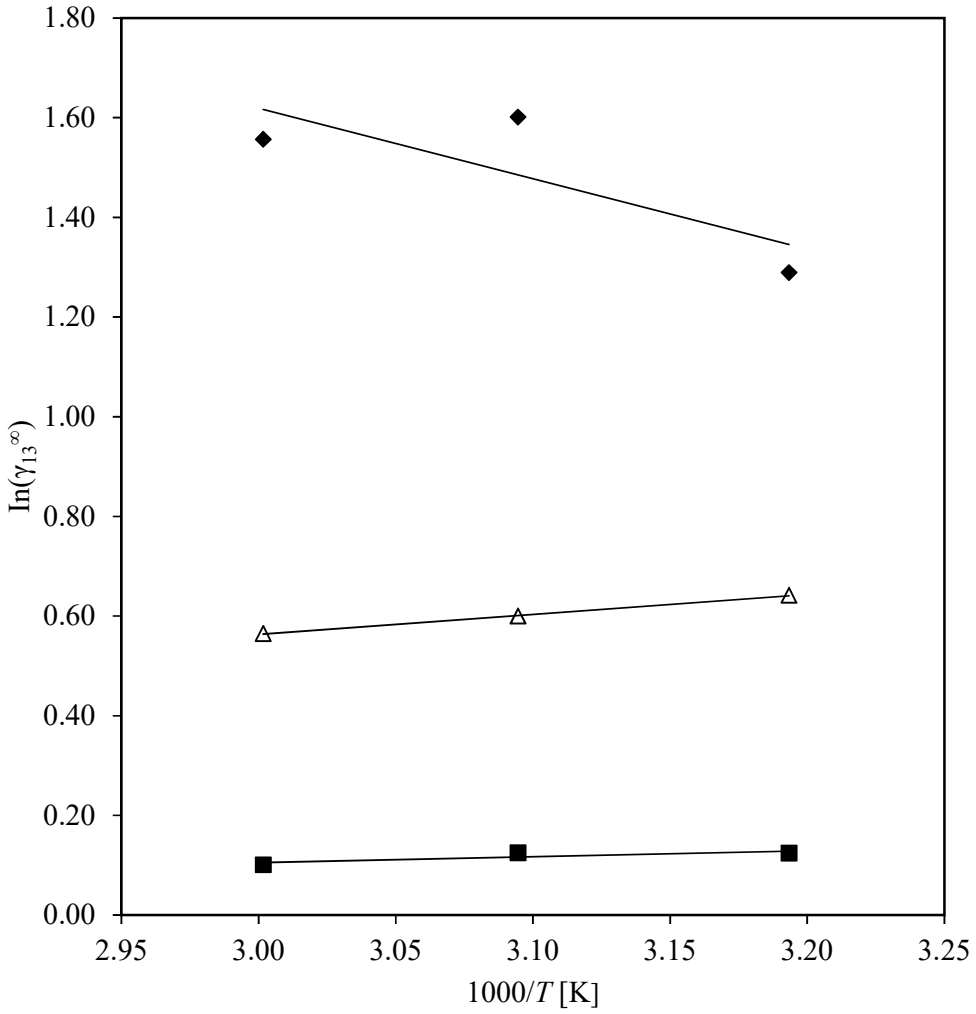

Figure 5.16: Graph of $\mathbf{ln\gamma_{13}^{\infty}}$ against 1/T of various solutes (1); 1-propanol (Δ), ethanol (■) and methanol (♦) in IL: 1-butyl-3-methyimidazolium hydrogen sulfate (3)

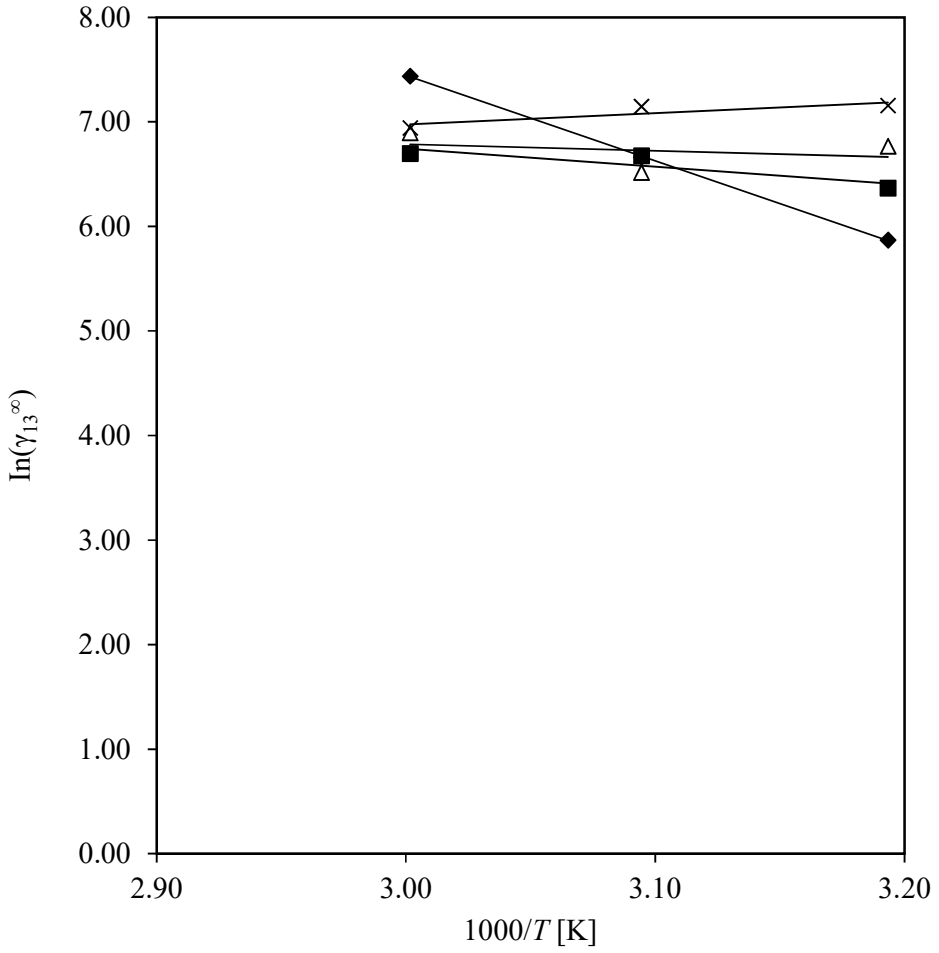

Figure 5.17: Graph of $\mathbf{ln\gamma_{13}^{\infty}}$ against 1/*T* of various solutes (1); heptane (Δ), hexane (■), octane (×), and pentane (♦) in IL: 1-butyl-3-methyimidazolium hydrogen sulfate (3).

Table 5.10 lists the partial molar excess enthalpies at infinite dilution of selected organic solutes in [BMIM][HSO_4].

Table 5.10: Partial molar excess enthalpies at infinite dilution, $\Delta \boldsymbol{H_1^{E,\infty}}$ for organic solutes in 1-butyl-3-methylimidazolium hydrogen sulfate, computed using the Gibbs-Helmholtz (equation 3.44)

Solutes	$\Delta H_1^{E,\infty} kJ.mol^{-1}$	R^2
n-Pentane	-67.950	1.00
n-Hexane	-14.357	0.82
n-Heptane	-5.279	0.10
n-Octane	9,094	0.77
Cyclopentane	10.960	0.61
Cyclohexane	29.521	0.99
Cyclooctane	14.695	1.00
Benzene	4.817	0.92
Toluene	1.979	0.95
o-Xylene	3.301	0.93
m-Xylene	3.301	0.93
p-Xylene	2.310	0.77
Methanol	-11.754	0.65
Ethanol	1.000	0.72
1-Propanol	3.325	1.00
Hex-1-ene	4.459	0.30
Non-1-ene	-12.360	0.77
Dec-1-ene	-17.520	0.76
Hex-1-yne	1.249	0.01
Hept-1-yne	-2.602	0.95
Octy-1-yne	-22.515	0.88
Pyridine	20.403	0.88
Thiophene	-1.723	0.63
Acetonitrile	-1.598	0.59
Dichloromethane	-14.796	0.99
Acetone	34.200	0.79
3-Pentanone	1.702	0.70
Ethylacetate	2.512	0.99

Table 5.11: Selectivity at infinite dilution at T = 323.15 K for the ionic liquid studied in this research, industrial separation agents and for other ionic liquids for different separation problems

	Selectivity at infinite dilution, S_{12}^{∞}								
	hexane/ benzene	heptane/ benzene	he/benzene	methanol/ benzene	ethanol/ benzene	hexane/ hex-1-ene	heptane/ pyridine	heptane/ thiophene	methanol/ acetone
[BMIM][HSO_4] (This work)	121.77	103.97	35.47	0.76	0.17	3.22	29.79	202.67	1.37
[1][BMIM][CH_3SO_4]	10.82	24.05	9.02	-	-	-	-	-	-
[2][BMIM][SbF_6]	20.53	26.32	11.13	1.26	1.67	2.01	-	-	3.72
[3][BMIM][NFf_2]	14.05	19.42	8.34	1.33	1.56	1.78	-	-	3.18
[4][BMIM][SCN]	71.28	91.05	20.28	0.18	0.31	3.26	-	156.90	-
[5][EMIM][CF_3SO_4]	29.79	43.39	14.15	0.31	0.50	2.33	-	-	-
[6][EMIM][$MDEGSO_4$]	39.00	60.83	17.23	0.16	0.28	3.38	-	-	0.25
[7][HDABCO][NTf_2]	12.72	15.45	6.25	1.34	1.59	-	25.88	-	-
[8][N_{1112}OH] [NTf_2]	25.97	40.66	13.03	0.33	0.46	2.24	332.88	50.11	2.28
[9][BMMOR][TCM]	34.95	52.23	14.10	0.52	0.80	2.40	108.00	78.51	1.08
[10]Sulfolane	16.84	22.16	8.33	0.86	1.16	-	45.73	-	1.25
[11]NMP	10.38	-	6.48	-	-	0.81	-	-	-

[1](Ge *et al.* 2014), [2](Olivier *et al.* 2011), [3]Singh *et al.* (2016), [4](Domańska and Laskowska 2009), [4](Domańska and Laskowska 2009), [5](Olivier *et al.* 2010),[4](Domańska and Laskowska 2009), [6](Bahadur *et al.* 2014), [7](Marcinkowski, Kloskowski and Namieśnik 2014), [8](Domańska, Królikowski and Acree 2011), [9](Domańska, Wlazło and Karpińska 2016) , [10](Möllmann and Gmehling 1997), [11](Krummen, Gruber and Gmehling 2000).

Table 5.12: Capacity at infinite dilution at T = 323.15 K for the ionic liquid studied in this research, industrial separation agents and other ionic liquids for different separation problems

	Limiting capacity, k_2^{∞}				
	benzene	hex-1-ene	pyridine	thiophene	acetone
[BMIM][HSO_4]	0.154	0.004	0.044	0.300	0.276
[BMIM][CH_3SO_4]	0.177	-	-	-	0.250
[BMIM][SbF_6]	0.752	0.074	-	-	2.212
[BMIM][NFf_2]	1.099	0.139			2.63
[BMIM][SCN]	0.461	0.022	-	0.788	-
[EMIM][CF_3SO_4]	0.446	0.040			
[EMIM][$MDEGSO_4$]	0.415	0.023	-		0.680
[HDABCO][NTf_2]	0.910	-	1.522	-	-
[N_{1112}OH] [NTf_2]	0.397	0.450	3.048	0.488	2.551
[BMMOR][TCM]	0.645	0.047	1.337	0.962	1.333
Sulfolane	0.432	-	0.954	-	0.648
NMP	0.952	0.166			-

Chapter 6

DISCUSSION

6.1 Density

6.1.1 Effect of Temperature on Density

It was observed that the density for all binary mixtures decrease with an increase in temperature (Table 5.1-5.3). The plot of experimental density, ρ, for binary systems ([BMIM][NO_3] + pyridine) or ([BMIM][NO_3] + acetonitrile) and ([BMIM][NO_3] + thiophene) at at T = 298.15 K;◊, T = 303.15 K;□ , T = 308.15 K;Δ , T = 313.15 K; X and , ∗ T = 318.15 K over the complete composition range are given in figures 6.1-6.3. The density is positive and decreases as the organic solute composition increases for ([BMIM][NO_3] + pyridine) and ([BMIM][NO_3] + acetonitrile) but for ([BMIM][NO_3] + thiophene) slightly decrease as the solute composition increases. It can also be seen from figures 6.1-6.3 that the temperature effects of density is more prominent than for speed of sound for all systems. A small size of IL molecule was established to have a significant influence on densities of the mixture with increase in temperature and a small size anion and cation give a better interaction with aromatic nitrogen/ sulfur molecules (Anantharaj and Banerjee 2011).

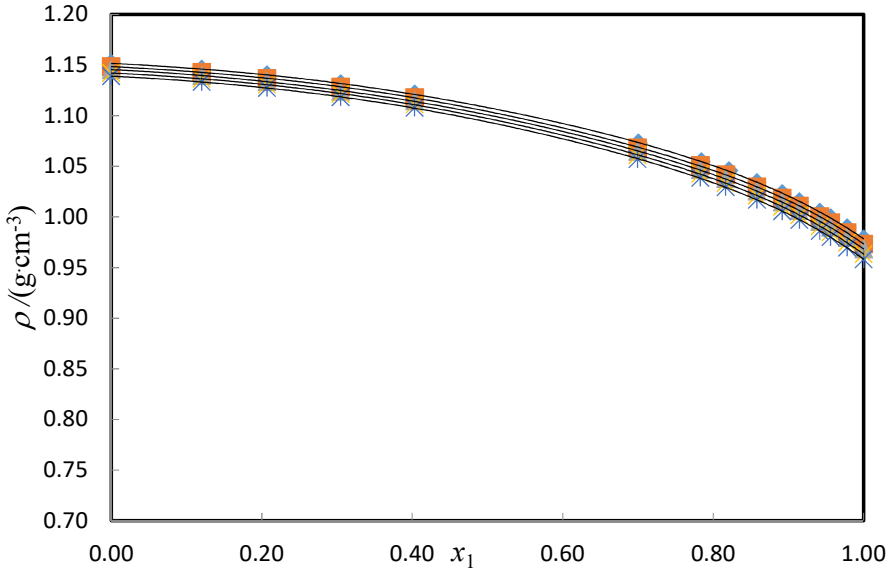

Figure 6.1: Experimental density, ρ,of the binary mixture of {[BMIM][NO_3] (x_2) + pyridine (x_1)} versus mole fraction x_1 of pyridine at T = 298.15 K;◊, T = 303.15 K;□ , T = 308.15 K;△ , T = 313.15 K; X and , ✳ T = 318.15 K

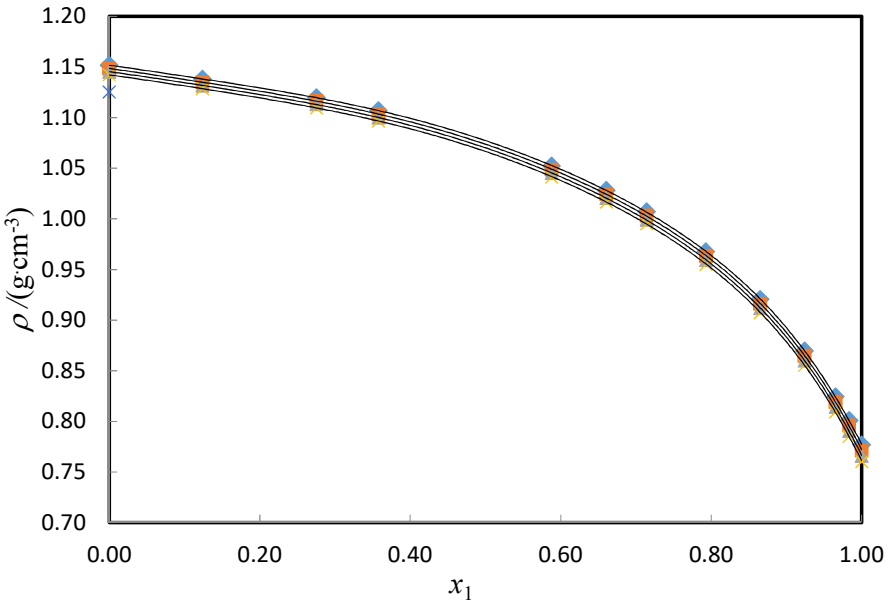

Figure 6.2: Experimental density, ρ, of the binary mixture of {[BMIM][NO_3] (x_2) + acetonitrile (x_1)} versus mole fraction x_1 of acetonitrile at T = 298.15 K;◊, T = 303.15 K;□ , T = 308.15 K;△ , T = 313.15 K; X and , ✳ T = 318.15 K

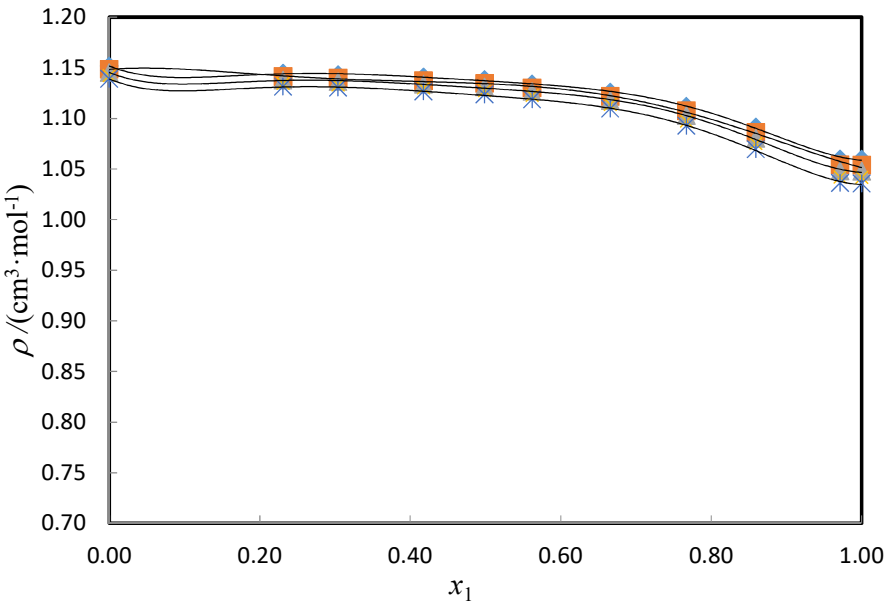

Figure 6.3: Experimental density, ρ, of the binary mixture of {[BMIM][NO_3] (x_2) + thiophene (x_1)} versus mole fraction x_1 of thiophene at T = 298.15 K;◊, T = 303.15 K;□ , T = 308.15 K;Δ , T = 313.15 K; X and , ∗ T = 318.15 K

6.1.2 Effect of Composition on Density

The density of mixture decreases with increasing in mole fraction of (([BMIM][NO_3] + pyridine or thiophene or acetonitrile) Tables 5.1 to 5.3. The ionic liquid, [BMIM][NO_3] can play a major role when interact with aromatic or nonaromatic structure compounds by (1) CH–π interaction, (2) π–π interaction, and (3) n–π interaction, where n = N, O, F and S atoms are located on the aromatic/non-aromatic compound or ionic liquid structure (Anantharaj and Banerjee 2011). The nitrogen/ sulfur atom of aromatic compounds forms hydrogen bond with hydrogen in imidazolium ring or with hydrogen located on the alkyl group of the imidazolium (Anantharaj and Banerjee 2011). The influence of composition have strong interaction with

similar molecules like thiophene since it has a similar five membered ring as compared to imidazolium ring, therefore it play important role in enhancing the solubility.

6.2 Excess Molar Volume

Rafiee and Frouzesh (2016) reported that two important factors affect excess molar volume, V_m^E behavior in binary mixtures: (a) the intermolecular interaction (including dipole-dipole interactions, cohesive and dispersive forces and hydrogen-bonding) and (b) the size, shape and packing ability of component's molecules (geometric factors in solution.

Excess molar volumes are the difference between the real partial molar volume of the mixture and the ideal partial volume. It is useful in comparing a substance or a component of a combination (Gomez *et al.* 2006).

Negative excess molar volumes indicate strong interactions between different molecules or could be due to an association of species involved, bringing the molecules closer together whereas positive excess molar volumes indicate a strong interaction between similar molecules (Redhi 2003).

Excess factors related with a liquid mixture are a numerical measure of change in the behavior of the liquid mixture from ideality. These functions are established to be sensitive to intermolecular forces and also on the variance in size and shape of the molecules. Excess volumes of liquid mixtures reveal the outcome of diverse contributions emanating from structural variations experienced by the pure co-solvent (Shah *et al.* 2013).

The temperature effect on excess molar volumes, of the mixtures, is critical, which can be used to investigate the microstructures of the system. In general, specific interactions in mixtures, typically hydrogen bonding, decreases as the temperature increases, while the dependence on temperature of the non-specific interactions is smaller and can usually be

neglected (Qian *et al.* 2012). Therefore, as the temperature increases, the V_m^E values of the mixtures will be less negative due to reduced hydrogen bonding in the mixtures (Rafiee and Frouzesh 2016).

6.2.1 Effect of Composition on Excess Molar Volume

For each binary mixture ([BMIM][NO_3] + pyridine), ([BMIM][NO_3] + acetonitrile) and ([BMIM][NO_3] + thiophene), excess molar volume V_m^E is plotted against mole fraction of solvents namely: pyridine, acetonitrile, and thiophene at all temperatures and are given in figure 5.1-5.3, and the results are presented in Table 5.1-5.3. The negative magnitude of excess molar volume (V_m^E signifies the closer packing of the central solute or ion by the surrounding solvents molecules or a more attractive force of interaction between ions of the IL and the solvents. The values of V_m^E for the binaries ([BMIM][NO_3] + pyridine) and ([BMIM][NO_3] + acetonitrile) were found to be negative to all range of temperatures. This reveals that there was more efficient packing and attractive interactions between the $[Bmim]^+/[NO_3]^-$ ions and pyridine or acetonitrile molecules in the studied binary solutions. This clearly indicates that the [BMIM][NO_3] interacts with pyridine, acetonitrile and thiophene molecules through hydrogen bonding, dipole-dipole interactions, dispersive forces, and dipolar interactions (Deenadayalu and Bhujrajh 2006). This data shows negative of V_m^E for (BMIM][NO_3] + thiophene) mixture at low compositions of [BMIM[NO_3], which indicates strong interaction between the [BMIM][NO_3] and thiophene molecules, but it becomes positive at higher composition (x_1 = 0.9) of thiophene which implies the breaking-up of the ion-ion interactions in the IL and self-interaction between similar molecules (thiophene-thiophene) (Anantharaj and Banerjee 2011). Figure 5.3 does not follow a certain trend because thiophene is unstable and volatile therefore, thiophene does not mix well with

[BMIM][NO_3]. At T = 298.15 K the $V_{m,\min}^{E}$ values for ([BMIM][NO_3] + pyridine) at x_1 = 0.4033 is -1.332 $cm^3 \cdot mol^{-1}$, for ([BMIM][NO_3] + acetonitrile) x_1 = 0.7144 is -1.464 $cm^3 \cdot mol^{-1}$, and for ([BMIM][NO_3] + thiophene) x_1 = 0.6140 is -1.6315 $cm^3 \cdot mol^{-1}$. $V_{m,\min}^{E}$ values increases in order thiophene < acetonitrile < pyridine. $V_{m,\min}^{E}$ for thiophene is less than pyridine and acetonitrile because the structure of thiophene is similar to imidazolium ring (both are 5- membered) therefore, it result in greater intermolecular interaction (Anantharaj and Banerjee 2011).

6.3 Speed of Sound

6.3.1 Effect of Temperature and Composition on Speed of Sound

The speed of sound is an important property to define the interactions such as solute-solvent, solvent-solvent, and solute-solute that occur in liquid mixtures (Roy, Ekka and Dewan 2011). The results of the speed of sound, *u*, for the binary systems ([BMIM][NO_3] + pyridine), ([BMIM][NO_3] + acetonitrile) and ([BMIM[NO_3] + thiophene) at various temperatures are presented in Tables 5.1- 5.3 and binary mixtures is plotted against the mole fraction or pyridine, acetonitrile and thiophene at all temperatures are given in figures 6.4-5.6. It is the evident from the results reported in Tables 5.1-5.3 and figures 6.4 -6.6 that speed of sound (u) values decreases with an increase in temperature and increasing composition of solvents, (pyridine, acetonitrile or thiophene).

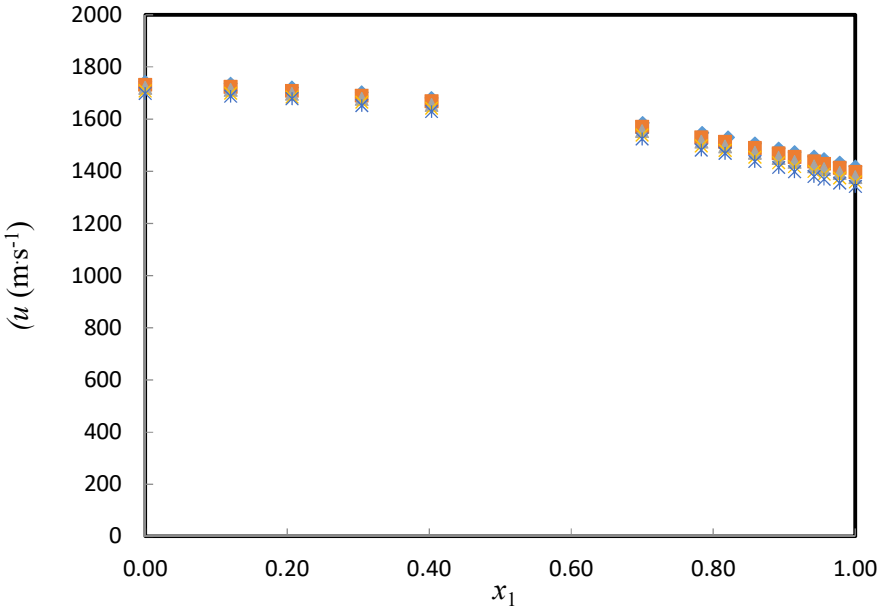

Figure 6.4: Experimental speed of sound, u ,of the binary mixture of {[BMIM][NO_3] (x_2) + pyridine (x_1)} versus mole fraction x_1 of pyridine at T = 298.15 K;◊, T = 303.15 K;□ , T = 308.15 K;Δ , T = 313.15 K; X and , ✳ T = 318.15 K

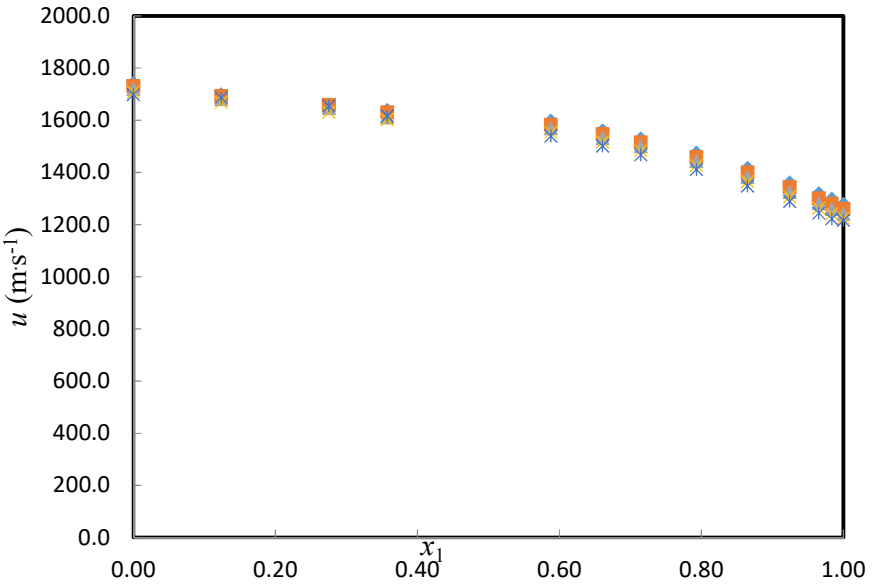

Figure 6.5: Experimental speed of sound, u, of the binary mixture of {[BMIM][NO_3] (x_2) + acetonitrile (x_1)} versus mole fraction x_1 of acetonitrile at T = 298.15 K;◊, T = 303.15 K;□ , T = 308.15 K;△ , T = 313.15 K; X and , ✳ T = 318.15 K

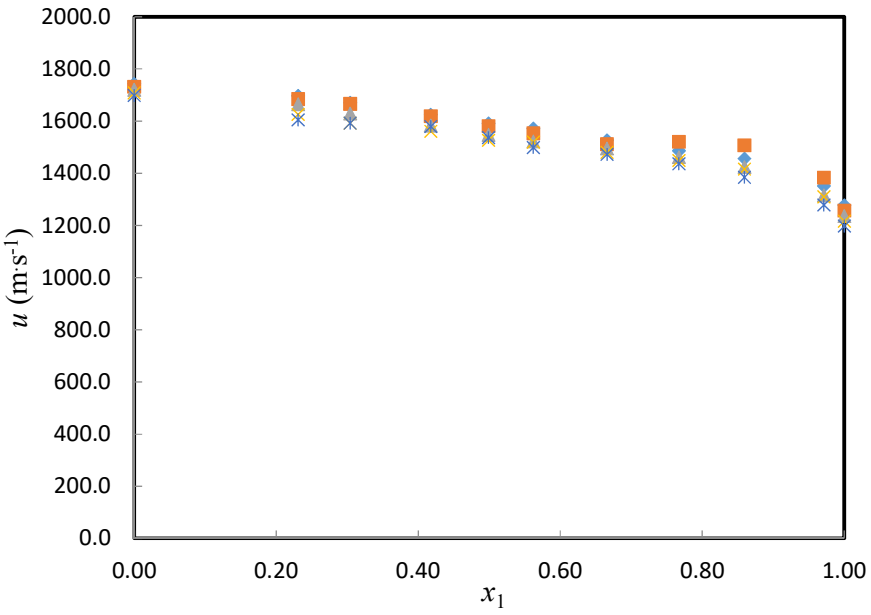

Figure 6.6: Experimental speed of sound, *u*, of the binary mixture of {[BMIM][NO_3] (x_2) + thiophene (x_1)} versus mole fraction x_1 of thiophene at T = 298.15 K;◊, T = 303.15 K;□ , T = 308.15 K;Δ , T = 313.15 K; X and , ✳ T = 318.15 K

6.3.2 Isentropic Compressibility

The results of isentropic compressibility, κ_s, for the binary systems ([BMIM][NO_3] + pyridine), ([BMIM][NO_3] + acetonitrile) and ([BMIM[NO_3] + thiophene) at various temperatures are presented in Tables 5.1- 5.3 and binary mixtures is plotted against the mole fraction or pyridine, acetonitrile and thiophene at all temperatures are given in figures 5.4-5.6. Isentropic compressibility (κ_s) of solutions were determined by the Newton-Laplace equation (equation 3.10) (Hirschfelder *et al.* 1954).

It is the an evident from the results reported in Tables 5.1-5.3 and figures 5.4-5.6 that isentropic compressibility values increases with an increase in temperature and increasing composition of solvents, (pyridine, acetonitrile or thiophene) which predicts more

compressibility of binary ionic liquid in solutions (Zafarani-Moattar and Shekaari 2005). Isentropic compressibility is positive at all temperatures is obviously due to the stronger interactions between [BMIM][NO_3] and solvent (pyridine, acetonitrile, and thiophene) molecules making the bulk solvent more compressible than the ideal mixture. This is also an indication of the closer approach of the ionic liquid molecule or ions and solvents with stronger interactions that result to increase in compressibility of the binaries (Gowrisankar *et al.* 2013). For each system, κ_s was positive over the entire composition range and at all temperatures indicating that the binary mixtures are more compressible than the ideal mixture. The $\kappa_{s,\min}$ value at T = 298 K at for ([BMIM][NO_3] + pyridine) x_1 = 0.0000 is 2.86 TPa^{-1}, ([BMIM][NO_3] + acetonitrile) x_1 = 0.0000 is 2.86 TPa^{-1}, and ([BMIM][NO_3] + thiophene) T = 298 K at x_1 = 0.0000 is 2.86 TPa^{-1}.

6.4 Refractive Index

6.4.1 Effect of Temperature and Composition on Refractive Index

Refractive index is an optical parameter to predict types of interaction occurring in binary solutions and can provide useful information when studying the interaction forces between molecules or their behavior in solution, and the change in refractive index, Δn, can be physically interpretable as the deviation of the reduced free volume. It is the evident from the results reported in Tables 5.4 and 5.6 and figures 6.7and 6.9 that the n values increases with an increases in temperature. Table 5.5 and figure 6.8 shows decrease with an increase in temperature and concentration for ([BMIM][NO_3] + acetonitrile). This behavior can be clarify by an efficient packing in ([BMIM][NO_3] + pyridine) and ([BMIM][NO_3] + thiophene) compared to ([BMIM][NO_3] + acetonitrile). The proportion of van der Waals and coulombic

force causes the refractive index of mixture to decrease with an increase in temperature molecules (Anantharaj and Banerjee 2011).

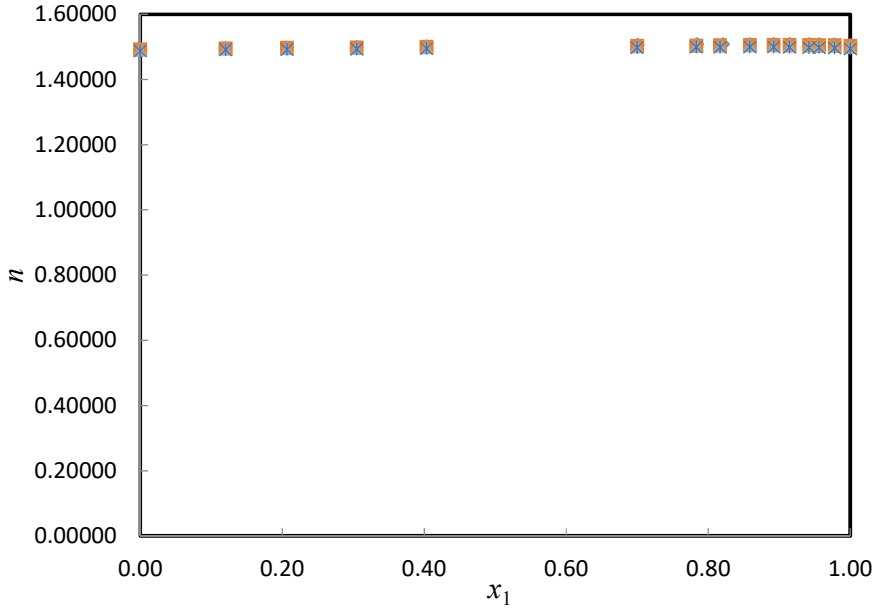

Figure 6.7: Experimental refractive index, *n*, of the binary mixture of {[BMIM][NO_3] (x_2) + pyridine (x_1)} versus mole fraction x_1 of pyridine at T = 298.15 K;◊, T = 303.15 K;□ , T = 308.15 K;Δ , T = 313.15 K; X and , ∗ T = 318.15 K

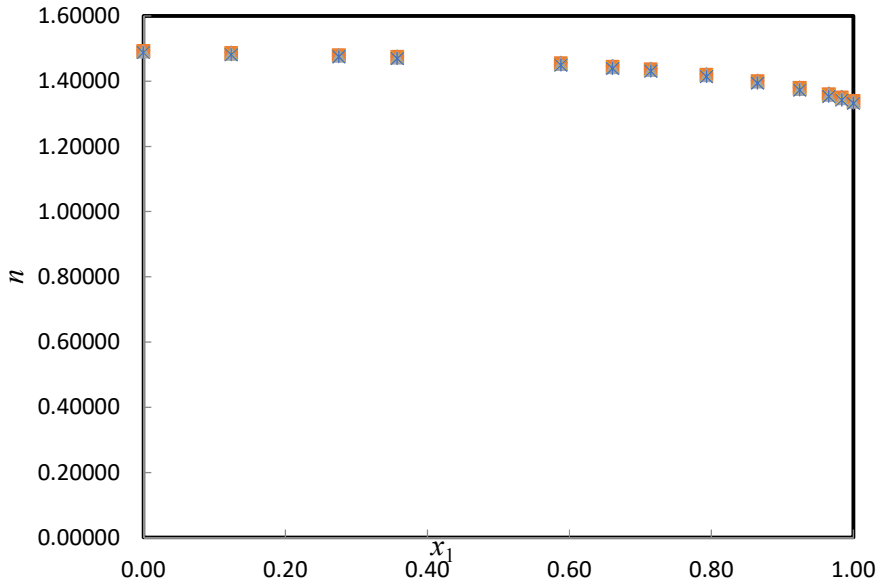

Figure 6.8: Experimental refractive index, *n*, of the binary mixture of {[BMIM][NO_3] (x_2) + acetonitrile (x_1)} versus mole fraction x_1 acetonitrile at $T = 298.15$ K;◊, $T = 303.15$ K;□ , $T = 308.15$ K;Δ , $T = 313.15$ K; X and , ✳ $T = 318.15$ K

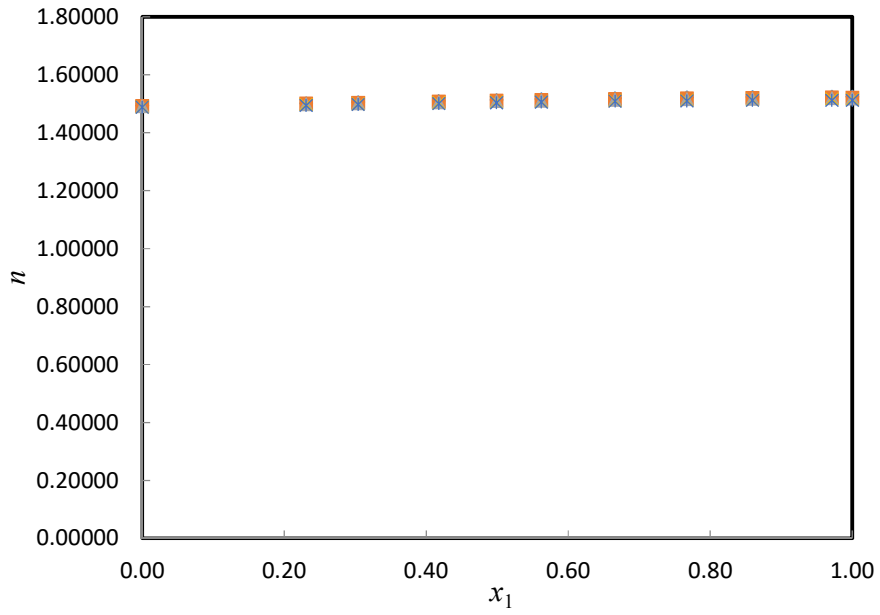

Figure 6.9: Experimental refractive index, *n*, of the binary mixture of {[BMIM][NO_3] (x_2) + thiophene (x_1)} versus mole fraction x_1 thiophene at T = 298.15 K;◊, T = 303.15 K;□ , T = 308.15 K;Δ , T = 313.15 K; X and , ∗ T = 318.15 K

6.4.2 Change in Refractive Index

Tables 5.4-5.6 shows the experimental data for change in refractive index (Δn) and figures 5.7- 5.9 shows change in refractive index (Δn) of the binary solutions plotted against mole fraction of pyridine or acetonitrile or thiophene, respectively at all temperatures. The change in refractive index (Δn) from ideal mixtures is positive in magnitude for all the binary solutions ([BMIM][NO_3] + pyridine), ([BMIM][NO_3] + acetonitrile) and ([BMIM][NO_3] + thiophene) across the whole composition range and at all temperatures. The results show the closely packing of molecules or a strong ion-solvent/solute-solvent interaction. At T = 298.15 K, the $\Delta n_{,max}$ at x_1 = 0.8584 is 0.00477 for ([BMIM][NO_3] + pyridine), x_1 = 0.6609 is 0.05323 for ([BMIM][NO_3] + acetonitrile) and at x_1 = 0.6658 is 0.00495 for ([BMIM][NO_3] + thiophene). The $\Delta n_{,max}$ for the binary mixtures increases in order acetonitrile > thiophene > pyridine.

6.5 Correlation and Predictions

6.5.1 Lorentz-Lorenz Equation

6.5.1.1 Prediction of Density by Lorentz-Lorenz (L-L) Equation

The density values obtained/predicted for the Lorentz-Lorentz equation are given in Table 5.8. The Lorentz–Lorentz equation gives a better correlation for the density for the system of ([BMIM][NO_3] + pyridine), but poor correlation for ([BMIM][NO_3] + acetonitrile) and ([BMIM][NO_3] + acetonitrile).

6.5.1.2 Prediction of Refractive Index by Lorentz-Lorenz (L-L) Equation

The Lorentz-Lorenz approximation for *n* gives better predict for ([BMIM][NO_3] + thiophene) and ([BMIM][NO_3] + acetonitrile). The prediction for ([BMIM][NO_3] + pyridine) was poor.

6.5.1.3 Correlation of Excess Molar Volumes by Lorentz-Lorenz Equation

The Lorentz-Lorenz approximation for excess molar volumes gives poor correlation for ([BMIM][NO_3] + pyridine), ([BMIM][NO_3] + thiophene) and ([BMIM][NO_3] + acetonitrile).

6.5.2 Redlich-Kister Correlation

The Redlich–Kister fitting smoothing polynomial was used to obtain the fitting parameters of the binary systems together with the standard deviations. Table 5.7 provides the correlation parameters for the Redlich-Kister smoothing polynomial. The Redlich-Kister polynomial fit for the Δn and excess molar volumes values (figure 5.2 and figure 5.8) provides the best fit for the ([BMIM][NO_3] + acetonitrile) binary mixture. ([BMIM][NO_3] + thiophene) gives a

poor polynomial fit in both change in refractive index and excess molar volumes. The Redlich-Kister polynomial fit for the Δn values (figure 5.6) give poor polynomial fit and excess molar volumes values (figure 5.1) for ([BMIM][NO_3] + pyridine) binary mixture. From the Table 5.8 provide Lorentz-Lorenz correlation of excess molar volumes gave the best prediction for all binary systems {([BMIM][NO_3] + pyridine), ([BMIM][NO_3] + acetonitrile), ([BMIM][NO_3] + thiophene)}.

6.6 Activity Coefficients at Infinite Dilution

It is evident from Table 5.9 that alkanes, cycloalkanes, and alkenes have the highest γ_{13}^{∞} when compared to the other solutes. This implies that they have weakest solute-solvent interactions. It can be seen from the Table 5.9 that the higher the number of carbons in a compound the higher γ_{13}^{∞} values. Cycloalkanes have lower γ_{13}^{∞} when compared to alkanes and alkenes, this could be due to stronger attractive interactions between the imidazolium ring and the cyclic structure of the cycloalkanes. Alkynes have the lowest γ_{13}^{∞} values when compared to their homologous series: alkanes, cycloalkanes and alkenes because of the triple bond in alkynes where the π electrons interact with the π electrons of the ($[BMIM]^+$) ions. The aromatic hydrocarbons benzene and toluene have the lowest γ_{13}^{∞} values when compared to the alkanes, alkenes, alkynes and cycloalkanes; this could be due to the π-delocalized electrons in the benzene and toluene structures and the polar [BMIM][HSO_4]. The alcohols have the second lowest γ_{13}^{∞} for all solutes, due to hydrogen bonding, between the hydrogen atom of the alcohol and the oxygen atoms of the hydrogen sulphate anion ($[HSO4]^-$) and the lone pair of electrons on the oxygen atom of the alcohol and hydrogen atoms of the cation ($[BMIM]^+$). Other polar solutes γ_{13}^{∞} increase in the order: pyridine > ethylacetate > 3-pentanone > acetone > thiophene > acetonitrile > dichloromethane. The γ_{13}^{∞} values for dichloromethane is the

lowest for all solutes, indicating that most polar solutes has the best solubility in the ionic liquid because of the higher solute/ solvent interactions.

6.6.1 Effect of Temperature on Activity Coefficients at Infinite Dilution

Activity coefficients at infinite dilution for various solutes in the ionic liquid [BMIM][HSO_4] were determined at three temperatures (313.15, 323.15, 333.15) K. The overall trend for activity coefficient at infinite dilution was increasing or decreasing with an increase with temperature.

6.6.2 Thermodynamic Functions at Infinite Dilution

The results were evaluated in terms of interactions between the solutes and the solvent. The partial excess molar property: enthalpy at infinite dilution were determined from the temperature dependence of the Inγ_{13}^{∞} versus temperature as claimed by Gibbs-Helmholtz equation given in 3.43.

The results were evaluated in terms interactions between the solutes and the solvent. The partial molar excess enthalpies at infinite values, $\Delta H_1^{E,\infty}$ shown in Table 5.10, outline the temperature dependence of γ_{13}^{∞} values. Figures 5.10-5.17, reveal the natural logarithm of γ_{13}^{∞} values as a function of the inverse absolute temperature for all solutes. The values, $\Delta H_1^{E,\infty}$ values are positive except pentane, n-hexane,n-heptane, methanol, alkenes, alkynes, thiophene, acetonitrile and dicholoromethane. The negative values of $\Delta H_1^{E,\infty}$ values for the solutes: methanol, alkenes, alkynes, thiophene, acetonitrile and dicholoromethane, indicate stronger solute-solvent interactions which corroborates with the lower γ_{13}^{∞} values. The positive values of $\Delta H_1^{E,\infty}$ for solutes implies disruption of intramolecular bonds in the solute.

6.6.3 Selectivities and Capacities

The purpose of the study is to evaluate the performance of the [BMIM][HSO_4] as a solvent for chemical separation problems in extractive distillation. The results obtained for selectivity and capacity, were calculated using equation 3.44 and 3.45. The results presented in Table 5.11 contain literature values for ionic liquids containing the same or similar cation or anion. Selectivity and capacity for other important industrial solvents such as N-methyl-2-pyrrolidinone (NMP) and sulfolane are also submitted for the purpose of comparison.

In order for the solvent to be suitable as an entrainer it should have both high selectivity and high capacity for the components to be separated. The selectivity value for the separation of heptane and thiophene in [BMIM][HSO_4] was 203. It was high compared to [BMIM][SCN] which is 156.90.The selectivity for the separation of hexane/ benzene was 121.77 in [BMIM][HSO_4] was reasonably high when compared to the values of NMP (10.3) and sulfolane (16.84). These results suggest the potential of [BMIM][HSO_4] for use in industrial separation processes. Hexane appears as the best limiting selective in [BMIM][HSO_4] because it has the largest selectivity. However, extractive distillation is to be considered, then the mixture of hexane and benzene in [BMIM][HSO_4] must be equally soluble. The capacity of benzene was 0.154 it indicates that the system will not be soluble in the concentrations required for effective separation. The results shows that the alkanes are not soluble in [BMIM][HSO_4] and that the solubility of alkanes decreases with increasing carbon number.

Chapter 7

CONCLUSION

In this study the thermophysical properties, which include density, speed of sound and refractive index were measured as a function of temperature and composition for the binaries ([BMIM][NO_3] + pyridine), ([BMIM][NO_3] + acetonitrile) and ([BMIM][NO_3] + thiophene) at T = (298.15, 303.15, 308.15, 313.15, and 318.15) K. Therefore, thermodynamic relevant parameters such as V_m^E, κ_s, have been calculated using density and speed of sound to confirm intermolecular interactions which occur in the mixtures. The isentropic compressibility is positive for all systems. The isentropic compressibility is an indication of the compressibility of the mixture, and the positive values indicate that the mixtures are compressible. The calculated values of excess molar volumes and change of refractive index on mixing were compared with the results obtained by applying the Lorentz- Lorentz equation to correlate excess molar volume. The study also clearly indicates the ion-solvent/solute-solvent interaction is dominant over the self-interaction like solvent-solvent/ion-ion/solute-solute. The Redlich-Kister smoothing expression was utilized successfully for the correlation of excess molar volumes and change in refractive index data. In this study, the gas liquid chromatography technique was used to calculate activity coefficients at infinite dilution for 28 polar and non-polar organic solutes in the IL: 1-butyl-3-methylimidazolium hydrogen sulfate. The interactions of organic solutes with 1-butyl-3-methylimidazolium hydrogen sulfate was studied. The partial molar excess enthalpies were calculated from the temperature dependence of $\ln\gamma_{13}^{\infty}$. Selectivities and limiting capacities were also calculated from the measured values of activity coefficient at infinite dilution for

various solutes separation problems. The highest selectivity value was obtained for the separation of hexane; it indicates that [BMIM][HSO_4] may be used in industrial separation processes.

REFERENCES

Alfonsi, K., Colberg, J., Dunn, P. J., Fevig, T., Jennings, S., Johnson, T. A., Kleine, H. P., Knight, C., Nagy, M. A. and Perry, D. A. 2008. Green chemistry tools to influence a medicinal chemistry and research chemistry based organisation. *Green Chemistry*, 10 (1): 31-36.

Ali, A., Tariq, M. and Nabi, F. 2008. Density, viscosity, refractive index, and speed of sound in binary mixtures of pyridine and 1-Alkanols (C6, C7, C8, C10) at 303.15 K. *Chinese Journal of Chemistry*, 26 (11): 2009-2015.

Allen, D. T., Shonnard, D. and Prothero, S. 2002. Evaluating environmental performance during process synthesis. *Green Engineering: Environmentally Conscious Design of Chemical Processes. Prentice Hall, New Jersey*: 199-249.

Alonso, I., Mozo, I., De La Fuente, I. G., González, J. A. and Cobos, J. C. 2011. Thermodynamics of ketone+ amine mixtures 7. Volumetric and speed of sound data at (293.15, 298.15 and 303.15) K for 2-pentanone +aniline, or + n-methylaniline, or + pyridine systems. *Journal of Molecular Liquids*, 160 (3): 180-186.

Alptekin, E. and Canakci, M. 2008. Determination of the density and the viscosities of biodiesel–diesel fuel blends. *Renewable Energy*, 33 (12): 2623-2630.

Anantharaj, R. and Banerjee, T. 2011. Physiochemical properties of hydrodenitrification and hydrodesulphurization inhibiting compounds with 1-ethyl-3-methylimidazolium ethylsulphate at T = (298.15 to 323.15) K and *Journal of Thermodynamics*, 2011

Antony, J. H., Mertens, D., Breitenstein, T., Dölle, A., Wasserscheid, P. and Carper, W. R. 2004. Molecular structure, reorientational dynamics, and intermolecular interactions in the neat ionic liquid 1-butyl-3-methylimidazolium hexafluorophosphate. *Pure and Applied Chemistry*, 76 (1): 255-261.

Aralaguppi, M., Jadar, C. and Aminabhavi, T. 1996. Density, refractive index, viscosity, and speed of sound in binary mixtures of 2-ethoxyethanol with dioxane, acetonitrile, and tetrahydrofuran at (298.15, 303.15, and 308.15) K. *Journal of Chemical & Engineering Data*, 41 (6): 1307-1310.

Azevedo, R., Gomes, R., Szydlowski, J., Pires, P., Esperança, J., Guedes, H. and Rebelo, L. 2004. A novel non-intrusive microcell for sound-speed measurements in liquids. Speed of sound and thermodynamic properties of 2-propanone at pressures up to 160 MPa. *Journal of Chemical Thermodynamics*, 36 (3): 211-222.

Aznarez, S. B. and Postigo, M. A. 1998. Excess molar volumes of binary mixtures of acetonitrile with n-alkanols at 25 C. *Journal of Solution Chemistry*, 27 (11): 1045-1053.

Bahadur, I., Govender, B. B., Osman, K., Williams-Wynn, M. D., Nelson, W. M., Naidoo, P. and Ramjugernath, D. 2014. Measurement of activity coefficients at infinite dilution of

organic solutes in the ionic liquid 1-ethyl-3-methylimidazolium 2-(2-methoxyethoxy) ethylsulfate at T = (308.15, 313.15, 323.15 and 333.15) K using gas+ liquid chromatography. *Journal of Chemical Thermodynamics*, 70: 245-252.

Barceló González, P. 2010. Thermodynamics of room-temperature ionic liquids: Modelling and experiment. Masters, University of Aberdeen.

Barghi, S., Adibi, M. and Rashtchian, D. 2010. An experimental study on permeability, diffusivity, and selectivity of CO_2 and CH_4 through [BMIM][PF_6] ionic liquid supported on an alumina membrane: Investigation of temperature fluctuations effects. *Journal of Membrane Science*, 362 (1): 346-352.

Battino, R. 1971. Volume changes on mixing for binary mixtures of liquids. *Chemical Reviews*, 71 (1): 5-45.

Berthod, A. and Carda-Broch, S. 2004. Uses of ionic liquids in analytical chemistry. *reactions* 1: 6. Available: http://doi.org/10.1021/ac070742b (Accessed 25 June 2017).

Bottomley, G. and Scott, R. 1974. A grease-free continuous dilution dilatometer; excess volumes for benzene+ carbon tetrachloride. *Journal of Chemical Thermodynamics*, 6 (10): 973-981.

Brennecke, J. F. and Maginn, E. J. 2001. Ionic liquids: innovative fluids for chemical processing. *American Institute of Chemical Engineers*, 47 (11): 2384-2389.

Brocos, P., Piñeiro, Á., Bravo, R. and Amigo, A. 2003. Refractive indices, molar volumes and molar refractions of binary liquid mixtures: concepts and correlations. *Physical Chemistry Chemical Physics*, 5 (3): 550-557.

Canales, R. I. and Brennecke, J. F. 2016. Comparison of ionic liquids to conventional organic solvents for extraction of aromatics from aliphatics. *Journal of Chemical & Engineering Data*, 61 (5): 1685-1699.

Ceriani, R., Paiva, F. R., Goncalves, C. B., Batista, E. A. and Meirelles, A. J. 2008. Densities and viscosities of vegetable oils of nutritional value. *Journal of Chemical & Engineering Data*, 53 (8): 1846-1853.

Checoni, R. F. and Francesconi, A. Z. 2006. Partial molar enthalpy properties and correlation of excess molar enthalpy data of acetonitrile+ diethylamine or S-butylamine mixtures at various temperatures and atmospheric pressure. *Thermochimica Acta*, 450 (1): 126-131.

Chen, F., Yang, Z., Chen, Z., Hu, J., Chen, C. and Cai, J. 2015. Density, viscosity, speed of sound, excess property and bulk modulus of binary mixtures of γ-butyrolactone with acetonitrile, dimethyl carbonate, and tetrahydrofuran at temperatures (293.15 to 333.15) K. *Journal of Molecular Liquids*, 209: 683-692.

Cheong, W.-J. 2002. A study of the gas liquid partition coefficients of eleven normal, branched and cyclic alkanes in sixty nine common organic liquids: the effect of solute structure. *Bulletin of the Korean Chemical Society*, 23 (3): 459-468.

Chum, H. L., Koch, V., Miller, L. and Osteryoung, R. 1975. Electrochemical scrutiny of organometallic iron complexes and hexamethylbenzene in a room temperature molten salt. *Journal of the American Chemical Society*, 97 (11): 3264-3265.

Cruickshank, A., Windsor, M. and Young, C. 1966. The use of gas-liquid chromatography to determine activity coefficients and second virial coefficients of mixtures. I. Theory and verification of method of data analysis. In: Proceedings of *Proceedings of the Royal Society of London A: Mathematical, Physical and Engineering Sciences*. The Royal Society, 259-270.

Cunha, D. L., Coutinho, J. A., Daridon, J. L., Reis, R. A. and Paredes, M. L. 2013. An atomic contribution model for the prediction of speed of sound. *Fluid Phase Equilibria*, 358: 108-113.

Deenadayalu, N. and Bhujrajh, P. 2006. Excess molar volumes and partial molar volumes for (propionitrile + an alkanol) at T= 298.15 K and p = 0.1 MPa. *Journal of Chemical Thermodynamics*, 38 (3): 278-282.

Deenadayalu, N., Letcher, T. M. and Reddy, P. 2005. Determination of activity coefficients at infinite dilution of polar and nonpolar solutes in the ionic liquid 1-ethyl-3-methyl-

imidazolium bis (trifluoromethylsulfonyl) imidate using gas− liquid chromatography at the temperature 303.15 K or 318.15 K. *Journal of Chemical & Engineering Data*, 50 (1): 105-108.

Dikio, E. D., Nelana, S. M., Isabirye, D. A. and Ebenso, E. E. 2012. Density, dynamic viscosity and derived properties of binary mixtures of methanol, ethanol, n-propanol, and n-butanol with pyridine at T = (293.15, 303.15, 313.15 and 323.15) K. *International Journal of Electrochemical Science*, 7 (11): 11101-11122.

Domańska, U. and Królikowska, M. 2010. Measurements of activity coefficients at infinite dilution in solvent mixtures with thiocyanate-based ionic liquids using GLC technique. *Journal of Physical Chemistry B*, 114 (25): 8460-8466.

Domańska, U., Królikowski, M. and Acree, W. E. 2011. Thermodynamics and activity coefficients at infinite dilution measurements for organic solutes and water in the ionic liquid 1-butyl-1-methylpyrrolidinium tetracyanoborate. *Journal of Chemical Thermodynamics*, 43 (12): 1810-1817.

Domańska, U. and Laskowska, M. 2009. Measurements of activity coefficients at infinite dilution of aliphatic and aromatic hydrocarbons, alcohols, thiophene, tetrahydrofuran, MTBE, and water in ionic liquid [BMIM][SCN] using GLC. *Journal of Chemical Thermodynamics*, 41 (5): 645-650.

Domańska, U., Wlazło, M. and Karpińska, M. 2016. Activity coefficients at infinite dilution of organic solvents and water in 1-butyl-3-methylimidazolium dicyanamide. A literature review of hexane/hex-1-ene separation. *Fluid Phase Equilibria*, 417: 50-61.

Everett, D. 1965. Effect of gas imperfection on GLC measurements: a refined method for determining activity coefficients and second virial coefficients. *Transactions of the Faraday Society*, 61: 1637-1645.

Fan, W., Zhou, Q., Sun, J. and Zhang, S. 2009. Density, excess molar volume, and viscosity for the methyl methacrylate+ 1-butyl-3-methylimidazolium hexafluorophosphate ionic liquid binary system at atmospheric pressure. *Journal of Chemical & Engineering Data*, 54 (8): 2307-2311.

Fortin, T. J., Laesecke, A., Freund, M. and Outcalt, S. 2013. Advanced calibration, adjustment, and operation of a density and sound speed analyzer. *Journal of Chemical Thermodynamics*, 57: 276-285.

Franks, F. and Smith, H. 1967. Apparent molal volumes and expansibilities of electrolytes in dilute aqueous solution. *Transactions of the Faraday Society*, 63: 2586-2598.

Furtado, A., Batista, E., Spohr, I. and Filipe, E. 2009. Measurement of density using oscillation-type density meters calibration, traceability and uncertainties. *Instituto Portugûes da Qualidade (IPQ), Portugal*,

Gabriel, S. and Weiner, J. 1888. Ueber einige abkömmlinge des propylamins. *European Journal of Inorganic Chemistry*, 21 (2): 2669-2679.

Gadžurić, S., Tot, A., Zec, N. a., Papović, S. a. and Vraneš, M. 2014. Volumetric properties of binary mixtures of 1-butyl-1-methylpyrrolidinium tris (pentafluoroethyl) trifluorophosphate with n-methylformamide, n-ethylformamide, n, n-dimethylformamide, n, n-dibutylformamide, and n, n-dimethylacetamide from T = (293.15 to 323.15) K. *Journal of Chemical & Engineering Data*, 59 (4): 1225-1231.

Ge, M.-L., Deng, X.-M., Zhang, L.-H., Chen, J.-Y., Xiong, J.-M. and Li, W.-H. 2014. Activity coefficients at infinite dilution of organic solutes in the ionic liquid 1-butyl-3-methylimidazolium methyl sulfate. *Journal of Chemical Thermodynamics*, 77: 7-13.

Ge, M., Xiong, J. and Wang, L. 2009. Theoretical prediction for the infinite dilution activity coefficients of organic compounds in ionic liquids. *Chinese Science Bulletin*, 54 (13): 2225-2229.

Ghafeli, D. and Almasi, M. 2016. The measurement of excess molar volumes in two-component mixture containing ethyl formate and 1-pantanol in the temperature range from 293.15 K to 323.15 K. *American Journal of Oil and Chemical Technologies*, 4 (1): 1-15.

Gil, I., Uyazán, A., Aguilar, J., Rodríguez, G. and Caicedo, L. 2008. Separation of ethanol and water by extractive distillation with salt and solvent as entrainer: process simulation. *Brazilian Journal of Chemical Engineering*, 25 (1): 207-215.

Gomez, E., Gonzalez, B., Domínguez, Á., Tojo, E. and Tojo, J. 2006. Dynamic viscosities of a series of 1-alkyl-3-methylimidazolium chloride ionic liquids and their binary mixtures with water at several temperatures. *Journal of Chemical & Engineering Data*, 51 (2): 696-701.

Govender, U., Letcher, T., Garg, S. and Ahluwalia, J. 1996. Effect of temperature and pressure on the volumetric properties of branched and cyclic ethers. *Journal of Chemical & Engineering Data*, 41 (1): 147-150.

Gowrisankar, M., Venkateswarlu, P., Sivakumar, K. and Sivarambabu, S. 2013. Ultrasonic studies on molecular interactions in binary mixtures of n-methyl aniline with methyl isobutylketone,+ 3-pentanone, and+ cycloalkanones at 303.15 K. *Journal of Solution Chemistry*, 42 (5): 916-935.

Gutiérrez Hernández, J. P. 2013. *Extractive distillation with ionic liquids as solvents: selection and conceptual process design*. Eindhoven: Technische Universiteit Eindhoven.

Gwala, N. V. 2009. Activity coefficients at infinite dilution for ILs: methyltrioctylammonium cation and bis (trifluoromethylsulfonyl) imide or thiosalicylate anions using glc. Master of Technology in Chemistry, Durban University of Technology.

Handa, Y. P. and Benson, G. C. 1979. Volume changes on mixing two liquids: a review of the experimental techniques and the literature data. *Fluid Phase Equilibria*, 3 (2-3): 185-249.

Heintz, A., Kulikov, D. V. and Verevkin, S. P. 2002. Thermodynamic properties of mixtures containing ionic liquids. 2. Activity coefficients at infinite dilution of hydrocarbons and polar solutes in 1-methyl-3-ethyl-imidazolium bis (trifluoromethyl-sulfonyl) amide and in 1, 2-dimethyl-3-ethyl-imidazolium bis (trifluoromethyl-sulfonyl) amide using gas-liquid chromatography. *Journal of Chemical & Engineering Data*, 47 (4): 894-899.

Hirschfelder, J. O., Curtiss, C. F., Bird, R. B. and Mayer, M. G. 1954. *Molecular theory of gases and liquids*. Wiley New York.

Huddleston, J. G., Willauer, H. D., Swatloski, R. P., Visser, A. E. and Rogers, R. D. 1998. Room temperature ionic liquids as novel media for 'clean'liquid–liquid extraction. *Chemical Communications*, (16): 1765-1766.

Hudson, G. and McCoubrey, J. 1960. Intermolecular forces between unlike molecules. A more complete form of the combining rules. *Transactions of the Faraday Society*, 56: 761-766.

Huo, Y., Xia, S. and Ma, P. 2007. Densities of ionic liquids, 1-butyl-3-methylimidazolium hexafluorophosphate and 1-butyl-3-methylimidazolium tetrafluoroborate, with benzene, acetonitrile, and 1-propanol at T = (293.15 to 343.15) K. *Journal of Chemical & Engineering Data*, 52 (5): 2077-2082.

Iglesias-Otero, M. A., Troncoso, J., Carballo, E. and Romaní, L. 2008. Density and refractive index in mixtures of ionic liquids and organic solvents: Correlations and predictions. *Journal of Chemical Thermodynamics*, 40 (6): 949-956.

Iloukhani, H. and Almasi, M. 2009. Densities, viscosities, excess molar volumes, and refractive indices of acetonitrile and 2-alkanols binary mixtures at different temperatures: Experimental results and application of the Prigogine–Flory–Patterson theory. *Thermochimica Acta*, 495 (1): 139-148.

José-Alberto, M.-H. and Jorge, A. 2011. Current knowledge and potential applications of ionic liquids in the petroleum industry. *Ionic liquids: Applications and Pperspectives, In Tech*: 439-456.

Karkamkar, A., Aardahl, C. and Autrey, T. 2007. Recent developments on hydrogen release from ammonia borane. *Material Matters*, 2 (2): 6-9.

Keyes, D. B. and Hildebrand, J. H. 1917. A study of the system aniline-hexane. *Journal of the American Chemical Society*, 39 (10): 2126-2137.

Knoop, C., Tiegs, D. and Gmehling, J. 1989. Measurement of. gamma.. infin. using gas-liquid chromatography. 3. Results for the stationary phases 10-nonadecanone, n-formylmorpholine, 1-pentanol, m-xylene, and toluene. *Journal of Chemical and Engineering Data*, 34 (2): 240-247.

Kozlova, S. A., Verevkin, S. P., Heintz, A., Peppel, T. and Köckerling, M. 2009. Activity coefficients at infinite dilution of hydrocarbons, alkylbenzenes, and alcohols in the paramagnetic ionic liquid 1-butyl-3-methyl-imidazolium tetrachloridoferrate (III) using gas–liquid chromatography. *Journal of Chemical Thermodynamics*, 41 (3): 330-333.

Krummen, M., Gruber, D. and Gmehling, J. 2000. Measurement of activity coefficients at infinite dilution in solvent mixtures using the dilutor technique. *Industrial & Engineering Chemistry Research*, 39 (6): 2114-2123.

Kumaran, M. and McGlashan, M. 1977. An improved dilution dilatometer for measurements of excess volumes. *Journal of Chemical Thermodynamics*, 9 (3): 259-267.

Lehmann, J., Rausch, M. H., Leipertz, A. and Fröba, A. P. 2010. Densities and excess molar volumes for binary mixtures of ionic liquid 1-ethyl-3-methylimidazolium ethylsulfate with solvents. *Journal of Chemical & Engineering Data*, 55 (9): 4068-4074.

Letcher, T., Harris, R., Ramjugernath, D. and Raal, J. 2001. Activity coefficients of hydrocarbon solutes at infinite dilution in monoethanolamine from gas–liquid chromatography. *Journal of Chemical Thermodynamics*, 33 (12): 1655-1662.

Letcher, T. M. ed. 2004. *Chemical Thermodynamics for Industry*. Letchworth: Royal Society of Chemistry.

Letcher, T. M., Domańska, U., Marciniak, M. and Marciniak, A. 2005a. Activity coefficients at infinite dilution measurements for organic solutes in the ionic liquid 1-butyl-3-methyl-imidazolium 2-(2-methoxyethoxy) ethyl sulfate using glc at T = (298.15, 303.15, and 308.15) K. *Journal of Chemical Thermodynamics*, 37 (6): 587-593.

Letcher, T. M., Marciniak, A., Marciniak, M. and Domańska, U. 2005b. Determination of activity coefficients at infinite dilution of solutes in the ionic liquid 1-butyl-3-methylimidazolium octyl sulfate using gas− liquid chromatography at a temperature of 298.15 K, 313.15 K, or 328.15 K. *Journal of Chemical & Engineering Data*, 50 (4): 1294-1298.

Lide, D. R. 2009. *CRC Handbook of Chemistry and Physics*. 90th ed. Boca Raton, FA.: CRC Press.

Lo, T. and Schwietzer, P. 1996. *Handbook of Separations Techniques for Chemical Engineers*. New York: McGraw-Hill.

Luning Prak, D. J. and Lee, B. G. 2016. Density, viscosity, speed of sound, bulk modulus, surface tension, and flash point of binary mixtures of 1, 2, 3, 4-tetrahydronaphthalene and trans-decahydronaphthalene. *Journal of Chemical & Engineering Data*, 61 (7): 2371-2379.

Marciniak, A. 2010. Influence of cation and anion structure of the ionic liquid on extraction processes based on activity coefficients at infinite dilution. A review. *Fluid Phase Equilibria*, 294 (1): 213-233.

Marcinkowski, Ł., Kloskowski, A. and Namieśnik, J. 2014. Measurement of activity coefficients at infinite dilution of organic solutes in the ionic liquid 1-hexyl-1,4-diaza[2.2.2]bicyclooctanium bis(trifluoromethylsulfonyl)imide using gas–liquid chromatography. *Journal of Chemical Thermodynamics*, 71: 84-90.

Martin, A. and Synge, R. M. 1941. A new form of chromatogram employing two liquid phases: A theory of chromatography. 2. Application to the micro-determination of the higher monoamino-acids in proteins. *Biochemical Journal*, 35 (12): 1358.

Martins, M. A., Coutinho, J. A., Pinho, S. P. and Domańska, U. 2015. Measurements of activity coefficients at infinite dilution of organic solutes and water on polar imidazolium-based ionic liquids. *Journal of Chemical Thermodynamics*, 91: 194-203.

Matzke, M., Arning, J., Ranke, J., Jastorff, B. and Stolte, S. 2010. Design of inherently safer ionic liquids: toxicology and biodegradation. *Handbook of Green Chemistry*,

McGlashan, M. and Potter, D. 1962. An apparatus for the measurement of the second virial coefficients of vapours; the second viral coefficients of some n-alkanes and of some mixtures of n-alkanes. In: Proceedings of *Proceedings of the Royal Society of London A: Mathematical, Physical and Engineering Sciences*. The Royal Society, 478-500.

Micaelo, N. M., Baptista, A. M. and Soares, C. M. 2006. Parametrization of 1-butyl-3-methylimidazolium hexafluorophosphate/nitrate ionic liquid for the GROMOS force field. *Journal of Physical Chemistry B*, 110 (29): 14444-14451.

Mokhtarani, B., Sharifi, A., Mortaheb, H. R., Mirzaei, M., Mafi, M. and Sadeghian, F. 2009. Density and viscosity of 1-butyl-3-methylimidazolium nitrate with ethanol, 1-propanol, or 1-butanol at several temperatures. *Journal of Chemical Thermodynamics*, 41 (12): 1432-1438.

Möllmann, C. and Gmehling, J. 1997. Measurement of activity coefficients at infinite dilution using gas− liquid chromatography. Results for n-methylacetamide, n, n-dimethylacetamide, n, n-dibutylformamide, and ulfolane as stationary phases. *Journal of Chemical & Engineering Data*, 42 (1): 35-40.

Mota-Martinez, M. T., Althuluth, M., Berrouk, A., Kroon, M. C. and Peters, C. J. 2014. High pressure phase equilibria of binary mixtures of light hydrocarbons in the ionic liquid 1-hexyl-3-methylimidazolium tetracyanoborate. *Fluid Phase Equilibria*, 362: 96-101.

Nayak, J. N., Aralaguppi, M. I., Toti, U. S. and Aminabhavi, T. M. 2003. Density, viscosity, refractive index, and speed of sound in the binary mixtures of tri-n-butylamine + triethylamine,+ tetrahydrofuran,+ tetradecane,+ tetrachloroethylene,+ pyridine, or + trichloroethylene at T = (298.15, 303.15, and 308.15) K. *Journal of Chemical & Engineering Data*, 48 (6): 1483-1488.

Olivier, E., Letcher, T. M., Naidoo, P. and Ramjugernath, D. 2010. Activity coefficients at infinite dilution of organic solutes in the ionic liquid 1-ethyl-3-methylimidazolium trifluoromethanesulfonate using gas–liquid chromatography at T = (313.15, 323.15, and 333.15) K. *Journal of Chemical Thermodynamics*, 42 (1): 78-83.

Olivier, E., Letcher, T. M., Naidoo, P. and Ramjugernath, D. 2011. Activity coefficients at infinite dilution of organic solutes in the ionic liquid 1-butyl-3-methylimidazolium hexafluoroantimonate using gas–liquid chromatography at T = (313.15, 323.15, and 333.15) K. *Journal of Chemical Thermodynamics*, 43 (6): 829-833.

Orge, B., Rodríguez, A., Canosa, J. M., Marino, G., Iglesias, M. and Tojo, J. 1999. Variation of densities, refractive indices, and speeds of sound with temperature of methanol or ethanol with hexane, heptane, and octane. *Journal of Chemical & Engineering Data*, 44 (5): 1041-1047.

Patil, P., Patil, S., Borse, A. and Hundiwale, D. 2011. Density, excess molar volume and apparent molar volume of binary liquid mixtures. *Rasayan Journal of Chemistry*, 4 (3): 599-604.

Pereiro, A., Araújo, J., Esperança, J., Marrucho, I. and Rebelo, L. 2012. Ionic liquids in separations of azeotropic systems–A review. *Journal of Chemical Thermodynamics*, 46: 2-28.

Pereiro, A. B. and Rodríguez, A. 2007. Thermodynamic properties of ionic liquids in organic solvents from (293.15 to 303.15) K. *Journal of Chemical & Engineering Data*, 52 (2): 600-608.

Plechkova, N. V. and Seddon, K. R. 2008. Applications of ionic liquids in the chemical industry. *Chemical Society Reviews*, 37 (1): 123-150.

Poling, B. E., Prausnitz, J. M. and O'Connell, J. P. 2000. *The Properties of Gases and Liquids*. 5th ed. New York: McGraw-Hill Professional.

Qian, W., Xu, Y., Zhu, H. and Yu, C. 2012. Properties of pure 1-methylimidazolium acetate ionic liquid and its binary mixtures with alcohols. *Journal of Chemical Thermodynamics*, 49: 87-94.

Rafiee, H. R. and Frouzesh, F. 2016. The study of partial and excess molar volumes for binary mixtures of nitrobenzene and benzaldehyde with xylene isomers from T = (298.15 to 318.15) K and P = 0.087 MPa. *Journal of Advanced Research*, 7 (5): 769-780.

Redhi, G. 2003. Themodynamics of liquid mixtures containing carboxylic acids Doctor of Philosophy, University of Natal.

Rogers, R. D. and Seddon, K. R. 2003. Ionic liquids - solvents of the future? *Science*, 302 (5646): 792-793.

Roy, M. N., Ekka, D. and Dewan, R. 2011. Physico-chemical studies of some bio-active solutes in pure methanoic acid. *Acta Chimica Slovenica*, 58: 792-796.

Saini, N., Jangra, S. K., Yadav, J., Sharma, D. and Sharma, V. 2011. Thermodynamic properties of binary mixtures of tetrahydropyran with pyridine and isomeric picolines: Excess molar volumes, excess molar enthalpies and excess isentropic compressibilities. *Thermochimica Acta*, 518 (1): 13-26.

Schult, C. J., Neely, B. J., Robinson, R., Gasem, K. and Todd, B. A. 2001. Infinite-dilution activity coefficients for several solutes in hexadecane and in n-methyl-2-pyrrolidone (NMP): experimental measurements and UNIFAC predictions. *Fluid Phase Equilibria*, 179 (1): 117-129.

Seader, J. and Henley, E. 2006. Adsorption, ion exchange, and chromatography. *Separation Process Principles*: 568-570.

Shah, M. R., Anantharaj, R., Banerjee, T. and Yadav, G. D. 2013. Quaternary (liquid+ liquid) equilibria for systems of imidazolium based ionic liquid + thiophene + pyridine + cyclohexane at 298.15 K: Experiments and quantum chemical predictions. *Journal of Chemical Thermodynamics*, 62: 142-150.

Shana'a, M. and Canfield, F. 1968. Liquid density and excess volume of light hydrocarbon mixtures at–165° C. *Transactions of the Faraday Society*, 64: 2281-2286.

Shekaari, H., Zafarani-Moattar, M. T. and Behrooz, N. J. 2015. Volumetric, acoustic, and refractometric properties of (thiophene+ hexane/cyclohexane) solutions in the presence of some imidazolium based ionic liquids at T= 298.15 K. *The Journal of Chemical Thermodynamics*, 86: 188-195.

Sibiya, P. 2009. Excess molar volumes, partial molar volumes and isentropic compressibilities of binary systems (ionic liquid + alkanol). Masters Degree in Technology, Durban University Of Technology.

Singh, S. 2013. Correlation and prediction of the physical and excess properties of the ionic liquid 1-butyl-3 methylimidazolium methyl sulphate with several alcohols at T = (298.15 to 313.15) K. Masters Degree in Technology, Durban University Of Technology.

Singh, S., Bahadur, I., Naidoo, P., Redhi, G. and Ramjugernath, D. 2016. Application of 1-butyl-3-methylimidazolium bis (trifluoromethylsulfonyl) imide ionic liquid for the different types of separations problem: Activity coefficients at infinite dilution measurements using gas-liquid chromatography technique. *Journal of Molecular Liquids*, 220: 33-40.

Singh, S., Bahadur, I., Redhi, G. G., Ramjugernath, D. and Ebenso, E. E. 2014. Density and speed of sound measurements of imidazolium-based ionic liquids with acetonitrile at various temperatures. *Journal of Molecular Liquids*, 200: 160-167.

Skoog, D. A., Holler, F. J. and Crouch, S. R. 2007. *Principles of Instrumental Analysis*. 6th ed. Belmont, CA: Thomson Brooks/Cole.

Sobota, M., Dohnal, V. r. and Vrbka, P. 2009. Activity coefficients at infinite dilution of organic solutes in the ionic liquid 1-ethyl-3-methyl-imidazolium nitrate. *Journal of Physical Chemistry B*, 113 (13): 4323-4332.

Stark, A. and Seddon, K. R. 2007. Ionic liquids. In: Seidel, A. ed. *Kirk-Othmer Encyclopedia of Chemical Technology*. New York: Wiley.

Steltenpohl, P. and Graczová, E. 2014. Use of ionic liquids in extraction. *Acta Chimica Slovaca*, 7 (2): 129-133.

Strechan, A., Kabo, A., Paulechka, Y., Blokhin, A., Kabo, G., Shaplov, A. and Lozinskaya, E. 2008. Thermochemical properties of 1-butyl-3-methylimidazolium nitrate. *Thermochimica Acta*, 474 (1): 25-31.

Taib, M. M. and Murugesan, T. 2011. Density, refractive index, and excess properties of 1-butyl-3-methylimidazolium tetrafluoroborate with water and monoethanolamine. *Journal of Chemical & Engineering Data*, 57 (1): 120-126.

Tiegs, D., Gmehling, J., Medina, A., Soares, M., Bastos, J., Alessi, P. and Kikic, I. 1986. Activity coefficients at infinite dilution; DECHEMA Chemistry Data Series *Main: Frankfurt*, Vol. IX, 4 parts.

Tumba, K. A. 2010. Infinite dilution activity coefficient measurements of organic solutes in fluorinated ionic liquids by gas-liquid chromatography and the inert gas stripping method. Master of Science (Chemical Engineering), Faculty of Engineering, School of Chemical Engineering, University of KwaZulu-Natal.

Van Dyk, B. and Nieuwoudt, I. 2000. Design of solvents for extractive distillation. *Industrial & Engineering Chemistry Research*, 39 (5): 1423-1429.

Walden, P. 1914. Molecular weights and electrical conductivity of several fused salts. *Bulletin de l'Academie Imperiale de Sciences de Saint-Petersbourg (St. Petersburg)*, 8: 405-422.

Wasserscheid, P., van Hal, R. and Bösmann, A. 2002. 1-n-Butyl-3-methylimidazolium ([BMIM]) octylsulfate—an even 'greener'ionic liquid. *Green Chemistry*, 4 (4): 400-404.

Welton, T. 1999. Room-temperature ionic liquids. Solvents for synthesis and catalysis. *Chemical Reviews*, 99 (8): 2071-2084.

Wilkes, J. S., Levisky, J. A., Wilson, R. A. and Hussey, C. L. 1982. Dialkylimidazolium chloroaluminate melts: a new class of room-temperature ionic liquids for electrochemistry, spectroscopy and synthesis. *Inorganic Chemistry*, 21 (3): 1263-1264.

Wilkes, J. S. and Zaworotko, M. J. 1992. Air and water stable 1-ethyl-3-methylimidazolium based ionic liquids. *Journal of the Chemical Society, Chemical Communications*, (13): 965-967.

Williams-Wynn, M. 2012. An Investigation Into the Potential of NFM, DEG and TEG as Replacement Solvents for NMP in Separation Processes. Master of Science (Chemical Engineering), University of KwaZulu-Natal.

Wood, S. E. and Brusie, J. P. 1943. The Volume of Mixing and the Thermodynamic Functions of Benzene—Carbon Tetrachloride Mixture1. *Journal of the American Chemical Society*, 65 (10): 1891-1895.

Zafarani-Moattar, M. T. and Majdan-Cegincara, R. 2007. Viscosity, density, speed of sound, and refractive index of binary mixtures of organic solvent + ionic liquid, 1-butyl-3-methylimidazolium hexafluorophosphate at T = 298.15 K. *Journal of Chemical & Engineering Data*, 52 (6): 2359-2364.

Zafarani-Moattar, M. T. and Shekaari, H. 2005. Apparent molar volume and isentropic compressibility of ionic liquid 1-butyl-3-methylimidazolium bromide in water, methanol, and ethanol at T = (298.15 to 318.15) K. *Journal of Chemical Thermodynamics*, 37 (10): 1029-1035.

Zafarani-Moattar, M. T. and Shekaari, H. 2006. Application of Prigogine–Flory–Patterson theory to excess molar volume and speed of sound of 1-n-butyl-3-methylimidazolium

hexafluorophosphate or 1-n-butyl-3-methylimidazolium tetrafluoroborate in methanol and acetonitrile. *Journal of Chemical Thermodynamics*, 38 (11): 1377-1384.

Zhou, Q., Wang, L.-S. and Chen, H.-P. 2006. Densities and viscosities of 1-butyl-3-methylimidazolium tetrafluoroborate + H_2O binary mixtures from T = (303.15 to 353.15) K. *Journal of Chemical & Engineering Data*, 51 (3): 905-908.

APPENDICES

Critical constants and ionization energy of the solutes and the carrier gas used in the calculation of the virial coefficients.

Solute	T_c/ K	P_c/ KPa	V_c/ ($cm^3 \cdot mol^{-1}$)	I/ eV
n-Pentane	469.70	3370.00	311.00	10.35
n-Hexane	507.60	3025.00	368.00	10.13
n-Heptane	540.20	2740.00	428.00	9.92
n-Octane	568.70	2490.00	492.00	9.82
Cyclopentane	5.11.60	4508.00	260.00	10.51
cyclohexane	553.93	4073.00	308.00	9.86
Cyclooctane	647.20	3570.00	410.00	9.76
Benzene	562.05	4895.00	256.00	9.25
Toluene	591.75	4108.00	316.00	8.82
o-Xylene	630.30	3732.00	370.00	8.56
m-Xylene	617.00	3541.00	375.00	8.57
p-Xylene	616.20	3511.00	378.00	8.45
Methanol	512.64	8097.00	118.00	10.85
Ethanol	513.92	6148.00	167.00	10.47
1-Propanol	536.78	5175.00	219.00	10.22
Hex-1-ene	504.00	3143.00	355.10	9.44
Hept-1-ene	537.30	2920.00	409.00	9.44
Oct-1-ene	567.00	2680.00	468.00	9.43
Non-1-ene	594.04	2330.00	526.00	9.42

Solute	T_c/ K	P_c/ KPa	V_c/ ($cm^3 \cdot mol^{-1}$)	I/ eV
Dec-1-ene	615.00	2200.00	650.00	9.42
Hex-1-yne	529.04	3691.00	333.50	9.95
Hept-1-yne	559.69	3295.00	389.50	9.95
Octy-1-yne	586.86	2960.00	445.50	9.95
Pyridine	620.00	5670.00	254.00	9.30
Thiophene	580.00	5660.00	219.00	8.87
Acetonitrile	574.90	4830.00	173.00	12.20
Dichloromethane	510.00	6100.00	189.50	12.10
Acetone	508.10	4700.00	209.00	9.70
3-Pentanone	561.50	3730.00	336.00	9.31
Ethylacetate	523.20	3830.00	286.00	10.01
Helium	5.20	227.00	57.30	24.59

Saturated vapour pressure P_1^*, molar volume V_1^*, virial coefficients B_{11} and B_{12} used in the calculation of γ_{13}^{∞} at T = (313.15, 323.15 and 333.15) K

Solutes	T/ K	P_1^*/ kPa	V_1^*(cm^3·mol^{-1})	B_{11}(cm^3·mol^{-1})	B_{12}(cm^3·mol^{-1})
n-Pentane	313.15	115.77	118.84	-1054.32	48.08
	323.15	159.45	121.00	-973.79	48.63
	333.15	214.88	123.30	-902.64	49.15
n-Hexane	313.15	37.95	133.70	-1647.74	53.86
	323.15	54.07	135.74	-1510.53	54.46
	333.15	76.37	137.90	-1390.43	55.03
n-Heptane	313.15	12.34	149.99	-2474.07	59.90
	323.15	18.90	152.01	-2252.23	60.55
	333.15	28.05	154.13	-2059.51	61.14
n-Octane	313.15	4.14	167.93	-3599.35	66.26
	323.15	6.71	169.99	-3256.52	66.96
	333.15	10.48	172.14	-2960.35	67.61
Cyclopentane	313.15	73.99	97.37	-1101.26	41.39
	323.15	103.93	98.78	-1013.43	41.94
	333.15	142.66	100.27	-936.23	42.45
Cyclohexane	313.15	24.64	110.70	-1771.09	47.00
	323.15	36.26	112.07	-1616.21	46.99
	333.15	52.00	113.51	-1481.37	47.55
Cyclooctane	313.15	1.72	139.12	-4612.79	56.04
	323.15	2.87	140.42	-1443.14	56.75
	333.15	4.59	141.77	-3739.76	57.42

Solutes	T/ K	P_1^*/ kPa	V_1^*($cm^3 \cdot mol^{-1}$)	B_{11}($cm^3 \cdot mol^{-1}$)	B_{12}($cm^3 \cdot mol^{-1}$)
Benzene	313.15	24.37	90.18	-1536.68	40.57
	323.15	36.17	91.28	-1401.18	41.13
	333.15	52.19	92.43	-1283.32	41.65
Toluene	313.15	7.89	107.97	-1639.43	47.14
	323.15	12.29	109.18	-1458.68	47.75
	333.15	18.55	110.44	-1304.64	48.32
o-Xylene	313.15	2.04	123.45	-3802.57	52.65
	323.15	3.40	124.69	-3420.45	53.30
	333.15	5.44	125.98	-3091.89	53.92
m-Xylene	313.15	2.55	124.40	-3586.07	53.41
	323.15	4.19	125.71	-3229.57	53.30
	333.15	6.62	127.07	-2922.76	54.67
p-Xylene	313.15	2.65	125.45	-3599.04	53.83
	323.15	4.34	126.78	-3241.49	54.07
	333.15	6.86	128.15	-1485.34	55.09
Methanol	313.15	35.44	37.64	-339.87	24.08
	323.15	55.56	38.28	-321.20	24.49
	333.15	84.52	38.95	-304.04	24.87
Ethanol	313.15	17.90	56.09	-541.40	30.29
	323.15	29.48	56.98	-507.15	30.75
	333.15	47.00	57.93	-476.29	31.19
1-Propanol	313.15	6.98	75.33	-870.65	36.27
	323.15	12.15	76.39	-808.66	37.00
	333.15	20.29	77.49	-753.54	37.29

Solutes	T/ K	P_1^*/ kPa	V_1^*(cm^3·mol^{-1})	B_{11}(cm^3·mol^{-1})	B_{12}(cm^3·mol^{-1})
Hex-1-ene	313.15	45.05	130.19	-1559.00	52.78
	323.15	64.70	132.20	-1429.47	53.37
	333.15	91.00	134.32	-1316.24	53.91
Hept-1-ene	313.15	14.93	146.22	-2326.22	58.14
	323.15	22.60	148.18	-2118.26	58.77
	333.15	33.22	150.23	-1937.55	59.37
Oct-1-ene	313.15	5.05	163.35	-3391.03	47.69
	323.15	8.07	165.32	-3068.56	48.19
	333.15	12.47	167.38	-2789.93	48.67
Non-1-ene	313.15	1.71	170.65	-4785.95	47.95
	323.15	2.90	172.64	-4307.31	48.47
	333.15	4.72	174.70	-3895.54	48.93
Dec-1-ene	313.15	0.65	230.03	-7165.00	81.99
	323.15	1.13	232.34	-6420.52	82.76
	333.15	1.19	234.72	-5782.22	83.49
Hex-1-yne	313.15	32.69	124.50	-1678.45	49.63
	323.15	48.18	126.16	-1535.42	50.23
	333.15	69.19	126.16	-1535.42	50.27
Hept-1-yne	313.15	13.14	127.59	-2508.34	55.28
	323.15	19.56	129.28	-2278.94	55.93
	333.15	28.39	131.04	-2080.05	56.53
Octy-1-yne	313.15	14.88	155.44	-3608.68	60.88
	323.15	22.05	157.18	-3259.16	61.57
	333.15	22.04	157.18	-3259.16	61.57

Solutes	T/ K	P_1^*/ kPa	V_1^*($cm^3 \cdot mol^{-1}$)	B_{11}($cm^3 \cdot mol^{-1}$)	B_{12}($cm^3 \cdot mol^{-1}$)
Pyridine	313.15	5.98	86.25	-1851.09	39.41
	323.15	9.55	87.13	-1686.54	40.00
	333.15	14.76	88.04	-1543.57	40.55
Thiophene	313.15	20.69	72.59	-1181.17	36.14
	323.15	31.01	73.47	-1086.23	36.67
	333.15	45.16	74.38	-1002.93	37.17
Acetonitrile	313.15	23.04	45.81	-641.75	30.06
	323.15	34.07	46.57	-600.45	30.57
	333.15	49.12	47.36	-536.29	31.05
Dichloromethane	313.15	956.34	62.87	-540.78	32.65
	323.15	1210.26	63.91	-511.06	33.16
	333.15	1508.24	65.00	-483.74	33.63
Acetone	313.15	56.62	69.02	-730.82	35.72
	323.15	81.95	70.17	-680.01	32.21
	333.15	115.60	71.40	-634.67	36.68
3-pentanone	313.15	10.04	118.40	-1836.64	49.66
	323.15	15.61	119.85	-1682.42	50.27
	333.15	23.55	121.37	-1547.65	50.83
Ethylacetate	313.15	25.11	98.89	-1178.51	44.36
	323.15	38.03	100.35	-1088.91	44.93
	333.15	55.89	101.89	-1009.77	45.64

Sample Calculations

Activity coefficient at infinite dilution for toluene using IL: 1-butyl-3-methylimidazolium hydrogen sulphate at T =313.15 K.

$$J_2^3 = \frac{2}{3}\left[\frac{(P_i/P_o)^3 - 1}{(P_i/P_o)^2 - 1}\right]$$

$$J_2^3 = \frac{2}{3}\left[\frac{(117674/99007.33)^3 - 1}{(117674/99007.33)^2 - 1}\right]$$

$$J_2^3 = 1.09698$$

$$U_O = U\left(1 - \frac{P_W}{P_O}\right)\frac{T}{T_f}$$

$$U_O = 5.04202E-07\ m^3{\cdot}s^{-1} * \left(1 - \frac{2905.86\ Pa}{99007.33}\right) * \frac{313.15\ K}{296.76\ K}$$

$$U_O = 5.16\ E-07\ m^3{\cdot}s^{-1}$$

$$V_N = (J_2^3)^{-1} U_o (t_R - t_G)$$

$$V_N = (1.09698)^{-1} * (5.16\ E-07\ m^3{\cdot}s^{-1}) * (712.64\ s - \ 30.00\ s)$$

$$V_N = 3.21\ E-04\ m^3$$

The activity coefficient is subdivided into three terms

Term 1

$$ln\frac{n_3 RT}{V_N P_1^*}$$

$$ln\frac{0.01270\ mol * 8.314\ Pa.\frac{m^3}{K}.mol * 313.15\ K}{3.21\ E-04\ m^3 * 7890.89\ Pa}$$

= 2.56807

$$\frac{(B_{11} - V_1^*)P_1^*}{RT}$$

$$\frac{\left(-0.001639\,\frac{m^3}{mol} - \frac{0.00010780\ m^3}{mol}\right) * 789089\ Pa}{8.314\ Pa.\frac{m^3}{K}.mol * 313.15\ K}$$

= -0.0053

Term 3

$$\frac{P_o J_2^3 (2B_{12} - V_1^\infty)}{RT}$$

$$\frac{99007.33\ Pa * 1.09698 * (2 * 4.714\ E - 05 m^3/mol - 0.0001080\ m^3/mol)}{8.314\ Pa.\frac{m^3}{K}.mol * 313.15\ K}$$

= -0.00057

Therefore,

$$ln\gamma_{13}^\infty = ln\frac{n_3 RT}{V_N P_1^*} - \frac{(B_{11} - V_1^*)P_1^*}{RT} + \frac{P_o J_2^3 (2B_{12} - V_1^\infty)}{RT}$$

$ln\gamma_{13}^\infty =$ Term 1- Term 2 + Term 3

$ln\gamma_{13}^\infty =$ 2.5681- (-0.0053) + (-0.00057)

$\gamma_{13}^\infty =$ 13.10

Excess molar enthalpy at infinite dilution for using toluene using IL: 1-butyl-3-methylimidazolium hydrogen sulfate at T = 313.15 K.

$$\left[\frac{\partial In\gamma_i^{\infty}}{\partial(1/T)}\right] = \frac{\Delta H_1^{E\infty}}{R}$$

Where,

$\left[\frac{\partial In\gamma_i^{\infty}}{\partial(1/T)}\right]$ is equal to slope from the graph of $ln\gamma_{13}^{\infty}$ versus (1000/T) K^{-1}

From the graph, the slope benzene = 0.238

$$0.238 = \frac{\Delta H_1^{E\infty}}{8.314}$$

$\Delta H_1^{E\infty}$= 1.979 kJ/mol^{-1}

Selectivity at infinite dilution

$$S_{ij,s}^{\infty} = \frac{\gamma_i^{\infty}}{\gamma_j^{\infty}}$$

Where i refers to a solute (hexane) and j and refers to aromatic benzene at T = 323.15 K

And then

$$S_{ij,s}^{\infty} = \frac{791.079}{6.497} = 121.76$$

Capacity at infinite dilution

$$k_j^{\infty} = \frac{1}{\gamma_j^{\infty}}$$

$$k_j^{\infty} = \frac{1}{6.497} = 0.154$$